REPUBLIQUE ALGERIENNE DEMOCRATIQUE ET POPULAIRE
MINISTÈRE DE L'ENSEIGNEMENT SUPÉRIEUR ET DE LA RECHERCHE SCIENTIFIQUE

Université Mouloud Mammeri de Tizi-Ouzou
Faculté du Génie de la Construction
Déaprtement de Génie Mécanique

Mémoire en vue de l'obtention du diplôme de

MASTER en Génie Mécanique

Spécialité : Construction Mécanique

Thème :

Etude et conception d'une chaine cinématique d'un véhicule électrique

Réalisé par :

Dahbia Amini

Proposé et encadré par :

Prof. Ould Ouali Mohand

Année Universitaire 2020/2021

PEOPLE'S DEMOCRATIC REPUBLIC OF ALGERIA
MINISTRY OF HIGHER EDUCATION AND SCIENTIFIC RESEARCH

University Mouloud Mammeri of Tizi Ouzou
Faculty of Construction Engineering
Department of Mechanical Engineering

Dissertation submitted for the degree of Master's in mechanical engineering

Major: Mechanical design

Topic:

Design and study of a two – speed transmission powertrain for an electric vehicle

Done by:

Dahbia Amini

Proposed and supervised by:

Prof. Ould Ouali Mohand

Academic year 2020/2021

Abstract

Over the past decade, the automotive industry has shifted significantly into electrification. Electric vehicles are growing in popularity, but so far they have used almost exclusively single-ratio gearboxes. Using a dual gear ratio has several potential benefits, including enabling the electric motor and inverter to operate in a more efficient area, improving vehicle acceleration, gradeability and top speed, and reducing the mass and bulk of the overall traction system.

This thesis elaborates the steps of applying a two-speed gearbox to EVs according to the latest published papers on the topic. The current trends in EVs and insight into the industry are covered. The work discusses the steps of integrating a two-speed transmission into an EV powertrain, the design of components and dynamic analysis were also conducted.

While multi-speed EV traction systems do show considerable promise, more investigation is needed to finally determine under what circumstances they can outperform highly optimized single-speed systems.

Résumé

Au cours de la dernière décennie, l'industrie automobile a considérablement évolué vers l'électrification. Les véhicules électriques gagnent de popularité, mais jusqu'à présent, ils ont utilisé presque exclusivement des boîtes de vitesses à un seul rapport de transmission. L'utilisation d'un double rapport présente plusieurs avantages potentiels, notamment le fait de permettre au moteur électrique et au convertisseur de fonctionner plus en efficacité, d'améliorer l'accélération du véhicule, l'aptitude en pente et la vitesse de pointe, et de réduire la masse et l'encombrement de la chaine cinématique.

Cette thèse élabore les étapes d'application d'une boîte de vitesses à deux vitesses aux véhicules électriques selon les derniers articles publiés sur le sujet. Les tendances actuelles des véhicules électriques et un aperçu de l'industrie sont étudies. Le travail aborde les étapes d'intégration d'une transmission à deux vitesses dans une transmission pour un véhicule électrique, la conception des composants et une analyse dynamique ont également été menées.

Bien que les transmissions à plusieurs vitesses soient très prometteuses, une étude plus approfondie est nécessaire pour enfin déterminer dans quelles circonstances ils peuvent surpasser les systèmes à une vitesse hautement optimisés.

Acronyms and abbreviations

EV: Electrical Vehicle

BEV: Battery Electrical Vehicle

FCEV: Fuel Cell Electrical Vehicle

PHEV Plug-in Hybrid Electrical Vehicle

HEV: Hybrid electrical vehicle

OEM: Original Equipment Manufacturer

R&D: Research and Development

DSO: Days Sales Outstanding

EVSPL: Electrical Vehicle Solar Parking Lot

ICE: Internal Combustion Engine

DC: Direct Current

AC: Alternative Current

PV: Photovoltaic

PMSM: Permanent magnet synchronous motor

SRM: Switched reluctance motor

EU: European Union

NCAP: New Car Assessment Program

FMVSS: Federal Motors Vehicle Safety Standard

IDIADA : (Institut d'Investigació Aplicada de l'Automòbil) Applied Automotive Research Institute

To my late father,

To my mother, brother and to those who kept and keep supporting me…

Acknowledgments

I would like to thank my thesis advisor Prof. Ould Ouali Mohand of the Department of Mechanical Engineering at Mouloud Mammeri University of Tizi Ouzou. He consistently allowed this Master's thesis to be from my work and steered me in the right direction providing vital support, feedback, and encouragement, as well as recommendations and several revisions throughout the work period.

I would furthermost thank my family and friends who provide unconditional support and a chance to evade the stressful work environment.

I would here like to take the opportunity to thank all of those that had a positive impact during my thesis writing.

Contents

Introduction

The growing need to protect natural resources and environmental concerns stimulates the interest in the development of electric vehicles. These vehicles have various advantages compared to an internal combustion engine car. They are more efficient, less noisy and simpler, providing a smooth driving experience.

While most existing vehicles work with some form of internal combustion engines, the all-electric vehicle provides excellent performances running on an electric motor which allows constant power supply during high-speed ranges. These motors with lightweight, low cost and high efficiency. However, the main challenge is integrated high-speed motor with a 2-speed gearbox to significantly reduce speed and provide different speed ranges, as the standard in electric vehicles is a single-speed gearbox with a fixed ratio.

The main purpose of this paper is to design an electric vehicle powertrain with a two-speed gear transmission for a front-wheel-drive urban passenger car.

In high-speed transmissions, special attention must be paid to gear tooth geometry and selection of rolling bearings to maximize energy efficiency while controlling the noise generated, which is a major factor in electric vehicles as there is no noise from the combustion engine to suppress transmission noise.

Another challenge was to design a two-speed transmission and a differential for a one motor transmission. Mechanical design of components, assembling and manufacturing drawings will also be considered and the necessary ones are presented.

This work layout is structured in chapters, the references and included appendices are presented at the end of the document. The layout chapters begin after the introduction by background research regarding the history, the current electric vehicle types also and insight of the industry and a market analysis. Then, the second chapter focus on the specifications of the powertrain in an electric vehicle following a study of its geometry also dimensioning calculations for the powertrain components. The final chapter, rely on the data acquired from the previous one and shows the 3D modeling of the powertrain and the design was analyzed by SolidWorks. The conclusion offers a final observation on the dynamic study analysis and discusses further required studies.

Chapter I. Background theory

I.1 Introduction

The automotive industry is one of the biggest industries worldwide and in this recent years it achieved a great deal of development of new technologies and due to environmental awareness, electrical vehicles were the main subject of those advancements, although it is not particularly a new invention in the automobile industry as they were introduced decades ago. In this chapter, we start with a look back at the history of electrical vehicles then we dive into the recent market analysis of the industry; where we review current EVs users and OEMs points of view to get a perspective of possible improvements. After that, we study different types of electrical vehicles, their characteristics and drawbacks. Finally, we go into details about EVs configurations and main parts.

I.2 Origins and history of electrical vehicles

The invention of electric cars was serious of breakthroughs that go before that is of internal combustion vehicles. This concept can be traced back to 1828 when Hungarian inventor Anyos Jedlik came up with a small model car running on an electromagnetic device. After that, in 1837, the scot Robert Davidson built an electric locomotive with the capacity of 1.5 miles at 4 mph before changing the batteries.

The batteries were rechargeable by 1858 and in 1887, William Morrison, applied for a patent on a 4 horsepower electric locomotive reaching a top speed of 20 mph, running on 24 battery cells rechargeable every 50 miles. The Philadelphians Pedro Salom and Henry G. Morris also got a patent in 1894 on their 1.1 kW motor Elecrobat and sold their idea to Issac L. Rice the owner of the Electric Vehicle Company (ECV). By the early 1900s and with the help of partners and investors, the company managed to put 600 electric cabs on the streets of New York. They also managed to address the battery-recharging problem by transforming an ice arena into a battery-swapping station. In the end, the business collapsed in 1907 due to inner conflicts.

In 1908, Henry Ford introduced the Model T for gasoline cars that made gasoline-powered vehicles more available also due to the cheap prices of gasoline. That same year, Charles Kettering introduced the electric starter, eliminating the need for the hand crank, which increased gasoline-powered vehicle sales. Technology development in gasoline cars decreased electric vehicles usage.

After 30 years, gas shortages and oil rising prices in addition to development in the combustion engine created the need for alternative vehicles. Moreover, the most important breakthrough was made in 1973 by the British chemist M. Stanley Whittingham by inventing the first rechargeable lithium-ion battery. On the other hand, the environmental concern rising in the 1990s helped develop electric cars that have almost the same performances as the fuel-powered ones.

The real revival of electric cars was at the start of the 21st century and it was sparked by two major events. First, the introduction of the Toyota Prius relaying on a nickel-metal hybrid battery. It was released in Japan in 1997 and introduced worldwide in 2000. It was made the world's first mass-produced hybrid electric vehicle. Then, Tesla Motors began the production of electric sports cars running 200 miles in one charge.[21, 26, 38]

I.3 Insight on the worldwide EV industry

I.3.1 Electrical cars' market

A new research report on the EV market published by Meticulous Research entitled "Electric Car Market by Propulsion Type (BEV, FCEV, PHEV, HEV), Power Output (Less Than 100kW, 100 kW to 250 kW), End-Use (Private, Commercial), and - Global Forecast to 2028," showed that the electric car market is expected to reach 69.3 million units by 2028.

The global electric vehicles market is divided into sectors depending on propulsion type, power output, final usage, and geography.

Based on propulsion type, in 2021 the segment of hybrid vehicles is estimated to get the largest share of the market. That is due to the increasing automotive vehicles emission regulations, the demand for high fuel efficiency, large OEMs investments in the segment, and the low cost of hybrid cars compared to other types. However, by 2028, the fuel cell electric cars are expected to grow at the highest. The factors contributing to this growth are the good characteristics this type offers like fast refueling, no tailpipe emissions, increased driving range with a lighter battery pack, investments in R&D of hydrogen fuel cell technology and setting charging stations.

According to the power output, the electric vehicle market is subdivided into 100kW or less and 100kW to 250kW. In 2021, it is expected that the part below 100kW will account for the largest share of the entire electric vehicle market. The large share of this segment is mainly due to the increase in the use of light electric vehicles in the central business increase the implementation of electric vehicles in shared travel services in major cities around the world major cities, battery prices have fallen, and electric vehicle start-ups have increased investment in this area. However, during the forecast period, the 100kW to 250kW segment is expected to grow at the highest compound annual growth rate.

According to the end-user, the electric vehicle market is divided into private use and commercial use. In 2021, the private usage segment will occupy the largest share of the entire electric vehicle market. A large part of this is partly due to the increase in consumer demand for energy-saving and zero-emission vehicles, the government encourages the sales and manufacture of electric vehicles, tax rebates, and battery decline costs and fuel prices are rising. This market segment is expected to grow at a compound annual growth rate during the forecast period.

Geographically, the global electric cars market includes North America, Europe, Asia-Pacific, Latin America, and the Middle East &Africa. In 2021, Asia-Pacific will estimably get the biggest share of the global electric cars market by value and volume before Europe and North America. In this region, a large part is mainly attributable to the increasing demand for electric vehicles and related charging facilities, and more start-ups are providing numerous solutions and services in the electric vehicle industry. Also due to the attractive incentives in plans of electric vehicle buyers, and the existence of regional core competitiveness in countries such as China and the manufacturing and technological development in Japan, South Korea and India.

In Europe, the rapid growth of the regional market is attributed to the continuous development of strict EU regulations on emissions, so countries are trying to reduce the number of traditional cars on the road. Moreover, Europe's extensive charging infrastructure network, and increased investment in the development of sustainable road traffic infrastructure that can charge electric vehicles during the journey to minimize mileage anxiety related to electric vehicles. [3]

I.3.2 EV battery market

The focus in R&D of EV batteries is the reduction of size and the place occupied by the battery. The modification in the battery design includes changing the anode-cathode battery separator by Samsung SDI to reduce the size and CATL the Chinese EV battery manufacturer invented 1cm thick battery cells that will be stacked up to form a battery system.

Companies also are looking for different materials to improve battery performances, safety and lifetime. Therefore, Toshiba, Targray and Altairnano used lithium, titan and graphite as the anode-cathode materials. By 2025, Electrolyte is expected to be the largest segment in the li-ion battery component. It is located inside the battery to allow ions a free movement between positive and negative electrodes. This component improves the li-ion battery's safety and performance and unlike other electric solutions, it is compatible with other components due to its non-aqueous state. Although, it has a limited operating temperature [-20, +50] °C and out of this range the solution is damaged.

In addition to size and materials, there is a big emphasis to change the battery location as its large dimension occupies most of the car's space and is mostly installed at the bottom. To be able to place the battery closer to the wheels and narrow the drivetrain as much as possible, there must be a decrease in size and an increase in the density of the battery.

Even with the recent development in EV batteries, there still are many gaps to overcome as previously mentioned; the limited range, charging time, battery life and lack of charging stations. Therefore, manufacturers are looking for solutions by developing batteries with high performance.

In 2021, hybrid electric vehicles still occupy the largest market share. However, more and more attention is paid to replacing traditional internal combustion engine vehicles with environmentally

friendly vehicles running on pure electric energy, which is expected to double the BEV market and create opportunities for EV battery manufacturers.

Dividing the market into segments, the truck segment is expected to have the fastest growth in the forecast. Medium-duty trucks are usually used for distribution and garbage services, while heavy-duty trucks are more suitable for long-distance transportation. The use of electricity as fuel for medium and heavy trucks has prompted many OEMs to launch electric trucks in 2021, which will ultimately drive the electric vehicle battery market.

For example, Navistar, which has launched a new business unit NEXT eMobility Solutions, plans to launch an international medium-sized electric truck in 2021. Tesla Semi, an electric heavy-duty truck with a cruising range of 500 miles, is also started production in 2021.

During the forecast period, North America will lead the medium and heavy truck market. The existence of OEMs like Peterbilt, Freightliner, Kenworth and Navistar and their focus on producing electric mid-size trucks promote the market in the region.

All these projects and the increasing adoption of trucks will increase the global production of electric vehicle batteries, thereby promoting the development of the electric vehicles battery market.[3]

I.3.3 Charging station market

Charging stations are becoming an important necessity that must be provided to allow EV users to charge their vehicles away from home thus permitting more drive range, offering other services such as frequency and regulation of voltage. However, the limited availability of charging sockets and long charging time are still big issues to address.

One of the solutions offered is using reservations and decreasing the demand in charging stations by rising charging prices to influence clients to use specific periods by setting low or no reservation fees. The second strategy is to decrease the charging price and increase the demand but a reservation fee will guarantee the demand and allow for more flexibility (Figure I.3—1). The strategies give different outcomes depending on users. However, in the market, an increase in charging flexibility drops cost revenues of the stations so opting for reservation times that allow maximal usage of sockets can benefit both sides.

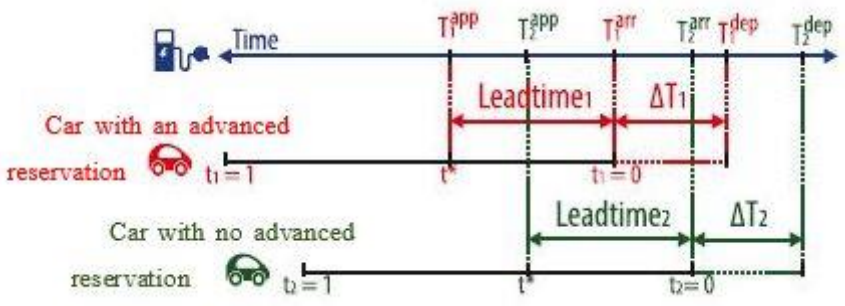

Figure I.3—1. Charging time difference of two cars[1]

In addition to flexibility, there are other operational objectives such as:

- Maximize the use of on-site renewable energy for power generation: generate electricity from renewable energy on-site at zero marginal cost, or sign bilateral supply contracts with local producers to ensure that the energy used to charge electric vehicles is purchased from the electricity market;
- Supporting distribution system operator (DSO) goals: Assumptions CS is a marketing agent independent of DSO; nevertheless, if a commercial agreement is pre-arranged, CS can still support DSO goals if DSO provides real-time incentives. In the case of a pre-arranged protocol, CS receives control commands from DSO to limit its power consumption at specific time intervals during the day, this can be directly modeled as an additional constraint on the aggregate CS charging profile;[29]

Another innovative solution is the introduction of an EV parking lot with a solar rooftop to offer charging services. The aim was to combine EV's and solar photovoltaic in a single power system, as the parking lot acts as a charging station with energy generated from photovoltaic.

Economically, in the case of capacity payment, EVSPL generates income by having available and synchronized power capacity, but also receiving additional payments for energy transmission. The revenue from the actual delivery of available capacity accounts for 4% to 7% of the total revenue of EVSPL agents. Still, EVSPL is affected by not providing the power regulation offered.

In addition to the specified economic benefits, EVSPL also provides important environmental benefits. These benefits include reducing the need for open land for the construction of renewable energy projects and using electricity generated from renewable energy to charge electric vehicles, thus eliminating any related emissions with operations used in electrical vehicles. Moreover, EVSPL is reducing the average emissions associated with the electrical grid.[18]

[1] Rodrigo Bernal, D.O., Matias Negrete-Pincetic, Álvaro Lorca, Management of EV charging stations under advance reservations schemes in electricity markets. Sustainable Energy, Grids and Networks, 2020: p. 11

The growth in the EV market will result directly in the growth of the charging stations market. Thus, the government's initiative to install charging stations will benefit the market growth in the Asia-Pacific region and is expected to be in a leading position until 2026. China is likely to play an important role in driving the growth in the region. This will happen when the Chinese government is implementing a national policy for the development of charging stations. In Japan and South Korea, the market will grow steadily due to the expansion of the electric vehicle industry.

On the other hand, Europe had an electric vehicle charging station market revenue of USD 8.49 billion in 2018. This increase can be attributed to the increasing installation of charging stations within 100 kilometers of national highways by many European governments. Due to the huge charging network of automakers throughout the United States, North America will grow exponentially.[2]

I.4 Consumers perspective influence on EV vehicle manufacturers

The improvement in electrical powertrains and batteries alongside the environmental and market pressures put on internal combustion engines (ICEs) increased the demand for electrical vehicles (EVs). In 2016, the sales of pure electrical cars excluding hybrids developed by approximately 45%, [27] but even now in 2021, despite the promising potential of EVs, their present and acceptability in the market are still insufficient and consumers' willingness to own electrical cars still not high enough when their preferences are based on space, appearance and power range. Therefore, to provide a product acceptable to consumers there should be optimization in the structure and performances of EVs.[9]

Table 2
Mean and median values of stated satisfaction with EV attributes.

EV attributes	Satisfaction Mean	50th percentile (Median)
Range-Recharge satisfaction (RRS)		
Battery range	3.54	4
Battery range during winter	3.90	3
Recharging duration	3.29	4
Cost satisfaction (CS)		
Purchase cost	3.83	4
Maintenance cost	3.95	4
Recharging cost	4.22	4
Policy measures satisfaction (PMS)		
Road toll exemption/reduction	4.40	5
Ferry fee exemption/reduction	3.62	0
Parking fee exemption/reduction	3.65	3
Access to bus lane (time-saving)	3.71	1
Environmental-attributes satisfaction (EAS)		
Tailpipe emission	4.59	5
Traffic noise	4.30	4
Type of energy usage	4.64	5
Other environmental consequences	4.24	4
Availability satisfaction (AS)		
Availability of dealers nearby	3.98	4
Availability of different EV models	3.62	3
Country of manufacturer	3.70	3
Manufacturer's reputation	3.99	4

Table 3
Mean and median values for each item of TPB constructs.

TPB Constructs	Mean	50th percentile (Median)
Subjective Norms (SN)		
People who are important to me are considering buying electric cars.	3.39	3
People who are important to me already own electric cars.	3.53	4
People who are important to me recommended that I buy an electric car.	3.28	3
People who are important to me support my interest in buying an electric car.	3.68	4
People who are important to me think electric cars promote a sustainable transportation system.	3.43	3
Perceived Functional Barriers (FB)		
I think that the driving performance of an electric car is inferior to that of conventional cars.	1.82	2
I think that an electric car has a lower maximum speed than conventional cars.	1.81	2
I consider conventional cars to be safer to drive than electric cars.	2.00	2
I am worried about running out of a charge while driving an electric car.	2.74	3
Attitude (ATT)		
I believe driving an electric car reduces (would reduce) the local air pollution in my residential area.	4.12	4
I believe driving an electric car saves (would save) money in the long term.	4.18	4
I believe driving an electric car reduces (would reduce) traffic noise.	3.91	4

Figure I.4—1. Consumers' behavior toward purchasing an EV vehicle[2]

An empirical study analyzed data from a survey made on the Norwegian EV market, which has a high market penetration rate in the field. The findings suggest that consumers' behavior in buying electrical powered cars is mainly influenced by the environmental values of EVs and the corresponding social pressure, as to lower air pollution, traffic noise also the economic benefit of saving money in the long term. These previous values' influence on consumers surpassed the client's perception about EV's technical functions. The same study finds that cost aspects have the strongest effect on satisfaction with EVs so it indicates that car manufacturers need to focus on cost reduction related to purchasing, recharging and maintenance of their products. On the other side, other significant attributes should be taken into consideration as power range, charging time along with environmental attributes and availability of electrical cars in the market.[24]

According to the survey, most of the consumers were focused on the social and environmental influence of purchasing an EV car and were not as much satisfied with the functional barriers.

In another study conducted on consumers' preferences for the features of EV's in South Korea (*Figure I.*4—2), they confirmed that Korean consumers focus more on technological attributes. Therefore, they favor high fuel economy, long power driving range and autonomous driving but also they were displeased by the high cost of purchasing the vehicle, the large distance to the charging station and the long charging time.

[2] Hasan, S., Assessment of electric vehicle repurchase intention: A survey-based study on the Norwegian EV market. Transportation Research Interdisciplinary Perspectives 2021: p. 13.

Table 5
Relative importance of attributes analysis results.

Classification	Attributes	Model 1		Model 2	
		Relative Importance (SD)	Relative Importance (SUM)	Relative Importance (SD)	Relative Importance (SUM)
Economic-related attributes	Fuel economy	20.35% (0.032)	51.0%	3.74% (0.016)	74.67%
	Purchase price	30.65% (0.037)		–	
	High purchase price over RP.	–		15.68% (0.031)	
	Low purchase price over RP.	–		55.25% (0.076)	
Technology-related attributes	Driving range with full battery/tank	10.86% (0.029)	22.48%	5.40% (0.014)	13.43%
	Charging time	7.96% (0.035)		6.85% (0.018)	
	Autonomous driving	3.66% (0.019)		1.18% (0.007)	
Infrastructure-related attributes	Distance to charging station: within 1 (dummy)	15.11% (0.034)	17.43%	6.20% (0.018)	8.35%
	Distance to charging station: within 3 km (dummy)	2.32% (0.017)		2.16% (0.010)	
Body types	Body type: SUV/minivan (dummy)	4.69% (0.029)	9.09%	2.34% (0.014)	3.55%
	Body type: mid/full-size car (dummy)	4.40% (0.028)		1.21% (0.009)	

Figure I.4—2. Preferred EV attributes of Korean consumers[3]

The study also showed through a market simulation that the shares of EVs highly increased when the purchase cost decreased in comparison with current EV prices due to extension in government sub-studies and/or lower manufacturing costs. In addition, when the charging time was reduced from 40 min to that is of a current ICEV (5 min), the shares went up. It increased then slightly when the driving range augmented from 400 km to 700 km same as the gasoline level. Lastly, the market shares were not affected by the improvement in fuel economy.

To expand the adoption of EVs, the article implicated that:

- Lowering purchase and recharge costs, as they were the key factor for changing from ICEVs to EVs. Therefore, the strategy of launching EVs with appropriate performances within the price range of the current ICEVs is better than introducing high-performance EVs with higher prices.
- R&D investments should be directed towards improving EVs performance such as developing battery technology to attend long driving range and faster charging time.
- Finally, promoting nearby and an adequate number of charging infrastructures in residential areas.[34]

I.5 Electrical vehicles market penetration in North Africa and Algeria in particular

With regions dependent on oil production income and/or with low vehicle market contribution, the introduction of EV vehicles could be a critical transition. A new analysis predicts that car sales in North Africa will shrink by 30.7% on average, as local production operations begin to close or warn of disruption due to Covid-19, downside risks are increasing, which will affect available inventory. Nissan has suspended the operation of its Egyptian plant from March 26 (the plant has not yet restarted), and due to the suspension of production in China, GB Auto is facing a delay in the complete phase-out of

[3] Sungsoon Jang, J.Y.C., Which consumer attributes will act crucial roles for the fast market adoption of electric vehicles. Estimation on the asymmetrical & heterogeneous consumer preferences on the EVs. Energy Policy, 2021: p. 11.

imported kits from Chery. Egyptian consumers are also subject to more movement restrictions, which will affect their activities. Other risks for sales come from the possibility that auto shows in the region could've been canceled in 2020, which is usually a driver of demand, such as the Morocco Auto Expo originally scheduled to be held in Casablanca in June 2020. However, the fair has then been postponed but Moroccan car sales may receive some support by the end of 2021.

Algerian cars market even before the Covid-19 outbreak; we had low near-term prospects of the new car sales. This is due to the 2020 budget increases the tax burden of ownership, the interruption of the supply of locally produced cars, and the weak economic outlook of the country due to the decline in oil production. Given that Covid-19, in particular, may have a significant impact on Q220 sales, the Algerian auto industry estimably, shrunk by at least 75% in 2020.[9]

But research-wise there are still rising opportunities for EVs in Algeria as mention Oussama Touaba a young Algerian researcher from the development center of renewable energies (CDER), who manufactured an electrical car from aluminum with a 2.5 m length, a driving range of 40kms/h. the car weighs less than 200kg and is equipped with two 1.2 Kwatts motors.[5]

I.6 EV types and comparison

An electrical vehicle is a control system fully or partially propelled by electric motors, which could be powered from a collector network, electricity generator, photovoltaic cells, or power turbines. The working process of an EV depends on its type and currently, there are three distinguished types according to their technology and settings; BEV, HEV, PHEV and FCEV.[14, 20]

I.6.1 Battery electric vehicle (BEV)

A battery electric vehicle (BEV), also known as an all-electric vehicle (AEV), runs entirely on batteries and electric drive systems. Therefore, BEVs use electric motors and systems instead of internal combustion engines (ICE) for propulsion. Electricity is stored in a large battery pack, which is charged by plugging into the grid. In return, the battery pack provides power for one or more electric motors to run electric vehicles.

Battery Electric Vehicles (BEV) include different types of vehicles, such as cruisers, bicycles, skateboards, rail cars, boats, forklifts, vehicles, trucks, and other vehicles.[17, 20]

I.6.1.1 Construction and operating principle

The figure (Figure I.6—1) below demonstrates the main component of a battery electric vehicle. To be able to operate a BEV need the following:

- Charging port: it allows the vehicle to communicate with an external power source to charge its battery. Then electricity is converted from DC batteries to AC power for use by electric motors;

- DC/DC converter: converts a high DC voltage to a low DC voltage because the low DC voltage helps to operate vehicle components and provides energy for the battery.
- Electric traction motor: uses electricity from the battery to rotate the wheels so that the vehicle can run. This type of motor can be used to drive or recover;
- Onboard charger: The purpose of this charger is to extract AC power from the household or any other power source; usually 240 V. Then, convert this AC power to DC power to charge the battery. It also checks the battery's voltage, current, temperature and various other factors;
- Power electronics controller: when it receives a signal from an accelerator, it helps to transmit the power from the battery, the speed and torque to control the vehicle;
- The traction battery pack: stores the power for further use by the engine of a BEV;
- Transmission: conveys the mechanical force from the motor to the wheels to run the vehicle;

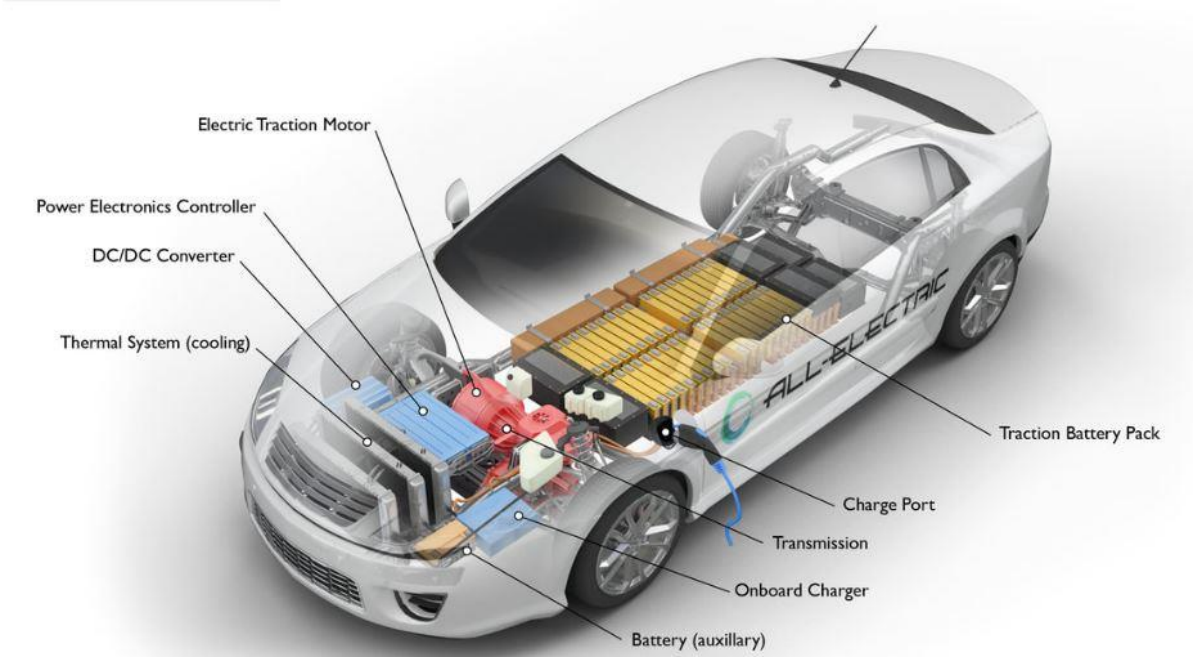

Figure I.6—1. Main components of a BEV[4]

Other parts are also included in BEV's for better functioning; the auxiliary battery offers a capacity to power vehicle accessories. In addition, the thermal system, to manage the temperature of the motor, engines…etc.

I.6.1.2 Current BEV's model's anatomy

- **Tesla Model S (**Figure I.6—2**):** an advanced BEV. In the two-car axles, there is an electric traction engine, in the front and the back, and both run independently and have their power

[4] Source : U.S. Department of Energy, Alternative Fuels Data Center, www.afdc.energy.gov

electronic controller. This gives the car an All Wheel Drive (AWD) ability and an increasing speed. In 2021, new features are added to the model and it is named Plaid.

Figure I.6—2. Tesla dual motor model S[5]

- **Rimac Concept One (**Figure I.6—3**):** it is referred to as a hyper car. The power strain of the vehicle relies on four separate engines, one in each wheel and each motor has its apparatus gearbox. One single-speed gearbox in the front and two-speed gearboxes in the back with carbon fiber grips. The battery is a T- shape form situated between the back and front axles.

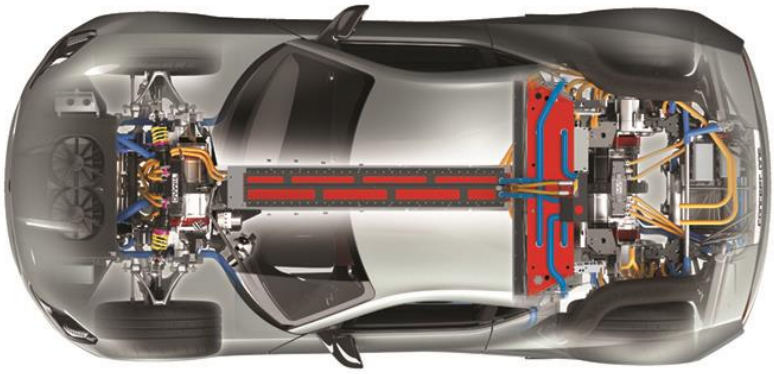

Figure I.6—3. Rimac Concept One model[6]

I.6.1.3 Key features

To compare a BEV to other EVs and even ICE vehicles, several characteristics should be considered:

- **Efficiency:** in a BEV the electric engine substitute the AC flow as it has a permanent magnet or an induction rotor that offers a basic efficiency of 65-80% and 90-97% at max, which is higher than ICE productivity of 10-40%;
- **Dynamic performance and torque vectoring:** the electric engine can transmit extreme torques at zero speed, which provides a good start for the vehicle. It also provides peak torque for a limited time measurement at the beginning and uninterrupted torque when the vehicle

[5] Source : https://www.veicolielettricinews.it/tesla-model-s-dual-motor-doppio-motore-trazione-integrale-e-prove-generali-di-guida-autonoma/

[6] Source : https://e-hike.net/tr/content/rimac-automobili-invents-croatian-auto-industry

is in a steady-state. Unlike ICE, it has a faster torque response and can improve stability by controlling the torque of the wheels;

- **Reliability:** BEV has fewer moving parts. Also due to high torque and a fast electric engine, it does not require a multi-stage gearbox, which means a separate propulsion mechanical gearbox is sufficient to meet the traction prerequisites. Although ICE vehicles have many moving parts thus many additional frames;
- **Energy Recuperation and Brake Regeneration:** the use of electric motors in BEVs is one of the obvious advantages of BEVs over other vehicles. Because, electric machines are reversible, which means they can provide torque when provided by electricity, they can also generate electricity due to the delay of the vehicles, when they have the energy of the input torque. Therefore, the electric machine is in engine mode when generating torque, and in generator mode when providing electrical energy;
- **Costs and maintenance:** Like ordinary internal combustion engine vehicles, pure electric vehicles have some leeway in terms of operating costs compared with different electric vehicles. The electricity cost to charge a pure electric vehicle is 33% as much per kilometer as buying oil. In addition, there are fewer moving parts and segments, so a BEV is simpler and the cost of keeping up is lower;
- **Environmental friendly:** less CO2 emissions related to BEVs so less pollution, the electricity for charging have better prospects to be generated from renewable resources. Moreover, some manufacturers are looking for ways to use eco-friendly materials and recycled ones from households to manufacturing some of the car parts;[17]

However, the current issue with BEV is the limited drive range and infrastructure for charging.

I.6.2 Fuel cell electric vehicle (FCEV)

A fuel cell electric vehicle (FCEV) is an electric vehicle that uses "fuel cell technology" to generate the electricity needed to run the vehicle. In this type of vehicle, fuel chemical energy, mainly derivate oxygen and hydrogen from the air is directly converted into electrical energy. These vehicles are considered zero-emissions although most hydrogen is extracted from natural gas.[20]

Some current model examples of FCEVs include Toyota Mirai, Hyundai Tucson FCEV, River simple Rasa, Honda Clarity Fuel Cell, and Hyundai Nexo.

I.6.2.1 Architecture and working principal

The main purpose of fuel cell integrated vehicles is to provide the electricity to run the vehicle within itself so it is generating power for two loads and charging the battery under normal operating conditions.[8]

An FCEV is composed of the main parts seen in (Figure I.6—4):

- Battery (auxiliary): In electric vehicles, the low-voltage auxiliary battery provides power to start the car before the traction battery is engaged; it also provides power for car accessories;
- Battery pack: This high-voltage battery stores the energy generated by regenerative braking and provides supplementary power for the electric traction motor;
- DC/DC converter: This device converts high-voltage direct current from the traction battery pack into low-voltage direct current required to run vehicle accessories and charge auxiliary batteries;
- Electric traction motor (FCEV): Using electricity from fuel cells and traction battery packs, this motor drives the wheels of the vehicle. Some vehicles use motor generators that perform driving and regeneration functions;
- Fuel cell stack: A single membrane electrode assembly that uses hydrogen and oxygen to generate electricity;
- Fuel filler: The nozzle of the fuel dispenser is connected to a container on the vehicle to fill the fuel tank;
- Fuel tank (hydrogen): Store hydrogen on the vehicle until the fuel cell needs it;

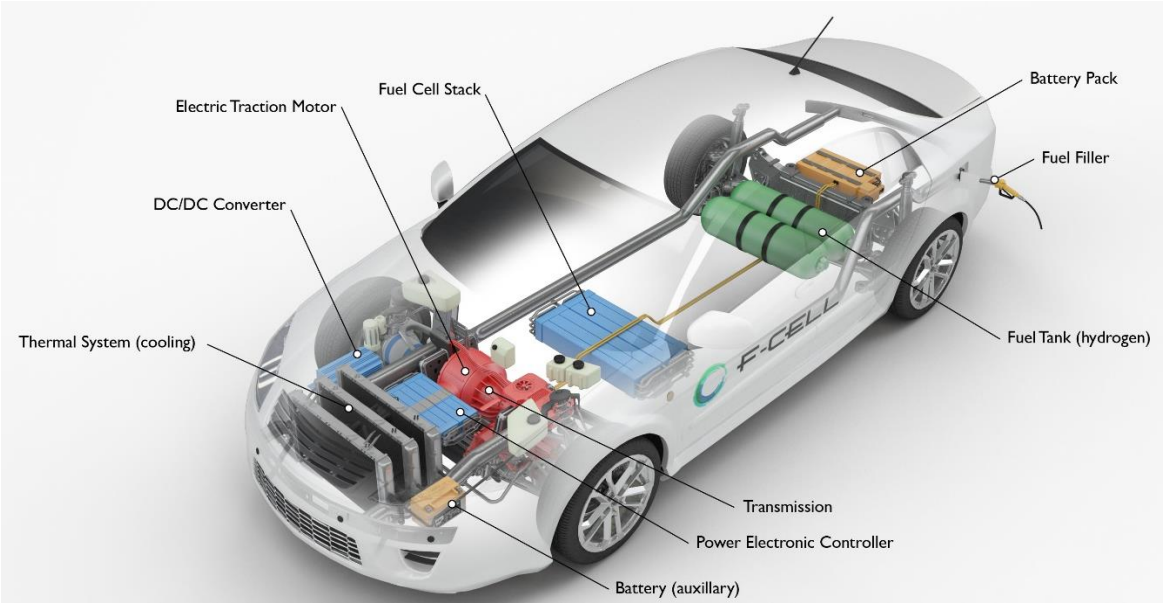

Figure I.6—4 Components of a fuel cell electric vehicle[7]

- Power Electronic Controller (FCEV): This unit manages the flow of electrical energy provided by the fuel cell and traction battery, and controls the speed of the traction motor and the torque it produces;
- Thermal System (Cooling)-(FCEV): This system maintains the proper operating temperature range of fuel cells, electric motors, power electronics and other components;

[7] U.S. Department of Energy, A.F.D.C. How Do Fuel Cell Electric Vehicles Work Using Hydrogen? [Cited 2021; Available from: https://afdc.energy.gov/vehicles/how-do-fuel-cell-electric-cars-work

- Transmission (electric): The transmission transmits mechanical power from the electric traction motor to drive the wheels;[37]

I.6.2.2 Features and limitations

Fuel cell vehicles have zero emissions, a longer lifespan, and can operate at 100°C. The fuel cell full-load efficiency is reported to be about 46%.

Compared with photovoltaic (PV) systems, fuel cells are specially integrated into electric vehicles due to their cleanliness, lower noise, and higher relative efficiency. However, FCHEV has some limitations, such as lack of storage capacity, slow dynamic response compared to BEV but the similar response in steady-state, lower tolerance to ripple, and cold start problems. For the above problems, FCEV is integrated with an auxiliary power supply (battery) to alleviate these problems mentioned in vehicle parts.[8]

I.6.3 Hybrid electric vehicles (HEV)

This type of hybrid vehicle is often referred to as a standard hybrid or a parallel hybrid. The HEV is driven by a combination of a traditional internal combustion engine and an electric engine. In this type of electric car, the internal combustion engine obtains energy from fuel (gasoline and other types of fuel), while the motor obtains electrical energy from the battery. The gasoline engine and electric motor rotate the transmission at the same time to drive the wheels.

The difference between PHEV and BEV is that HEV cannot be connected to the grid. The battery that provides energy for the electric motor is only charged with electricity generated by the internal combustion engine of the vehicle, or from regenerative braking by converting kinetic energy into electrical energy.[20, 32]

I.6.3.1 Working principal and components

The internal combustion engine powers the hybrid car and the electric motor, which uses energy stored in the battery. The battery is also charged through regenerative braking, which can power auxiliary loads and reduce engine idling when stopped. An HEV is mainly designed showing the following components (Figure I.6—5):

- Battery (auxiliary): in electric vehicles, the low-voltage auxiliary battery provides power to start the car before the traction battery is engaged; it also provides power for auto parts. In addition, the traction battery pack: stores electricity for traction motor use;
- DC/DC converter: the device converts high-voltage direct current from the traction battery pack into low-voltage direct current required to run vehicle accessories and charge auxiliary batteries;

- Dynamo: during braking, it generates electricity from the rotating wheels and transfers the energy back to the traction battery pack. Some vehicles use motor generators that perform driving and regeneration functions;
- Electric traction motor: this motor uses the power of the traction battery pack to drive the wheels of the vehicle. Some vehicles use motor generators that perform driving and regeneration functions;
- The exhaust system exhausts the gas from the engine through the exhaust pipe. The three-way catalyst is designed to reduce engine emissions in the exhaust system;
- Gas station: the nozzle of the fuel dispenser is connected to a container on the vehicle to fill the fuel tank which stores gasoline on the vehicle until the engine needs it;
- Internal combustion engine (spark ignition): in this configuration, fuel is injected into the intake manifold or the spark from the spark plug ignites the combustion chamber, where it is combined with air and the air/fuel mixture;

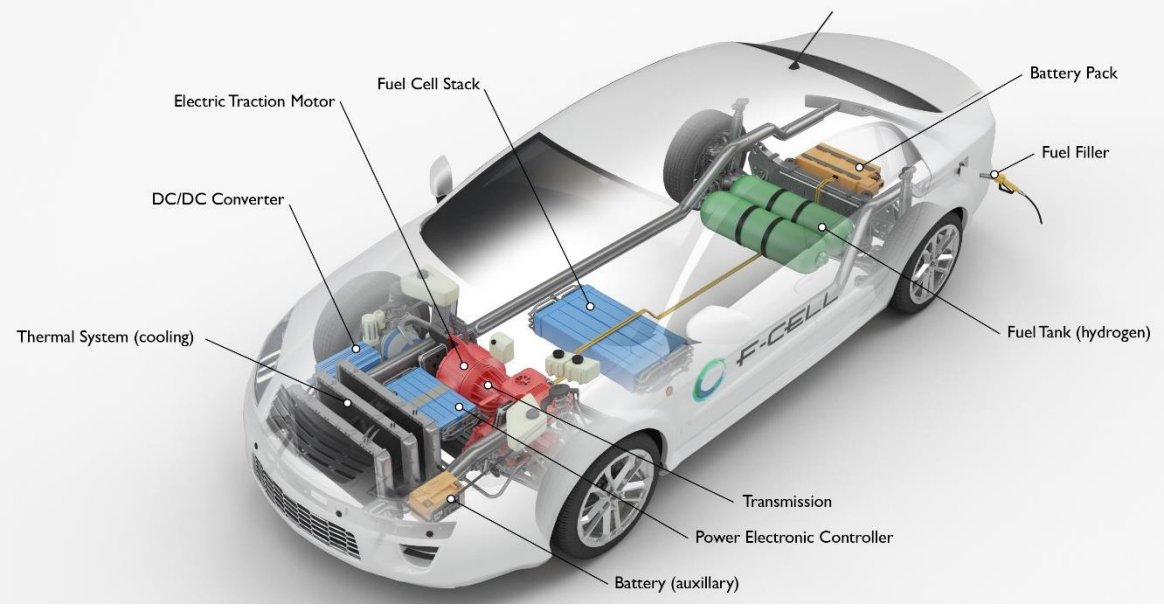

Figure I.6—5. HEV components[8]

- Power electronic controller: manages the flow of electrical energy provided by the traction battery and controls the speed of the traction motor and the torque it produces;
- Thermal system (cooling): This system maintains the proper operating temperature range of the engine, electric motor, and power unit, electronic equipment and other components;
- Gearbox: transmits mechanical power from the engine and/or electric traction motor to drive the wheels;

[8] Source: U.S. Department of Energy, A.F.D.C. [cited 2021; Available from: https://afdc.energy.gov/vehicles/

I.6.3.2 System design of HEVs

HEV can be mild hybrid or full hybrid, and full hybrid can be designed in series or parallel configuration.

- **Mild hybrid vehicles**: also called micro-hybrid vehicles use batteries and electric motors to power the vehicle and can turn off the engine when the vehicle is stopped, further improving fuel economy. However, they cannot use electricity alone to power vehicles.
- **Full-hybrid car:** With a larger battery and a more powerful electric motor, it can provide short-distance and low-speed power to the vehicle. The cost of these vehicles is higher than that of mild hybrids, but they have better fuel economy advantages.

There are many ways to combine the power of the electric motor and the engine. **Parallel hybrid vehicle:** The most common HEV design, connects the engine and electric motor to the wheels through a mechanical coupling. Both the electric motor and the ICE directly drive the wheels. **Series hybrid vehicles** only use electric motors to drive the wheels, which are more common in a plug-in hybrid vehicle.[37]

I.6.3.3 Main advantages and drawbacks

Hybrid vehicles have an auxiliary battery, which is added to the internal combustion engine and allows a certain electric autonomy to the vehicle. As a result, it offers a range similar to that of a traditional vehicle with a reduced tail-pipe emission.

The battery incorporated in the hybrid vehicle cannot be charged externally; therefore, it cannot operate at its full potential, which makes HEVs mainly depend on gas/fuel to run the car's engine.

Although the battery reduces the vehicle’s emissions, they are still considerably high. In addition, the weight of the dual-drive system makes the car less efficient than a BEV.[33]

I.6.4 Plug-in hybrid electric vehicles

PHEV is a hybrid vehicle with an ICE and a motor, often referred to as a series hybrid. This type of electric car is powered by conventional or alternative fuel and by a battery, which can be recharged with electricity by using an electrical outlet or an electric vehicle charging station.

PHEV can generally work in at least two modes; an all-electric mode, in which the engine and the battery supply all the energy for the car, and a hybrid mode, in which electricity and gasoline are used.[20]

I.6.4.1 Construction and working principal

PHEVs generally start in an all-electric mode and run on electricity until their battery is depleted. Some models switch to hybrid mode when they reach the cruising on the highway, typically over 60 miles per hour. Once the battery is empty, the engine takes it and the vehicle runs as an HEV.

In addition to plugging into an external power source, PHEV batteries can be recharged by internal combustion or regenerative braking. When braking, the electric motor acts as a generator to charge the battery and supplement the engine's power. As a result, smaller engines can be used, making the car fuel-efficient without compromising performance.[20]

The components of a plug-in hybrid electric car are as follows (Figure I.6—6):

- Auxiliary battery: gives power to vehicle accessories as well as low voltage electricity to start the vehicle before the traction battery is activated;
- Charge port: for connecting to an external power supply and charging the traction battery;
- DC/DC converter: converts higher-voltage DC power from the traction battery pack to lower-voltage DC power that can be used to power vehicle accessories and charge the auxiliary battery;
- Electric generator: Produces electricity from the rotating wheels when braking and transfers it to the traction battery pack. Some vehicles use motor generators that work both as a driver and as a regenerator;
- Electric traction motor: This motor powers the vehicle's wheels by drawing power from the traction battery pack. Some vehicles use motor generators that serve both as a driver and as a regenerator;

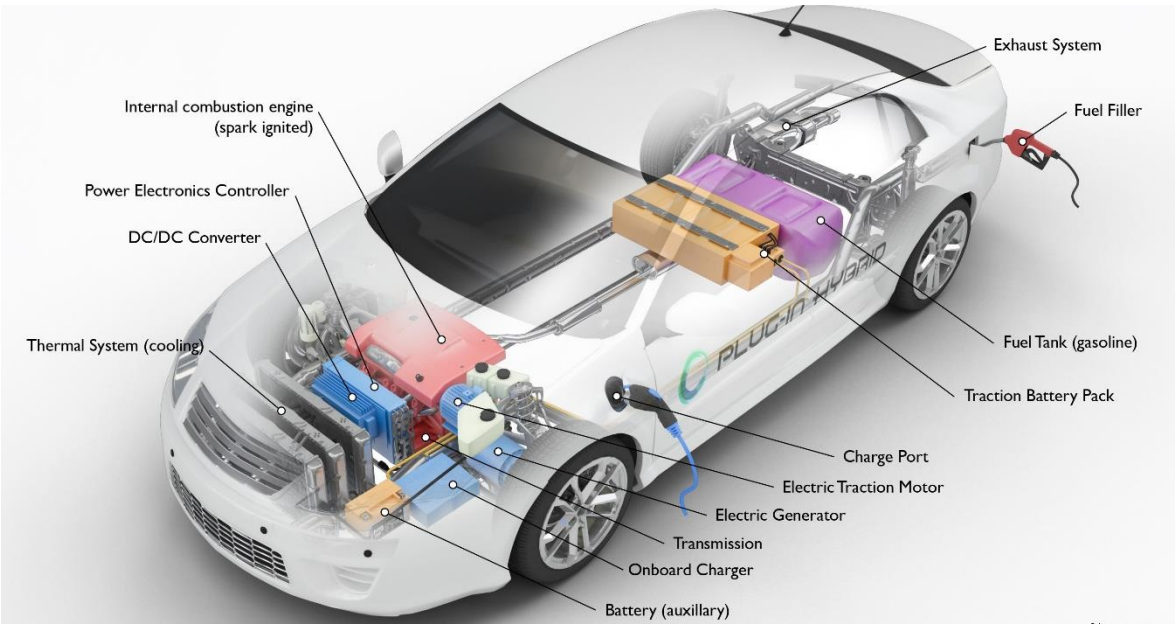

Figure I.6—6. PHEV main components[9]

- Exhaust system: The exhaust system is responsible for directing exhaust gases from the engine out the tailpipe. A three-way catalyst is intended to reduce engine-out emissions through the exhaust system;

[9] Source: U.S. Department of Energy, A.F.D.C. [cited 2021; Available from: https://afdc.energy.gov/vehicles/

- Fuel filler: A nozzle from a fuel dispenser attaches to the receptacle on the vehicle to fill the tank, which stores gasoline on board the vehicle until it is refueled;
- Internal combustion engine (spark-ignited): Fuel is injected into either the intake manifold or the combustion chamber in this design. Where it is combined with air, and the spark from a plug ignites the air/fuel mixture;
- Onboard charger: Converts incoming AC current from the charge port to DC power for charging the traction battery. While charging the pack, it also connects with the charging equipment and analyzes battery properties such as voltage, current, temperature, and state of charge;
- Power electronics controller: This unit handles the flow of electrical energy given by the traction battery, managing the speed and torque produced by the electric traction motor;
- Thermal system (cooling): This system keeps the engine, electric motor, power electronics, and other components within a safe operating temperature range;
- Traction battery pack: A battery pack that stores electricity for use by the electric traction motor;
- Transmission: The transmission is responsible for transferring mechanical power from the engine and/or electric traction motor to the wheels;[37]

I.6.4.2 Features and characteristics

A PHEV combines an internal combustion engine, an electric motor, and a massively charged battery. Unlike conventional crossbreeds, PHEVs can be linked and energized externally, allowing them to run only on electric motors. When the battery is depleted, the traditional motor kicks in and the car operates normally. Because they can run on grid electricity—and because power is a more consistent energy source than petrol or diesel. When in all-electric mode, PHEVs do not pollute the environment. They are more environmentally friendly because they have an electric motor and a battery.

They use less gasoline than traditional automobiles, lowering vehicle-operating costs. Although this cost is insignificant when computed for a single day, it reduces the entire cost of the car in the end. A plug-in hybrid electric car requires a 120 V outlet, which is typically available in residential homes, adding to the owner's luxury.

The financial benefit of PHEVs over conventional vehicles in terms of fuel consumption drives people to adopt PHEVs. These versions enhance the owner's luxury by providing the option of an all-electric range or hybrid mode.[33]

I.7 Challenges and improvements regarding electrical vehicles

In the last years, the field of the electric vehicle knew a great growth. However, there are still numerous aspects pending. To be able to look at new possible solutions exploring existing technologies in motor and battery design also the different charging modes.

I.7.1 Battery technologies and characteristics

The rising number of sales in EVs resulted in an increase in battery production by 66% and there were many technology developments in the sector related to battery characteristics. However, there are still many obstacles to overcome such as the driving range, the charging time and the weight of battery packs. In the following, there are some examples of battery types and features[23].

I.7.1.1 Lead-Acid batteries

The acid-filled battery is the cheapest and most popular car driving battery among electric vehicle batteries and deep-cycle batteries. The engine starter battery is designed to provide a low power percentage and start the machine's fast charge rate, while the low cycle battery, for example, chariots and golf carts are used to provide continuous energy for electric vehicles.

Deep-cycle batteries in recreational vehicles are often used as auxiliary batteries but they must be charged in stages. Flooded batteries must be checked at the electrolyte level, usually drained through water, and gas is collected during the normal charging period. In addition, the recent huge development of lead-acid, the battery has shown that other modern batteries are almost impossible to be replaced and soon, electric vehicles will completely use lead-acid batteries. These batteries are always used without basic problems, but certain behaviors under certain conditions are still unclear.

I.7.1.2 Nickel Metal hybrid

This type of battery is usually used in HEVs, they are made of Nickel Metal hybrid. Its related production is expected to increase due to the popularity of PHEVs and BEVs. The active ingredient is Hydrogen as a metal hybrid for negative electrodes and oxyhydroxide for positive electrodes, the two result in the oxidation of nickel into nickel hydroxide but after charging the pump the reverse process happens.

I.7.1.3 Molten Salt batteries

The molten salt battery is a type of battery that uses molten salt as an electrolyte. Provides good energy capacity and high power efficiency. The current type is not rechargeable thus; thermal batteries can stay in solid-state for a long time at room temperature before being inactivated by heating so Zebra cells are manufactured in the discharged state. Liquid salt NaAlCl4 vacuum impregnation in the porous mixture of nickel salts forming the cathode. Zebra cell charging capacity is calculated from the amount of salt (NaCl) present in the cathode. Zebra battery is durable, can be recycled thousands of times, and is non-toxic. The disadvantages of Zebra batteries include low specific capacity (<300 W/kg) and the

electrolyte being heated to about 270 °C (518 °F), which consumes some electricity and causes problems for long-term charging and storage and is potentially dangerous.

I.7.1.4 Lithium-Ion batteries

Compared with other commonly used batteries, lithium-ion batteries support higher energy costs, excellent power efficiency, longer service life and environmental protection, and have been proven to be widely used in electronic products. Nevertheless, the lithium-ion battery must be able to work properly, safely and consistently in environments with high temperatures and limited stress. Disabling the limitations of these windows will cause the battery to start quickly; amplification may even cause security difficulties. This also reduces electrolyte and generate combustible gas or combustible gas through relatively low voltage remaining.

Recent electric vehicles have used new lithium-ion chemical variants that have lost specific power and strength to provide fire safety, environmentally friendly loading and long service life (up to a few minutes).[14]

I.7.2 Current motor technologies used in EVs

Although motors do not signify any new invention with the recent development of EVs, it plays central importance apart from batteries. As EVs require fast start torque, significant electricity density and good efficiency, the new improvement in power electronics and control systems are offering multiple solutions and research prospects.[32]

I.7.2.1 Brushless DC motors

This is similar to a DC motor with permanent magnets. Brushless because there is no switch and brush device available which allows a free maintenance process. The brushless DC motor engine has traction performance, such as high starting torque and about 95-98% performance. This brushless DC motor is the most popular motor for electric vehicles applications due to its traction capabilities.

I.7.2.2 DC series motors

The advantage of this engine is that it is fast in terms of speed control; it has a good starting torque capability and can manage spontaneous power shifts. All of these functions make it an appropriate traction engine. Nevertheless, due to the brushes, the biggest disadvantage of the DC series engine is the high maintenance cost.

I.7.2.3 Permanent magnet synchronous motor (PMSM)

Similar to a brushless DC motor engine but with permanent magnets. These engines also have the same traction characteristics, such as high power density and high speed.

The higher-rated power is determined by a permanent magnet synchronous motor. PMSM is the perfect choice for demanding systems such as cars. Despite the high cost, PMSM can provide stable

resistance for induction motors due to its better performance than brushed DC motors. It is also better as a generator. Manufacturers of HEVs and BEVs prefer this motor category the most.

I.7.2.4 Three-phase AC induction motors

Induction engines do not have good starting torque compared with DC series engines, which operate under a fixed voltage and a fixed frequency. However, various control methods (such as FOC or voltage and frequency control) can be used to change this property. When the engine starts these control systems provide the best torque for traction.

Due to less maintenance, the squirrel-cage induction engine has a longer life cycle. In addition, powerful motors from 92% to 95% are possible to design. The drawback of this motor is the complicated process to do an inverting circuit. Tesla Model S is an example of an application to be able to reduce reliance on permanent magnets.

I.7.2.5 Switched reluctance motors (SRM)

Switched reluctance motors are robust and easy to install. SRM rotor is one-piece laminated steel without any windings or permanent magnets. This alleviates the inertia of the rotor also contributes to high acceleration.

The biggest disadvantage of SRM is the difficulty of switching circuit monitoring and passing. It also has some noise problems. When SRM joins the automobile industry, it should be able to supplement potential PMSM and induction engines.[14]

I.7.3 Charging classification

There are many concepts when classifying charging modes of EVs; the following classification is according to the IEC-62196 standard[10], which describes the main characteristics of charging processes and the energy supply methods. Therefore, there are four modes to be able to charge the vehicle.[32]

I.7.3.1 Fast charging

It is the easiest way to charge an electric car is especially suitable for DC loads. This is high and fast in two different categories. With DC, the output is up to 100KW, sometimes 150KW and up to 350KW when fast charging.

Quick chargers provide 7 to 22 kilowatts of electricity, usually charging electric cars for up to 3-4 hours. During the night service, a pure electric vehicle or two-quarter PHEV takes 8-12 hours. Electric vehicle charging requires complex devices with 3-pin or type two-socket connection cables.

[10] International Electro-technical Commission. Plugs, Socket-Outlets, Vehicle Couplers and Vehicle Inlets-Conductive Charging of Electric Vehicles—Part 1: General Requirements; Standard; IEC: Geneva, Switzerland, 2014.

I.7.3.2 Charging with a constant current

This mode allows a regulation of the charging device voltage and for the resistance related to the battery to maintain a current flow steadily. The constant current value changes capacity from beginning to end. However, the battery current capacity goes down proportionally with the continuous charging cycle which results in charging time overload and decreases the battery capacity even more.

I.7.3.3 Charging with a constant voltage

Constant voltage charging is a widely used charging technique that includes constant tension between battery poles. When the engine is in a running failure, the starter battery uses constant voltage charging. If the specified voltage constant value is appropriate, it can ensure that the battery does not lose moisture when charging. An alternative extension to the constant current or constant voltage algorithm is the new CC/CV charging algorithm for the converter. As an alternative to using constant voltage and constant current throughout the charging cycle, the charging efficiency

The first step is to increase the voltage amplification to make the battery reach about 30% of its average charging capacity. After that, the charging algorithm will be exchanged for standard CC/CV.

I.7.3.4 Non-contact charging method

This method relies on magnetic resonance to allow energy in the liquid phase in the device and battery, which gives a good energy conversion. In addition to being faster, cleaner it also contributes to decreasing EVs costs but on the other hand building such a system requires significant financial resources and it is dependent on electromagnetic fields to generate power, which may affect other near electronic components.[14]

I.8 Crash tests on electrical vehicles

The automotive market is mostly familiar with electric vehicles and their features are widely known but to guaranty their safety for usage they must submit the same tests as traditional vehicles. However, doing a crash test on an electric vehicle still represents a challenge to OEMs and also to test developers as EVs represent another additional danger when crashing due to an electric shock or battery spillage.

According to the EU laws (R94, R95, monetary unit NCAP) and American regulations (FMVSS 208, 214 and 301 new, 305), some voltage measurements when crashing ought to be taken and a few calculations have to be compelled to be created. In IDIADA, the internal safety protocol takes many restrictive precautions adopted for all cases. In addition, a show is mounted in a vehicle to understand, while not touching the vehicle, if the voltage is above allowed (60V). Moreover, an additional switch has to be put in in the vehicle and a temperature recording system has to be put in at the batteries to show if any fire risk exists. Finally, specific actions for emergency cases also are clear in case they are required.[6]

I.9 Conclusion

To conclude, according to the market many users are still hesitant about the transition into electrical vehicles despite the many advancements they showed as they still lack in other areas in comparison with conventional vehicles such as efficiency and flexibility and due to their high cost. Nowadays, there are four main categories of electric vehicles (BEV, HEV, PHEV, FCEV), they all offer features that suit certain demands and have areas to develop. Nevertheless, in general, current research in the field focuses on improving the vehicle organs without being exclusively belonging to a certain type; such as batteries, charging methods and engine technologies. In addition, developers also look at other ways to improve the safety of vehicles by conducting specialized crash tests also improving charging stations and road infrastructures to facilitate the transition to EVs.

Chapter II. Powertrain design specifications

II.1 Introduction

The dissertation's main objective is to design a two-speed transmission for an electric vehicle. In this chapter, we will a pre-dimensioning of the power strain of the vehicle through strength and other requirements analysis for the electrical and mechanical sub-systems. It will mostly rely on calculation and the acquired data in several resources such as existing components datasheets and commercial catalogs.

II.2 Powertrain of a Battery-Electric Vehicle (BEV)

In a BEV powertrain, the energy is stored in the battery, as chemical energy. The battery is connected to the electrical machine by a DC/AC power converter in addition to a control system to be able to control the frequency and the magnitude of the voltage applied to the electric machine depending on the driver's request. This last component is mostly a three-phase AC type, but also other types such as a hub wheel motor are used in some applications.

In-car designs, the dimensions of the electrical machine must be kept smaller to achieve good performance through a lightweight vehicle. This small design offers a maximum speed of 12000 and 16000 rpm, but on the other side, the speed vehicle of a typical BEV is [0 – 130] km/h which means the wheels spin at 1200 rpm. For this reason, a gear reduction ratio is needed between the electric machine and the driving wheel pair. The differential is used to allow traction of the wheels at slightly different speeds while turning the vehicle, it also serves as the last reduction ratio. Below is a schematic sketch of a typical BEV powertrain (Figure II.2—1), while this dissertation will focus on the mechanical sub-system.

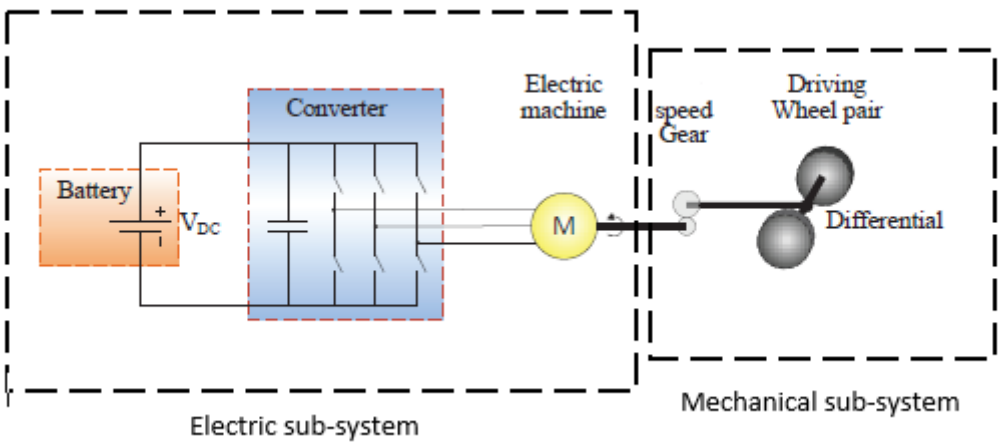

Figure II.2—1. Schematic sketch of a typical BEV powertrain

II.3 Road and driving patterns specifications

The knowledge of the purpose and utilization is essential in the design of any product as it is for the design of a car. Vehicles while driving can be affected by many factors such as the road and journey type, weather conditions and also the driver's behavior thus, all of these factors, need specific vehicle requirements. In the following, speed, acceleration and road specifications are identified to establish a BEV powertrain design criteria.

II.3.1 Speed levels

The study of the driving duration on specific speed levels according to different road types allows finding the suitable speed that can be reached with a certain vehicle. The table below (Table II.3—1), shows the time spend on three different roads (urban, rural and highway) with speed levels from 60 – 90 km/h and above 90 km/h.

Table II.3—1. Driving cycles in different road types at speed levels

	60 - 90 km/h	**> 90 km/h**
Urban	< 20 % of the time	≈ 0 % of the time
Rural	> 20 % of the time	< 20 % of the time
Highway	-	> 20 % of the time

In this work, we will focus on the rural road specifications and we will rely on the Artemis[11] rural cycle data to determine the vehicle performance at speeds of 50 – 100 km/h. In addition, we compare the data of the three road types using the same test cycle as the vehicle designed for rural conditions should be also able to perform in urban roads and highways.

Table II.3—2. Drive range and speed according to road types

Artemis test cycle	**Cycle duration (s)**	**Driven distance (m)**	**Max. speed (km/h)**	**Avg. speed (km/h)**	**Avg. running speed (km/h)**	**Std. speed (km/h)**
Rural	1082	17272	112	57	59	25
Urban	993	4870	58	18	25	17
Highway	1068	28736	132	97	98	35

Table II.3—3. Timeshare in a driving range according to road type

Artemis test cycle	**Timeshare (%)**			
	Standing	< 60 km/h	60 -90 km/h	> 90 km/h
Rural	4	47	42	7
Urban	33	66	0	0
Highway	2	18	10	70

[11] Grunditz, E.A., Design and Assessment of Battery Electric Vehicle Powertrain, with Respect to Performance, Energy Consumption and Electric Motor Thermal Capability, in Department of Energy and Environment2016, Chalmers University of technology: Göteborg, Sweden. p. 229

As shown in the tables above (Table II.3—2, Table II.3—3), the maximum performances of a vehicle are needed for a highway road type, a vehicle on a highway should be able to run 28736 and maintain a speed above 90 km/h for 70% of the time. In a rural road type also the driven distance is large (17272m) and the vehicle runs at below 60km/h 47% of the time and between 60-90 km/h for 42% of the time. On the other hand, the performance in urban road type is lower than the other types, thus designing a car according to performances of a rural road type with a max speed of 112 km/h will allow the car to function properly in the city as well as having good performance in a highway.

II.3.2 Acceleration levels

The vehicle acceleration provides the peak force and power for the wheels so it's necessary to study the acceleration levels of a car in different road types.

Table II.3—4. Acceleration levels in different road types

Artemis test cycle	**Max. pos. acc. (m/s²)**	**Max. neg. acc. (m/s²)**	**Avg. pos. acc. (m/s²)**	**Avg. neg. acc. (m/s²)**	**Std. pos. acc. (m/s²)**	**Std. neg. acc. (m/s²)**
Rural	2.4	-4.1	0.5	-0.5	0.4	0.6
Urban	2.4	-2.8	0.6	-0.7	0.5	0.6
Highway	1.7	-2.9	0.3	-0.4	0.3	0.5

Table II.3—5. Time share for different acceleration levels

Artemis test cycle	**Timeshare (%)**					
	Pos. acc.	Neg. acc.	a < 1 m/s²	1 < a < 2 m/s²	2 < a < 3 m/s²	a > 3 m/s²
Rural	41	40	96	3	0	0
Urban	38	35	92	8	0	0
Highway	48	37	97	3	0	0

The table (Table II.3—4) shows the acceleration levels of a vehicle in three different road types. The maximum positive acceleration reached in the rural and urban roads and the maximum negative acceleration occur in the rural road.

Then, the table (Table II.3—5) demonstrates the time spend in different acceleration levels according to road type. The values of positive and negative accelerations are almost similar ranging between [35-48] %, where a vehicle on a rural road spends 40% of acceleration time in a negative phase whereas a car on a highway spends 48% in a positive acceleration.

A vehicle's acceleration levels in three different road types spend between [92 – 97] % acceleration at below 1 m/s².

The duration of acceleration is [12 – 13] s for 80% of the acceleration in different road types (urban, rural and highway) and 50% of the acceleration is [5 – 6] s long or shorter according to[23].

II.3.3 Road grade and driven distances

Road grade levels are also important to determine a vehicle's load levels as speed and acceleration levels. According to[23], a grade level of 5% is recommended for speed up to 90 km/h and a 6% grade in mountain roads. For speed above 90 km/h, the maximum recommended grade level is 4%.

Furthermore, a driving range of a vehicle is determined by studying the usual distances traveled by drivers. The values depend on a lot of factors, such as the driver's need, the country, the city, and the lifestyle of the car owner for that we will rely on the current typical drive range of a BEV (291 km).

II.4 Vehicle performances

The drivetrain's components design of a vehicle depends on the performance requirements which are usually; speed, acceleration and drive range for BEVs. To be able to determine these requirements we analyzed the data of 5 top-selling BEVs in 2020 according to [13], the data that is relevant to our work includes curb weight, height and width to determine the car's area, drag coefficient Cd, top speed and acceleration time as well as driving range and energy consumption. The results are summarized in the tables below according to dimensions data (Table II.4—1), performances data (Table II.4—2), engine and battery data (Table II.4—3).

Table II.4—1. Vehicles dimensions data

Vehicle model	Weight (kg)	Height (mm)	Width (mm)	Estimated frontal area (m^2)	Wheel radius (mm)
Tesla model 3[35]	1843.8	1443	2088	2.22	508
Wuling HongGuang Mini EV[11]	665	1621	1493	2.4	-
Renault Zoe[30]	1563	1562	1730	2.7	457.2
Tesla model Y[36]	2003	1624	1921	3.1	482.6
Hyundai Kona EV	1535	1570	1800	2.8	406.4

Table II.4—2. Vehicles performances data

Vehicle model	Drag coef. Cd	Max. speed (km/h)	Acceleration time (s) (0 – 100 km/h)	Drive range (km)	Energy consumption (Wh/km)
Tesla model 3[35]	0.23	260.7	3.3	491	130
Wuling HongGuang Mini EV[11]	-	100	23.8	170	81
Renault Zoe[30]	0.29	135	11.4	245	178
Tesla model Y[36]	0.23	250	3.7	488	138
Hyundai Kona EV[15]	0.29	155	9.7	402.3	161.6

Table II.4—3. Vehicles engine and battery data

Vehicle model	Engine				Battery		
	Type	power (kW)	torque (Nm)	Type	Capacity (kWh)	Max charging power AC (kW)	Max charging power DC (kW)
Tesla model 3[35]	PMSM	336	636	lithium iron phosphate (LFP)	75	11.5	250
Wuling HongGuang Mini EV[11]	PMSM	20	85	Lithium - ion polymer (LMP)	13.8	-	-
Renault Zoe[30]	PMSM	101	245	Lithium - ion polymer (LMP)	52	22	50
Tesla model Y[36]	PMSM	336	639	lithium iron phosphate (LFP)	75	11.5	250
Hyundai Kona EV[15]	PMSM	100	395	Lithium - ion polymer (LMP)	39.2	11	50

From the data gathered in the tables above, we aim to build a theoretical model similar to the real car models demonstrated above to facilitate dynamic calculation and design drive trains for theoretical analysis purposes.

For the mentioned reason we calculated the mean values of each characteristic and for the type of motor and battery, all the models use a permanent magnet synchronous motor and a lithium-ion battery. Our theoretical model data are shown below (Table II.4—4).

Table II.4—4. Theoretical model A estimated data

Model A data	Estimated mean values				
Dimensions	Weight (kg)	Height (mm)	Width (mm)	Estimated frontal area (m^2)	Wheel radius (mm)
	1521,96	1564	1806,4	2,644	463,55
Performances	Drag coef. Cd	Max. speed (km/h)	Acceleration time (s) (0 – 100 km/h)	Drive range (km)	Energy consumption (Wh/km)
	0,26	160	10,38	359,26	137,72
Engine	Type	Power (kW)	Torque (Nm)		

	PMSM	178,6	400		
Battery	Type	Capacity (kWh)	Max charging power AC (kW)	Max charging power DC (kW)	
	Lithium – ion	51	14	150	

The vehicle dynamics will be calculated using the values shown above as a reference, which are estimated mean values of existing vehicle data.

Vehicle data may differ through calculation.

II.5 Calculation of vehicle dynamics

The vehicle dynamics describe the movement of the vehicle on road under the influence of the forces between the tires and the road surface, also including the aerodynamics and gravity effect. The study of the vehicle's dynamics allows us to know what loads and load levels the powertrain needs to support during driving as well as the powertrain's impact on the vehicle's performance.[23]

In this dynamic study, we assume that the vehicle is rigid and modeled as a lumped mass at the vehicle center of gravity, and it moves in the longitudinal forward direction.[19] So according to Newton's second law of mechanics, the movement of the vehicle is the sum of all forces acting on the vehicle in each instant of time.

$$ma = m\frac{d}{dt}v(t) = F_{tr}(t) - F_r(t) \qquad (II.5-1)$$

- m (kg): the mass accelerating;
- a (m/s²) and d/dt v(t) (m/s²) : the vehicle's acceleration;
- F_{tr} (Nm) is the sum of all the tractive forces increasing the vehicles speed;
- F_r (Nm): the sum of all the forces decreasing the vehicles speed;

The tractive forces are the forces exerted from the powertrain to the contact area between the wheels and the road, gravity also can serve as a tractive force during downhill driving.

The resistive forces include aerodynamic drag, rolling resistance, braking and gravity in case of driving uphill.

II.5.1 Aerodynamic drag

The aerodynamic drag in a simple explanation is the resistive airflow the vehicle experience during driving. Due to the complexity of the phenomena and that's of the shape of vehicles, we often rely on an empirical model using the following expression:

$$F_a = \frac{1}{2}\rho_a C_d A_f (v_{car} - v_{wind})^2 \qquad (II.5.1-1)$$

Where ρa (kg/m^3) is the air density, Cd is the aerodynamic drag coefficient, Af (m²) is the effective cross-sectional area of the vehicle, v_{car} (m/s) is the vehicle speed and v_{wind} (m/s) is the component of wind speed moving in the direction of the vehicle.[19]

The air density varies according to temperature, humidity and pressure. In a standardized condition ρa = 1.225 (kg/m^3) is used for T =15°C and P = 1013.25 Pa.

Cd is dimensionless, the typical range is 0.25 - 0.35. It is often the parameter focused on lowering the aerodynamic drag without compromising the vehicle shape.

Af is the cross-sectional area. Often not communicated in vehicle characteristics but can be estimated by the product of height and width of the vehicle.

If all the previous parameters are fixed, we can notice that the aerodynamic drag increase with wind speed depending on the vehicle's speed.

II.5.2 Rolling resistance

The rolling resistance is the friction force caused by wheels rolling on the road, this force works against the motion. Therefore, the rolling resistance is expressed through the equation below:

$$F_r = C_r m\, g \cos(\alpha) \qquad (II.5.2-1)$$

- m (kg): vehicle mass;
- g (m/s²) gravity constant;
- A (rad) road inclination angle;
- Cr: rolling resistance coefficient;[19]

The cos (α) is often neglected even with large road grades because it only influences with an error of less than 0.5% of the rolling resistance force.

The rolling resistance coefficient depends on various factors such as tire material and design, working pressure and temperature. However, during studies on vehicle performances, Cr is assumed to be constant for passenger car tires working on dry concrete or asphalt, with typical values of 0.011 to 0.015.[23]

II.5.3 Grading force

The grading force is referred to as the effect of gravity on a vehicle's dynamics in the case of a road grade (inclination).

$$F_g = m\, g \sin(\alpha)$$

Where α is the angle between the level road and the horizontal plane, expressed as the following:

$$\alpha = \arctan\left(\frac{rise}{run}\right) = \arctan\left(\frac{\%grade}{100}\right) \qquad (II.5.3-1)$$

Where "rise'' is the vehicle rise and "run'' is the horizontal distance run by the vehicle, the road grade is expressed in percentage.

The vehicle will be traveling uphill and downhill, so the grading force can be either a resistive or contributive force. However, typical values of vehicles acceleration result in the same wheel force as road grade levels.[23]

II.5.4 Wheel force

The wheel force is the force that comes to wheels to accelerate the vehicle, it is expressed as the sum of all forces acting on the vehicle.

$$F_{wheel}(t) = F_{acc}(t) + F_a(t) + F_r(t) + F_g(t) \qquad (II.5.4-1)$$

Where F_{acc} is the force required to accelerate the vehicle, it is expressed as the product of the mass and acceleration (F_{acc} = m a).

The maximum tractive force on the driving wheels can be limited by either the powertrain's maximum force capability or the maximum adhesive capability between tire and ground that is possible to be applied on the wheel without losing the grip to the road[19]. The latter is limited by the current normal force on the driving wheels, F_N and the coefficient of friction between the tire and the road μ, as follows:

$$F_{wheel,max} = \mu F_N \qquad (II.5.4-2)$$

Taking into account, the friction coefficient depends nonlinearly on the deformation of the tire during acceleration and deceleration.[23]

II.5.5 Wheel power and energy

The tractive power coming from the powertrain to maintain a certain speed level in each instant of time is P_{wheel}, the integration of this power gives us the total energy consumed at the wheels.

$$P_{wheel}(t) = F_{wheel}(t) v_{car}(t) \qquad (II.5.5-1)$$

$$E_{wheel} = \int P_{wheel}(t)dt \qquad (II.5.5-1)$$

The total energy over time is reduced during regenerative braking while F_{wheel} is negative.

II.6 Drivetrain electric components specifications

As mentioned above a drivetrain in a BEV is composed of two sub-systems (electrical and mechanical), that work together to power the car.

II.6.1 Lithium-ion battery

Lithium-ion (Li-ion) batteries have become the preferred onboard power supply for pure electric vehicles (EVs) due to their high power, high energy density, and long cycle life. However, they are also considered to be sensitive to changes in factors such as ambient temperature, vibration, and pressure.

In order to effectively use space in an EV, it is necessary to place the battery in an unused space. From the perspective of vehicle dynamics, the battery pack should be placed in a way that keeps the center of gravity of the vehicle low and minimizes the mechanical stress and fatigue on the mounting frame. From the perspective of heat dissipation, the battery pack should be placed in a place with proper air circulation to maximize heat dissipation. To solve electrical safety issues, the battery pack should be regarded as the main component of the electric drive system, similar to the engine of an internal combustion engine car. Therefore, it should be located outside the passenger compartment so that high-voltage components do not pose any threat to passenger safety.

In addition, the battery pack should be separated from the front or rear end of the vehicle structure to protect the battery from potential shocks. The ideal space for this type of storage is located in the center of the vehicle under the floor of the vehicle, but due to the limited ground clearance of passenger cars, any such support structure must be carefully designed to use the available space to achieve maximum efficiency.[7]

For the design analysis, in this thesis, we refer to the US Patent 8561743 that discloses a method of placing as many batteries as possible in the center of the EV without affecting vehicle dynamics or safety. The patent discloses a battery assembly design, in which one set of batteries S1 is located under the front seats, another set of S2 is located under the floor between the front and rear seats, and the last set of batteries S3 is located under the rear seats.[28]

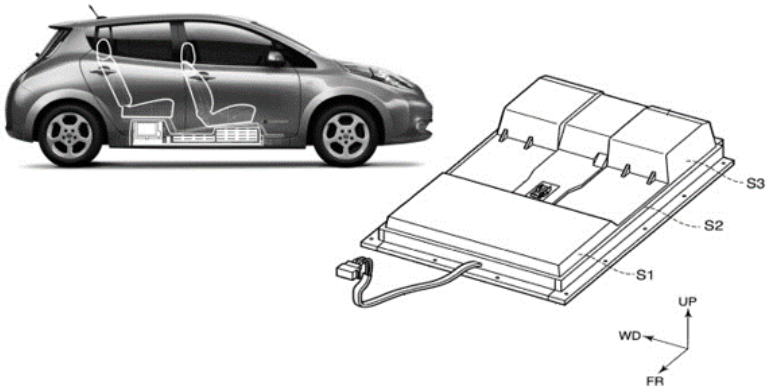

Figure II.6—1. Battery model pack in Nissan Leaf[28]

The battery model pack dimensions as shown in (Appendix A1) are 1547 x 1188 x 264 mm and a weight of 300 kg for a pack of 40 KWh. However, to stay up to the characteristics chosen in (Table II.4—4), to get a 51 KWh of capacity we assume the dimensions will increase by 5 mm in height in order to add more cells and generate more capacity.

II.6.2 DC – AC power converter

We use a DC – AC power converter (or referred to as an inverter) to convert the DC current output from the battery into an AC current as an input for a PMSM motor, which is asynchronous AC machine.

Mostly in commercial models, the motors come as an integrated model with their inverter, for that reason the dimensional specification of the inverter will be integrated with those of the motor and also depend on its specifications choice.

II.6.3 PMSM motor dimensioning

Motors have high efficiency in all speed ranges, especially high-speed motors, which have higher power density to help reduce weight and cost. Among the three main motors used in the automotive industry, permanent magnet synchronous motors (PMSM) seem to be the first choice for the A and B segments. It has high efficiency in the low and medium speed range, among which the vehicle will run most of the time.[31]

However, since the main object of this work is the design of the drivetrain, the motor will be selected from existing commercial models to provide the necessary data to model the mechanical sub-system. According to the first assumptions in (Table II.4—4), we have a permanent magnet synchronous motor with a peak power of 178.6 Kw and a torque of 400 Nm, relying on that we selected a PMSM motor from the Cascadia Motion catalog[4]. The recommended model for a passenger car is the iM-225-DX-D integrated module which is built using a CM200 inverter and HVH250 motor core to achieve a peak torque of 500Nm. The motor's features are summarized in the table (Table II.6—1) below.

Table II.6—1. PMSM motor features

Electrical features		Dimensional features	
Peak torque	500 Nm	**Weight**	64 kg
Peak power	225kW	**Total height**	405 mm
Continuous torque	230 Nm	**Axial length**	300 mm
Continuous power	110 – 135 kW	**Width**	170 mm
Maximum speed	12000 rpm		
Combined efficiency	95% peak (at 200 Nm, 5500 rpm)		
Max. Volt. With the inverter	480 V (DC)		

The connections used for assembly are one of the bolt patterns; 6 – bolt Cascadia pattern, 16 – bolt Remy pattern or 4 – bolt Porsche G50 pattern.

For the speed behavior according to power and torque variation, the power and torque curves are referred to in the (Appendix A2).

II.6.4 Vehicle performance with a PMSM motor

In order to check if, with the chosen PMSM motor, the vehicle model can attain the desired speed we first obtained the transmission ratio from the equation below.[31]

$$i_g = \frac{\pi N_{max} r_t}{30 v_{max}} \qquad II.6.4-1$$

Where the motor maximal speed is N_{max} = 12000 rpm, the wheel radius is r_t = 463.55 mm = 0.46 m and the maximum desired speed of the vehicle is v_{max} = 160km/h = 44.45 m/s. from the above equation we obtained a transmission ration of 13.

However, to reach the maximum speed, the vehicle must overcome the rolling resistance, the aerodynamic drag and since we consider a null road grade we neglect the grade force. The force transmitted to the wheels is F_{wheel}.

$$F_{wheel}(t) = F_{acc}(t) + F_a(t) + F_r(t) + F_g(t)$$

$$\begin{cases} F_r = C_r m\, g \cos(\alpha) = -179.17\ N \\ F_g = m\, g\, sin(\alpha) = 0 \\ F_a = \frac{1}{2}\rho_a C_d A_f (v_{car} - v_{wind})^2 = -499.71 N \\ F_{acc} = ma = 6513.99\ N \end{cases}$$

Taking into account the following values.

Table II.6—2. Calculation considered values

Vehicle mass m	1521.96 kg	**Vehicle acceleration a**	4.28 m/s²
Gravitational force g	9.81 m/s²	**Frontal area Af**	2.644 m²
Aero. Drag Cd	0.26	**Rolling res. Coef Cr**	0.012
Air density ρa	1.225 kg/m³	**Wind speed v_{wind}**	10 m/s

So we obtain F_{wheel} = 5835.11 N and the max limit is $F_{wheel,max} = \mu F_N = 4084.58\ N$, by considering the car runs on the dry road (μ = 0.7).

The wheel force value allows us to calculate the power and torque transmitted to the wheels and verify if they align with the characteristics of the chosen engine.

$$\begin{cases} P_{wheel} = F_{wheel,max} \times v_{car} = 181.6\ kW \\ T_{wheel} = \frac{F_{wheel,max} \times r_t}{i_g} = 145.65\ Nm \end{cases} \qquad II.6.4-2$$

From the equations above and by comparing to the engine characteristics in (Table II.6—1) we conclude that the max torque and max power transmitted to the wheels can be provided by the engine continuous and peak values.

II.7 Vehicle's transmission

The transmission is affected by the vehicle, electric motor and road conditions. When designing a transmission, technical and economic factors are very important. Over the years, extensive research and development have been carried out in transmission design to reduce losses and effectively transfer power from the engine to the wheels. Although sophisticated automotive transmissions (up to 7 speeds) have been developed for internal combustion engine vehicles, in the electric vehicle industry, single-speed transmissions are standard, reducing complexity and providing opportunities to explore other decisive factors such as material selection and gears design.[31]

However, single-speed ratio gearboxes have some limitations because they cannot always ensure that the electric traction machine (EM) and inverter operate in the best efficiency zone. Multi-speed gearboxes may be better suited to meet the load, traction, off-road, and top speed requirements of these vehicles. Nonetheless, researchers have shown that multi-speed gearboxes have the potential to reduce overall vehicle energy consumption, which can translate into a longer driving range, improved dynamic performance and gradeability for smaller battery packs. However, recent studies have shown that multiple gear ratio systems can reduce the energy consumption of various drive cycles by 2% to 20%.[16]

At the start of the design phase, the selection of an appropriate transmission arrangement is of extreme importance, since it will affect the subsequent decisions. Parallel gear sets are the standard choice in electric vehicle transmissions. They have greater mechanical efficiency and are more compact. One of the decisive factors is the number of stages, which is dependent on the overall ratio, which in turn is related to vehicle requirements and motor performance, as previously shown.

II.7.1 Geometry and overall transmission ratio

This work aims to design a 2-speed transmission. In most vehicles, the transmission is produced by a single-stage parallel gear ratio which is limited to 10:1, as with bigger values the dimensions and cost of production rise. For that reason, multi-stage gear trains will allow a multi-speed transmission and a more practical design.

With the input speed of 12000 rpm of the PMSM motor, the overall transmission ratio to achieve a max speed of 160 km/h is 13. In addition, to achieve a max speed of 138.7 km/h, we have a ratio of 15. To be able to design a gear train with a double transmission ratio, we rely on a planetary gear set on the second stage of transmission and we leave the first gear set and the differential gear the same for both ratios (Figure II.7—1).

In the following figure, the geometry is designed according to the design shown in [25]. The letters mean, D the differential gear unit, R the planetary gear set, M the motor shaft gear, in addition to the stage brakes that will allow the transition between transmission ratios.

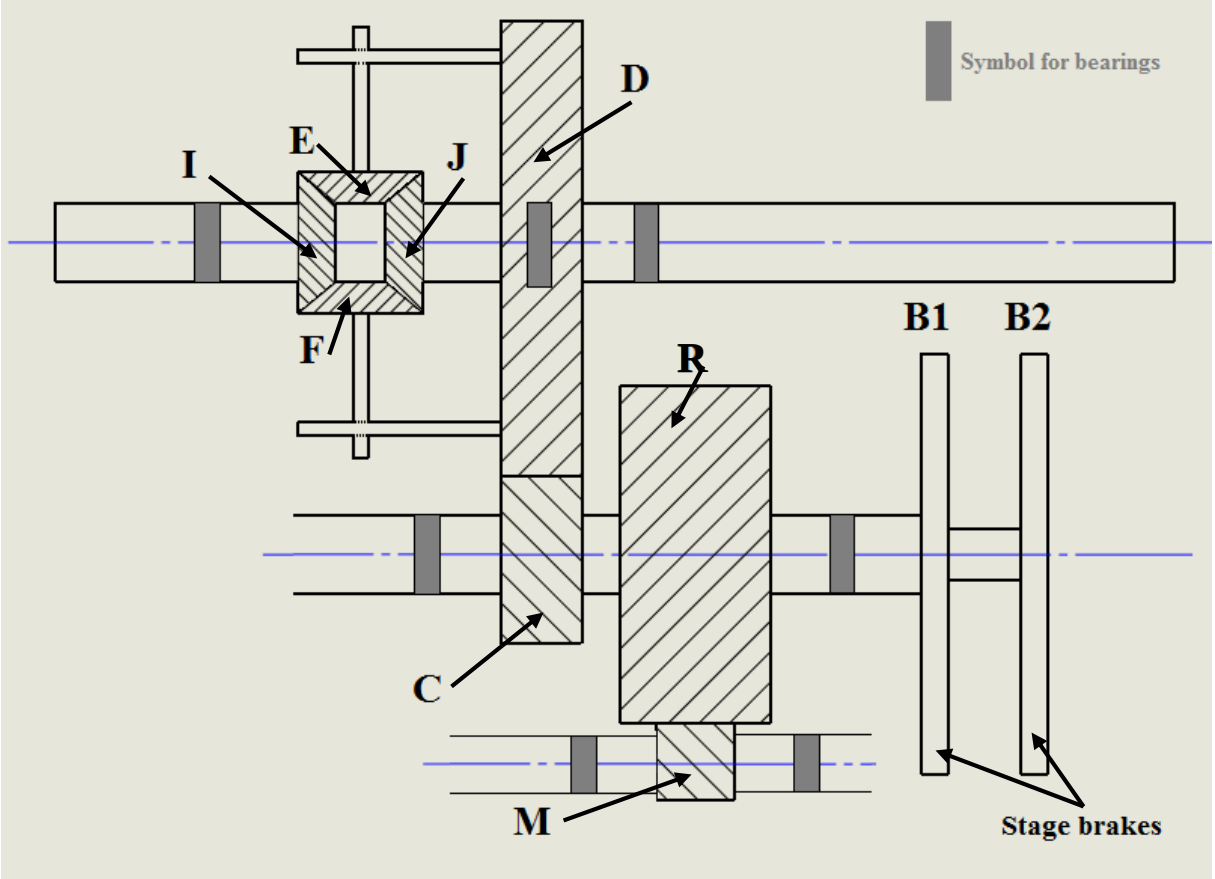

Figure II.7—1. The geometry of the transmission

The transmission ratio I (M – R) between the motor shaft and the planetary gear set is constant with the value of 2.6, also the differential ratio is constant to 4. Between the planetary gear set and the differential (C - D) we will have two different ratios to get two different vehicle speeds.

The gear design will rely on the previously mentioned ratios.

II.8 Gear sets design

The first step to designing the gearbox is to determine the characteristics of the gears it contains. Since the gearbox in our work will be designed to offer two-speed options, there will be two mechanisms the first one the planetary gear set R will be considered as two separate gears on a common shaft where the planetary gear set R is the input and the carrier C is the output, for that we will consider a ratio between M and R and another ratio between C and D.

Formulas and equations are taken from [12] and in the following calculation we consider this:

- The gears are spur gears for a simple and efficient application;
- The security coefficient s = 2 as we design for an automobile application;
- Teeth thickness factor K = 10;

- The material is steel alloy 20CrMo5 which is used typically for high-stress components such as gears and shaft, the yield is Re = 850 N/mm²;

II.8.1 Gear train M - R

The number of teeth and the speed of rotation are determined by the transmission ratio.

$$i_{M-R} = \frac{z_M}{z_R} = \frac{1}{2.6}; we\ take\ \boldsymbol{z_M = 24} \rightarrow \boldsymbol{z_R = 63} \qquad \text{II. 8.1} - 1$$

$$i_{M-R} = \frac{N_R}{N_M}\ et\ N_M = 12000\ rpm \rightarrow N_R = \frac{1}{2.6} \times 12000 \rightarrow \boldsymbol{N_R = 4615.38\ rpm} \qquad \text{II. 8.1} - 2$$

The module is determined by the following formula:

$$m_{M-H} \geq 2.22 \sqrt[3]{\frac{M_{tI}}{z_m K R_p}} \qquad \text{II. 8.1} - 3$$

With:

- Rp=R /s = 850/2 = 425 N/mm²;
- M_{tI} is the motor peak torque of 500 N.m multiplied by the gear's efficiency 0.97 and the bearings efficiency 0.98². Therefore for M_{tI} =465.79 N.m we get $m_{M\text{-}H} \geq 3.77$so we choose $m_{M\text{-}H} = 4$.

The specifications of the gear train M – H is summarized in the below table:

Table II.8—1. Gear train (M – P) specifications

Pressure angle α	Standard value	20
module	From II. 8.1 – 3	4
Number of teeth	From II. 8.1 – 1	$z_m = 24$; $z_p = 63$
pitch	$p = m.\pi$	12.57
Addendum h_a	$h_a = m$	4
Dedendum h_f	$h_f = 1{,}25.m$	5
Tooth depth h	$h = 2{,}25.m$	9
Pitch diameter d(M)	$d(M) = m.z_m$	96
Tip diameter d_a(M)	$d_a(M) = d(M) + 2m$	104
Root diameter d_f(M)	$d_f(M) = d(M) - 2{,}5m$	86
Pitch diameter d(P)	$d(P) = m.z_p$	252
Tip diameter d_a(P)	$d_a(P) = d(P) + 2m$	260
Root diameter d_f(P)	$d_f(P) = d(P) - 2{,}5m$	242
Tooth thickness b	$b = k.m$	40
Center distance a	$a = m(z_m + z_p)/2$	174

The load calculation of gears will allow us to rate the life and to select bearing later on, also to know the face width of the gear for design purposes.

The shaft rotating the gear M is the motor's output. Taking that into account we calculate the tangential load $F_T = M_{tI}/r = 465.79/0.048 = 9703.96$ N. The radial load is $F_R = F_T.\tan\alpha = 3531.95$ N and the contact load of the gear P on the gear M is $F_{P/M} = F_T/\cos\alpha = 10326.74$ N.

The face width of the gear will be calculated by the Lewis formula $\sigma = F_T.p/(F.Y)$. Where σ is the allowable stress on the gear, F_T is the tangential load, p is the pitch, F is the face width and Y is the Lewis Form Factor ($0.20 < Y < 0.55$, depending on number of teeth and type of gear – involute or stub).

Table II.8—2. Lewis form factors (pressure angle 20°)[12]

Table 1 Lewis form factors for various numbers of teeth (pressure angle 20°).

Number of Teetch	Lewis form Factor	Number of Teeth	Lewis form factor
10	0.176	34	0.325
11	0.192	36	0.329
12	0.210	38	0.332
13	0.223	40	0.336
14	0.236	45	0.340
15	0.245	50	0.346
16	0.256	55	0.352
17	0.264	60	0.355
18	0.270	65	0.358
19	0.277	70	0.360
20	0.283	75	0.361
22	0.292	80	0.363
24	0.302	90	0.366
26	0.308	100	0.368
28	0.314	150	0.375
30	0.318	200	0.378
32	0.322	300	0.382

Since the allowable stress is unknown we assume the face width is between 9 to 12 times of module according to [10], so we chose $F_{M-P} = 10.m = 40$ mm.

II.8.2 Gear train C – D

The number of teeth and the speed of rotation are determined by the transmission ratio.

$$i_{C-D} = \frac{z_C}{z_D} = \frac{1}{1.25}; we\ take\ \boldsymbol{z_C = 56} \rightarrow \boldsymbol{z_D = 70} \qquad \text{II.8.2} - 1$$

$$i_{C-D} = \frac{N_D}{N_C}\ et\ N_C = N_R = 4615.38\ rpm \rightarrow \boldsymbol{N_D = 3692.3\ rpm} \qquad \text{II.8.2} - 2$$

The module is determined by the following formula:

$$m_{C-D} \geq 2.22\sqrt[3]{\frac{M_{tII}}{z_C K R_p}} \qquad \text{II.8.2} - 3$$

With:

- Rp = R /s = 850/2 = 425 N/mm²;

[12] https://www.engineersedge.com/gears/lewis-factor.htm

- $M_{tII} = M_{tI} \times i_{C-D} \times \eta_{gears}^2 \times \eta_{bearings}^2 = 372.64 \times \frac{1}{1.25} \times 0.97^2 \times 0.98^2 = 336.73\ N.m.$

  Where η_{gears} is the efficiency of the gears and $\eta_{bearings}$ is the efficiency of the bearings.

From the previous calculation, we get the transmission ratio of $m_{C-D} \geq 2.49$ so we take $m_{C-D} = 3$.

The specifications of the gear train C – D are summarized in the below table:

Table II.8—3. Gear train (C-D) specifications

Pressure angle α	Standard value	20
Module	From II. 8.2 − 3	3
Number of teeth	From II. 8.2 − 1	$z_C = 56$; $z_D = 70$
Pitch	$p = m.\pi$	9.42
Addendum h_a	$h_a = m$	3
Dedendum h_f	$h_f = 1{,}25.m$	3.75
Tooth depth h	$h = 2{,}25.m$	6.75
Pitch diameter d(C)	$d(C) = m.z_C$	168
Tip diameter d_a(C)	$d_a(C) = d(C) + 2m$	174
Root diameter d_f(C)	$d_f(C) = d(C) - 2{,}5m$	160.5
Pitch diameter d(D)	$d(D) = m.z_D$	210
Tip diameter d_a(D)	$d_a(D) = d(D) + 2m$	216
Root diameter d_f(D)	$d_f(D) = d(D) - 2{,}5m$	202.5
Tooth thickness b	$b = k.m$	30
Center distance a	$a = m(z_C + z_D)/2$	189

The load calculation of gears will allow us to rate the life and to select bearing later on, also to know the face width of the gear for design purposes.

The gear C is the drive gear since it translates the torque to the gear D. Taking that into account we calculate the tangential load $F_T = M_{tII}/r = 336.73/0.084 = 4008.69$ N. The radial load is $F_R = F_T.\tan\alpha = 1459.04$ N and the contact load of the gear D on the gear C is $F_{P/M} = F_T/\cos\alpha = 4265.96$ N.

The face width of the gear will be calculated by Lewis formula $\sigma = F_T.p/(F.Y)$. Where σ is the allowable stress on the gear, F_T is the tangential load, p is the pitch, F is the face width and Y is the Lewis Form Factor ($0.20 < Y < 0.55$, depending on the number of teeth and type of gear – involute or stub).

Since the allowable stress is unknown we assume the face width is between 9 to 12 times of module according to [10], so we chose $F_{C-D} = 10.m = 30$ mm.

II.8.3 Differential gears

The overall transmission ratio for the differential is 4, and the specifications of the sun gear are previously calculated, and the gear symbols are according to (Figure II.7—1) therefore we get the following.

The number of teeth and the speed of rotation are determined by the differential transmission ratio.

$$i_D = i_{D-E} \times i_{E-J} \rightarrow we\ assume\ i_{D-E} = i_{E-J} = 1/2$$

We also assume the car is running in a straight road condition, so $N_J = N_I$ = 923.08 rpm which is obtained from the overall transmission ratio of 13 and the input speed of 12000 rpm.

Since we are designing a standard differential, we also have $z_E = z_F$ and $z_I = z_J$. From that we calculate the following:

$$i_{D-E} = \frac{z_E}{z_D} = \frac{1}{2.25}; we\ have\ \boldsymbol{z_D = 70} \rightarrow \boldsymbol{z_E = z_F = 30} \qquad \text{II.8.3} - 1$$

$$i_{J-E} = \frac{z_J}{z_E} = \frac{1}{1.78} \rightarrow \boldsymbol{z_J = z_I = 15} \qquad \text{II.8.3} - 2$$

In the case of a differential we assume, the module of the bevel gears is 3 and we calculate the torque transmitted by the gear E to be able to determine the distance from the center of the gear D to the axe of the gear. Therefore, we use the following equations:

$$m_{bevel\ gears} \geq 2.22 \sqrt[3]{\frac{M_{tIII}}{z_E K R_p}} \qquad \text{II.8.2} - 3$$

$$M_{tIII} = F_r \times r \qquad \text{II.8.2} - 4$$

Where Fr is the radial force applied to the gear D, Fr = 1459.04 N. and the other values are the same as previous. After calculation, we will obtain r ≤ 125.2 so we take r = 124 mm.

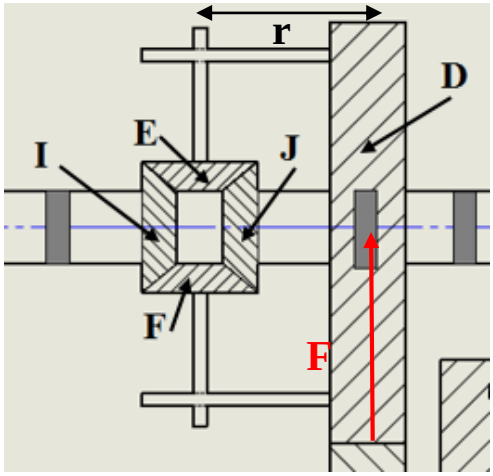

Figure II.8—1. Torque transmission in the differential

The bevel gears specifications are summarized in the table below according to[1]:

Table II.8—4. Bevel gears specifications

No. of teeth	Pitch dia. dp	A	B	Bore C (max)	Bore C (min)
15	45	66	40.3	12	22
30	90	56	55.3	16	36
No. of teeth	D	E	F	G	H
15	17	37.3	52.2	37.3	19.9
30	17	42.1	91.8	38	25

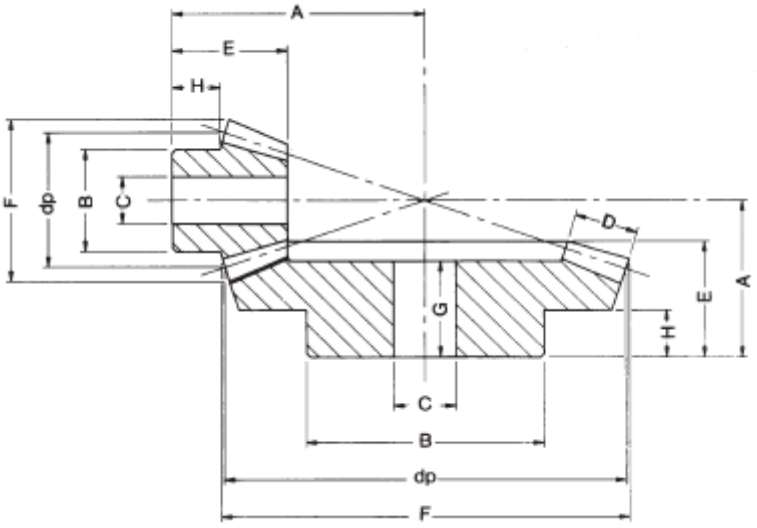

Figure II.8—2. Schematic representation of the bevel gears

The load calculation on the above bevel gears depends on the tangential force, which is calculated as follows:

$$P_t = \frac{M_{ta}}{r_m} = 7602.98\ N;$$

$$where\ M_{ta} = Fr\ \times \frac{d_D}{2} = 1459.04 \times 0.105 = \mathbf{153.2\ N.m}\ and\ r_m = \frac{B_I}{2} = \frac{40.3}{2} = \mathbf{20.15\ mm}$$

Fr is the force transmitted to the differential sun gear D, d_D is the diameter of the gear D and B_I is taken from the (Table II.8—4).

From that we calculate the radial and axial forces, taking into account the pressure angle $\alpha = 20°$ and $\theta = \tan^{-1}(dp_I/dp_E) = 26.6°$ where dp_I and dp_E are the pitch diameters of the gears I and E accordingly:

$$P_{rI} = P_{aE} = P_t \times tan\alpha \times cos\theta = \mathbf{2474.6\ N}$$

$$P_{aI} = P_{rE} = P_t \times tan\alpha \times sin\theta = \mathbf{1239.07\ N}$$

II.8.4 Planetary gears

The planetary gear set purpose is to provide transmission ratios for two different output speeds. The design is according to[25].

The planetary and sun gears will be dimensioned inside the previously designed gear R. the first speed will be given when the brake A is fixed and the 1st planetary gears are transmitting the motion to the 1st sun gear which comes as the carrier gear C output. The other way happens when brake B is fixed and the 2nd set of gears are transmitting the movement.

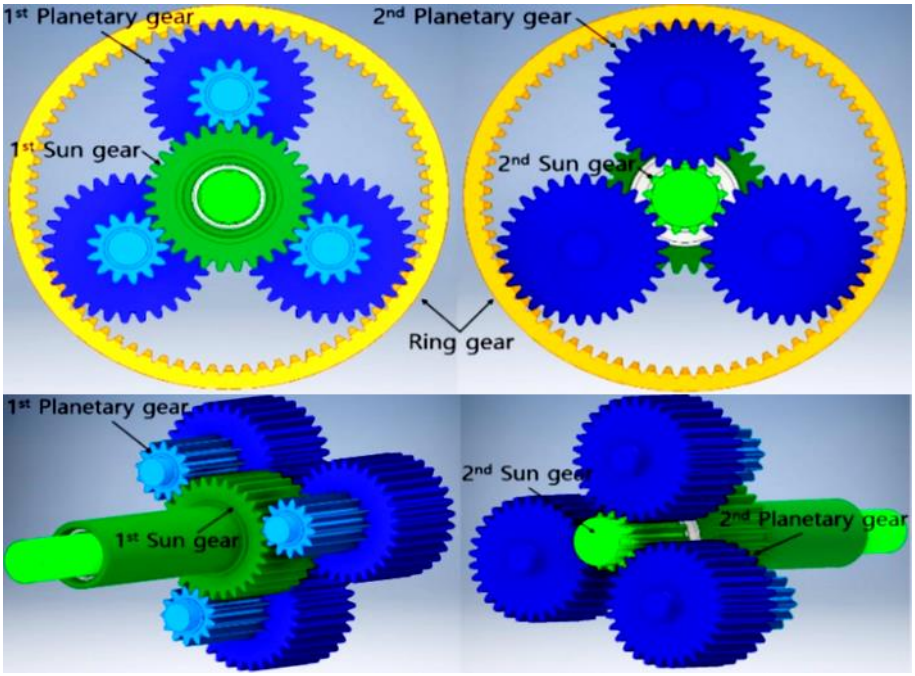

Figure II.8—3. Planetary gear set

We take the teeth number of the planetary gear 1 z_{P1} = 15 since it's the driving gear and we get the module m = 4 from this equations$m \geq 2.22\sqrt[3]{\frac{M_{tIII}}{z_{P1}KR_p}}$, from that we get r_{P1} = 25 mm. We also have the radius of the ring gear from previous dimensioning r_R = 126 mm and we take r_R = 100 for the internal radius. Finally $r_S = r_R - 2r_P = 100 - 2 \times 25 = 50$ mm. Knowing the module we get the teeth number of each gear as z_S = 25, z_P = 13, z_R = 50.

The gears specifications are in the table below according to [25]:

Table II.8—5. Planetary gear unit specifications

Ring gear		
Pressure angle α	Standard value	20
module	Calculated above	4
Number of teeth	Calculated above	50
pitch	p = m.π	12.57
Addendum h_a	h_a = m	4
Dedendum h_f	h_f = 1,25.m	5
Tooth depth h	h = 2,25.m	9
Pitch diameter d(R)	d (R) = m.z_R	200
Tip diameter d_a(R)	d_a (R) = d(R) + 2m	208
Root diameter d_f(R)	d_f (R) = d(R) – 2,5m	190
Tooth thickness b	b = k.m	40
Planetary gears and sun gear 1st set		
Pressure angle α	Standard value	20
module	Calculated above	4
Number of teeth	Calculated above	Z_{P1} = 13; z_{S1} = 25
pitch	p = m.π	12.75
Addendum h_a	h_a = m	4
Dedendum h_f	h_f = 1,25.m	5

Tooth depth h	h = 2,25.m	9
Pitch diameter d(P_1)	d (P_1) = m.z_{P1}	52
Tip diameter d_a(P_1)	d_a (P_1) = d(P_1) + 2m	60
Root diameter d_f(P_1)	d_f (P_1) = d(P_1) – 2,5m	42
Pitch diameter d(S_1)	d (S_1) = m.z_{S1}	100
Tip diameter d_a(S_1)	d_a (S_1) = d(S_1) + 2m	108
Root diameter d_f(S_1)	d_f (S_1) = d(S_1) – 2,5m	90
Tooth thickness b	b = k.m	40
Center distance a	a = m(z_{P1} + z_{S1})/2	76
Planetary gears and sun gear 2nd set		
Pressure angle α	Standard value	20
module	Calculated above	4
Number of teeth	Calculated above	Z_{P2} = 25; z_{S2} = 13
pitch	p = m.π	12.75
Addendum h_a	h_a = m	4
Dedendum h_f	h_f = 1,25.m	5
Tooth depth h	h = 2,25.m	9
Pitch diameter d(S_2)	d (S_2) = m.z_{S2}	52
Tip diameter d_a(S_2)	d_a (S_2) = d(S_2) + 2m	60
Root diameter d_f(S_2)	d_f (S_2) = d(S_2) – 2,5m	42
Pitch diameter d(P_2)	d (P_2) = m.z_{P2}	100
Tip diameter d_a(P_2)	d_a (P_2) = d(P_2) + 2m	108
Root diameter d_f(P_2)	d_f (P_2) = d(P_2) – 2,5m	90
Tooth thickness b	b = k.m	40
Center distance a	a = m(z_{P2} + z_{S2})/2	76

The load forces were calculated previously for the ring gear R.

II.9 Shafts design

The purpose of the shaft is to transmit torque along its axis to support the element, where it is located and bears the forces acting on these components. In the car transmission, torque is transferred from the input gear to the output gear. Torque transmission between the shaft and the gear is realized by mechanical elements, especially keys and splines.

Rolling bearings are widely used in mechanical transmission. They support the shaft, keep it in the correct position. They can also withstand the forces acting on the shaft, and transfer them to the housing and allow the shaft to rotate freely, minimizing friction.

For electric vehicle transmissions, rolling bearings need to withstand high speeds, considerable working temperature and when using light alloy housing (for example Aluminum), thermal expansion compensation is very important.[31]

II.9.1 Shaft layout considerations

A common shaft layout is a stepped cylinder, also called a multi-diameter shaft. With this structure, it is easy to manufacture and assemble its components.

General precautions for shafts design are the following:

- The shaft length must be minimized to limit the bending moment and deflection;
- The shaft shoulder is to axially locate the shaft element and bear thrust load;
- Parts with load-bearing capacities, such as gears, must be placed in support bearings (preferably two), and close to the bearing itself. This will result in reduced deflection and bending moment. In addition, this character is also related to increasing the critical speed of the shaft;
- The axial clearance between the components is necessary, the purpose is to easily disassemble and allow a normal flow of lubricant;
- Strict positioning of the components on the shaft is the key point, and accurate maintenance after positioning, make the coupling components aligned correctly;
- The diameter change in the shaft must be kept below the ratio of D/d = 1/4.

All the above factors are considered when designing the shaft layout. This process is not simple, because it must be constantly changing to meet the requirements and finally achieve the best layout design.

The conventional materials of the shaft are carbon steel and alloy steel. In the pinion shaft, the contact strength and bending strength of the teeth are required to withstand the load stress. Therefore, it has become necessary to use alloy steels and their respective processing methods.

In our design, we have two pinion shafts referred to previously as I and II, and the third one III is the wheel axle. However the three-shaft bear gears so it is preferable to use the same chosen material as gear (20CrMo5).[31]

II.9.2 Shaft load analysis

Since the load caused by bearing is previously calculated and the speed and torque related to the shafts are known, we rely on the MITcalc software to design the shafts.

The previously acquired data are summarized in the below table:

Table II.9—1. Shafts specifications

Shaft number	Torque (N.m)	Speed (rpm)	N° of gears	N° of bearings	Approx. length (mm)
I	465.79	12000	1	2	180
II	336.73	3692.3	2 + stage brakes unit	2	550
II	145.65	923.08	Differential + wheels	3	1600

II.9.2.1 Shaft I

To define the different diameter shifts we analyze the stress along the length of the shaft. For the shaft I the following graph shows the distribution of constraints along the shaft's length.

Table II.9—2. Distribution of constraints along the shaft I length

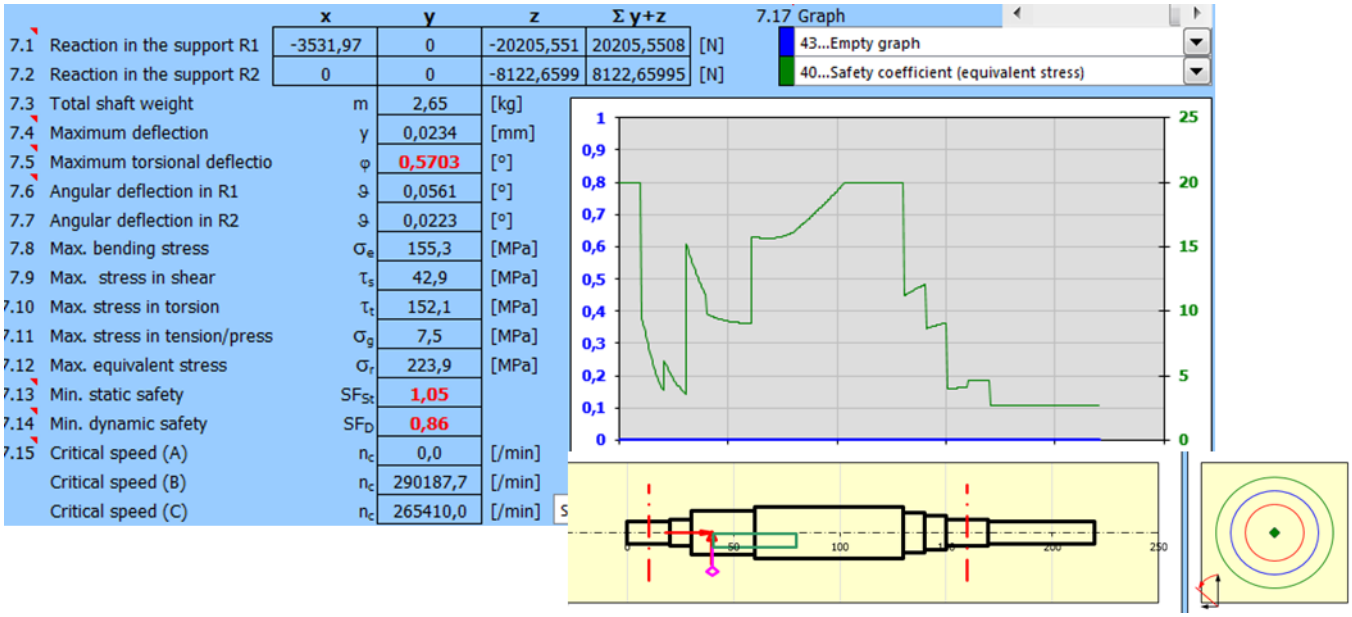

		x	y	z	Σ y+z	
7.1	Reaction in the support R1	-3531,97	0	-20205,551	20205,5508	[N]
7.2	Reaction in the support R2	0	0	-8122,6599	8122,65995	[N]
7.3	Total shaft weight	m	2,65			[kg]
7.4	Maximum deflection	y	0,0234			[mm]
7.5	Maximum torsional deflectio	φ	0,5703			[°]
7.6	Angular deflection in R1	ϑ	0,0561			[°]
7.7	Angular deflection in R2	ϑ	0,0223			[°]
7.8	Max. bending stress	σ_e	155,3			[MPa]
7.9	Max. stress in shear	τ_s	42,9			[MPa]
7.10	Max. stress in torsion	τ_t	152,1			[MPa]
7.11	Max. stress in tension/press	σ_g	7,5			[MPa]
7.12	Max. equivalent stress	σ_r	223,9			[MPa]
7.13	Min. static safety	SF_{St}	1,05			
7.14	Min. dynamic safety	SF_D	0,86			
7.15	Critical speed (A)	n_c	0,0			[/min]
	Critical speed (B)	n_c	290187,7			[/min]
	Critical speed (C)	n_c	265410,0			[/min]

According to the above graph, the constraints are concentrated on the middle section where the gears input the other sections have low concentration where the bearings will be installed. The other sections can be removed because they won't support any component.

Moreover, the moments of torsion and bending allow us to calculate the max diameter of the shaft.

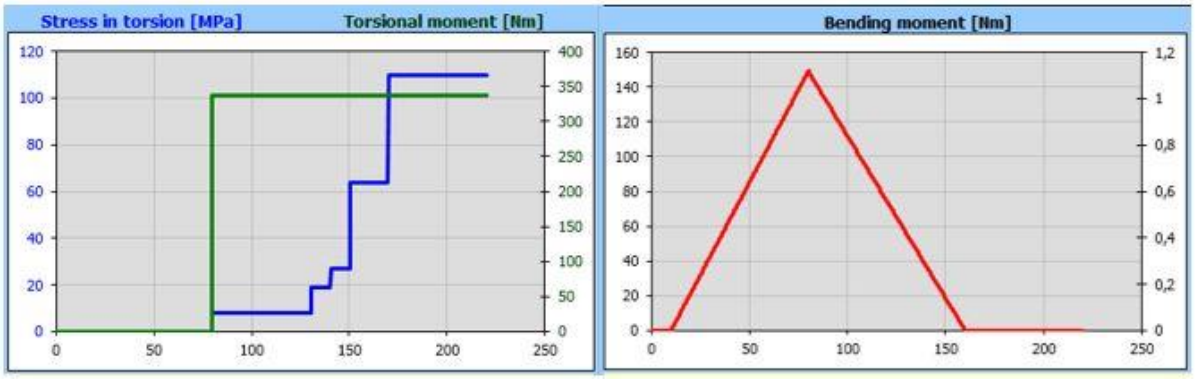

Figure II.9—1. Shaft I bending and torsion moments

From the above-shown graph, the maximal bending moment is Mb = 150 Nm and the maximal torsion moment is Mt = 340 Nm. Therefore the ideal moment is $M_i = \sqrt{M_b^2 + M_t^2} = 380.8\ Nm$ from that we get the maximal diameter $D_I \geq \sqrt[3]{\frac{32\ M_i}{\pi\ Rp}} \rightarrow D_I = 22\ mm$

II.9.2.2 Shaft II

The same procedure is for the other shafts. To define the different diameter shifts we analyze the stress along the length of the shaft. For shaft II the following graph shows the distribution of constraints along the shaft's length.

Table II.9—3. Distribution of constraints along the shaft II length

		x	y	z	Σ y+z	
7.1	Reaction in the support R1	-1459	0	-9844,5676	9844,56764	[N]
7.2	Reaction in the support R2	0	0	-7620,1207	7620,12071	[N]
7.3	Total shaft weight		m	2,65		[kg]
7.4	Maximum deflection		y	0,0183		[mm]
7.5	Maximum torsional deflectio		φ	0,5593		[°]
7.6	Angular deflection in R1		ϑ	0,0311		[°]
7.7	Angular deflection in R2		ϑ	0,0175		[°]
7.8	Max. bending stress		σ_e	75,7		[MPa]
7.9	Max. stress in shear		τ_s	20,9		[MPa]
7.10	Max. stress in torsion		τ_t	152,1		[MPa]
7.11	Max. stress in tension/press		σ_g	3,1		[MPa]
7.12	Max. equivalent stress		σ_r	223,9		[MPa]
7.13	Min. static safety		SF_{St}	1,05		
7.14	Min. dynamic safety		SF_D	1,77		
7.15	Critical speed (A)		n_c	0,0		[/min]
	Critical speed (B)		n_c	290187,7		[/min]
	Critical speed (C)		n_c	265410,0		[/min]

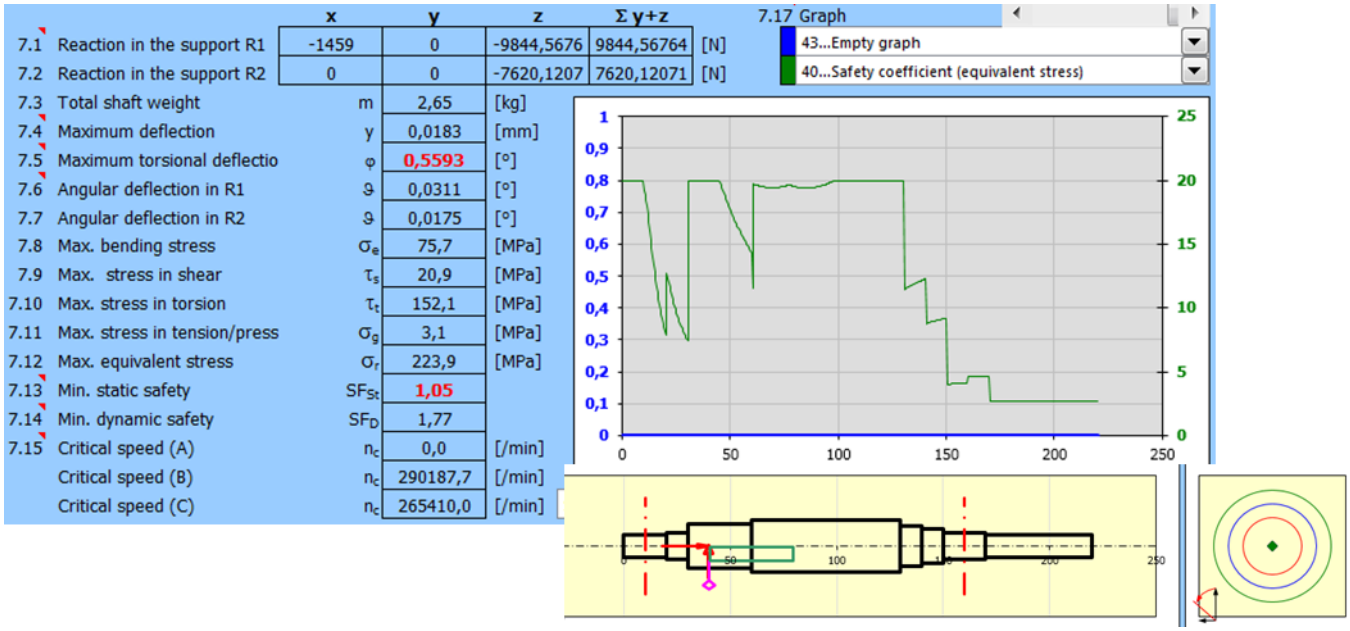

Unlike the shaft II the concentration of constraints are positioned in two sections due to the location of the gears, we only have to increase the diameter of the right end section to put the stage brakes unit.

Then, the moments allow us to calculate the diameter.

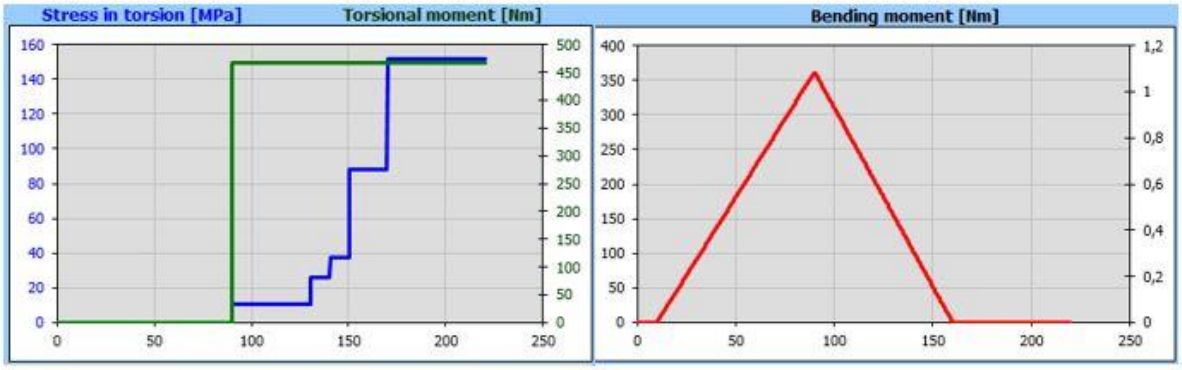

Figure II.9—2. Shaft II bending and torsion moments

From the above shown graph the maximal bending moment is Mb = 370 Nm and the maximal torsion moment is Mt = 470 Nm. Therefore the ideal moment is $M_i = \sqrt{M_b^2 + M_t^2} = 598.16 Nm$ from that we get the maximal diameter $D_{II} \geq \sqrt[3]{\frac{32\, M_i}{\pi\, Rp}} \rightarrow D_{II} = 35\ mm$

II.9.2.3 Shaft III

The third shaft is the wheel axle and the diameter shifts will be located in the middle only to support the bearing and the gears.

Table II.9—4. Distribution of constraints along the shaft III length

		x	y	z	Σ y+z	
7.1	Reaction in the support R1	-1459	0	-12198,229	12198,2291	[N]
7.2	Reaction in the support R2	0	0	-5266,4592	5266,45922	[N]
7.3	Total shaft weight	m	2,65			[kg]
7.4	Maximum deflection	y	0,0149			[mm]
7.5	Maximum torsional deflectio	φ	0,5703			[°]
7.6	Angular deflection in R1	ϑ	0,0344			[°]
7.7	Angular deflection in R2	ϑ	0,0142			[°]
7.8	Max. bending stress	σ_e	93,8			[MPa]
7.9	Max. stress in shear	τ_s	25,9			[MPa]
7.10	Max. stress in torsion	τ_t	152,1			[MPa]
7.11	Max. stress in tension/press	σ_g	3,1			[MPa]
7.12	Max. equivalent stress	σ_r	223,9			[MPa]
7.13	Min. static safety	SF_{St}	1,05			
7.14	Min. dynamic safety	SF_D	1,43			
7.15	Critical speed (A)	n_c	0,0			[/min]
	Critical speed (B)	n_c	290187,7			[/min]
	Critical speed (C)	n_c	265410,0			[/min]

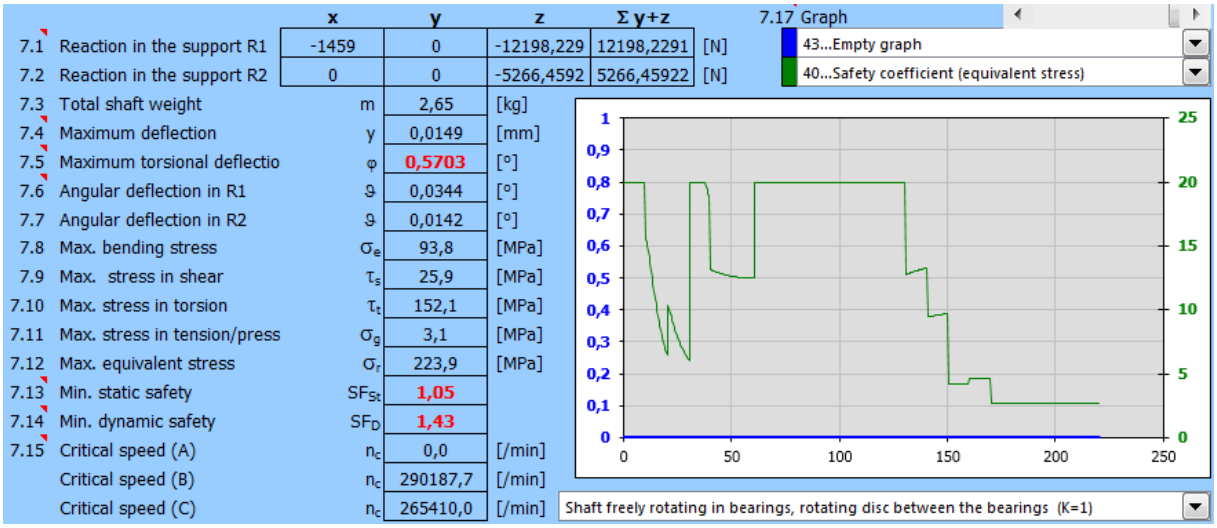

The concentration of constraints is on the sections bearing the gears and the section allowing the orientation of the axle.

Then, the moments allow us to calculate the diameter.

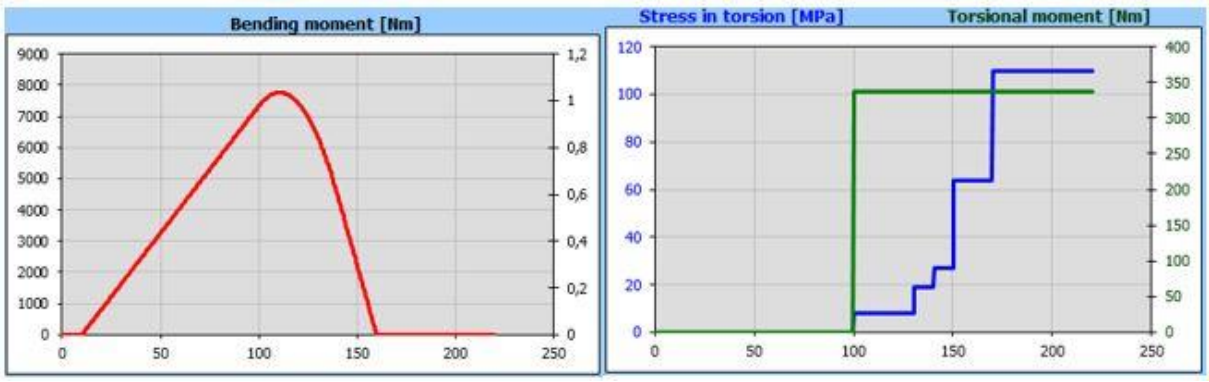

Figure II.9—3. Distribution of constraints along the shaft III length

We notice that the bending moment is bigger since the maximal length of the axle is bigger than the other shafts.

From the above-shown graph the maximal bending moment is Mb = 7900 Nm and the maximal torsion moment is Mt = 340 Nm. Therefore the ideal moment is $M_i = \sqrt{M_b^2 + M_t^2} = 7907.3\ Nm$ from that we get the maximal diameter $D_{III} \geq \sqrt[3]{\frac{32\ M_i}{\pi\ Rp}} \rightarrow D_{III} = 60\ mm$

II.9.3 Rolling bearings selection

When choosing a bearing, you need to consider several important factors. The first factor to consider is the load that the bearing can support (axial or radial).

Each type of bearing is more specifically designed to support an axial load or a radial load. Some bearings can even support both loads: this is called a combined load. If you have to withstand a combined load, for example, we advise you to go for a tapered roller bearing. If you need a bearing capable of supporting a large radial load, then we recommend a cylindrical roller bearing. On the other hand, if your bearing has to withstand less heavy loads, a ball bearing may be sufficient, because it is often less expensive.

The speed is another factor to consider. Some bearings can withstand high speeds. Thus, the presence of a cage for cylindrical roller bearings and needle bearings allows higher speeds than bearings without a cage. However, the choice of a higher speed is sometimes made to the detriment of the load.

Likewise, the conditions of use are of fundamental importance in choosing an ideal bearing. It is therefore necessary to analyze the environment of your application. Your bearing can be subject to some contaminations. Indeed, certain applications can be a source of noise inconvenience, shocks and / or vibrations. Your bearing must therefore withstand these shocks on the one hand and not be a hindrance on the other hand.

Another essential element to consider is the life of the bearing. Several factors, such as speed or repeated use, can affect the longevity of a bearing.[22]

From the above description, we selected cylindrical roller bearings because they support important radial loads and with an incorporated cage they can also bear important rotation speed with an extended lifetime. The following are the selected bearing for shaft I and shaft II, the complete information is found in (appendix A3-1).

Table II.9—5. Cylindrical roller bearing specifications for shaft I and II

Shaft	Number of bearings	Loads (N)	Speed (rpm)	Shaft diameter (mm)	Bearing designation
I	2	Fa = 0; Fr ≠ 0	12000	22	SZ - 204
II			3692.3	35	RN207

The third shaft because it needs to support also axial loads we have to choose tapper roller bearing due to their capacity to support high loads, axial, radial and combined types of loads. Also, there are the two perpendicular shafts that hold the bevel gears E and F.

The following are the selected bearing for shaft III, the complete information is found in (appendix A3-2, A3-3).

Table II.9—6. Cylindrical roller bearing specifications for shaft III and the bevel gears shafts

Shaft	Number of bearings	Loads (N)	Speed (rpm)	Shaft diameter (mm)	Bearing designation
III	3	$Fa \neq 0$; $Fr \neq 0$	923.08	60	32012X
Small shaft for the bevel gearings	2 (1 on each shaft)	$Fa \neq 0$; $Fr \neq 0$	518.6	17	30203A

II.10 Conclusion

After knowing the vehicle specifications and required performances, we had been able to choose the electrical components (the lithium-ion battery and the PMSM motor), also relying on existing datasheets of some electric vehicles brand. Then we check the adaptability of the PSMS motor chosen to our desired vehicle design. The motor data such as the output speed and torque were then applied to design the transmissions.

The two-speed transmission is designed to combine the gearbox and the differential in a compact geometry to reduce the size and weight of the vehicle which then allows better performance. The components of the transmission such as gears were designed through a strength analysis set of equations. Meanwhile, the design of the shaft was done through the MITcalc software and the bearing was selected through commercial catalogs.

These results will be applied in the next chapter to obtain 3D model drawings of the components and perform dynamic analyses.

Chapter III. 3D modeling and dynamic study of powertrain components

III.1 Introduction

In this chapter, we run a dynamic linear study on the gearbox components we designed in the previous chapter to check their behavior while on the motion. The parts we analyze consist of the gears and shafts.

For the gears, we look at the interaction between each gear train, the planetary gear set and the differential bevel gears. For the shafts, we assume the gears are remote masses acting as loads and the bearings are established as the connection between the shafts and the housing. The result analysis will show the stress on the parts through a Von Mises stress plot.

III.2 Design of powertrain components

The powertrain of the electric vehicle contain three main sections; the battery, the PMSM motor and the transmission. We used SolidWorks software to design the mentioned components, for the battery and motor we relied on the dimensions provided by the manufacturers (Appendix A1, Appendix A2), the 3D model show only the dimensions that allow us to position the transmission and have a visual reference of the powertrain.

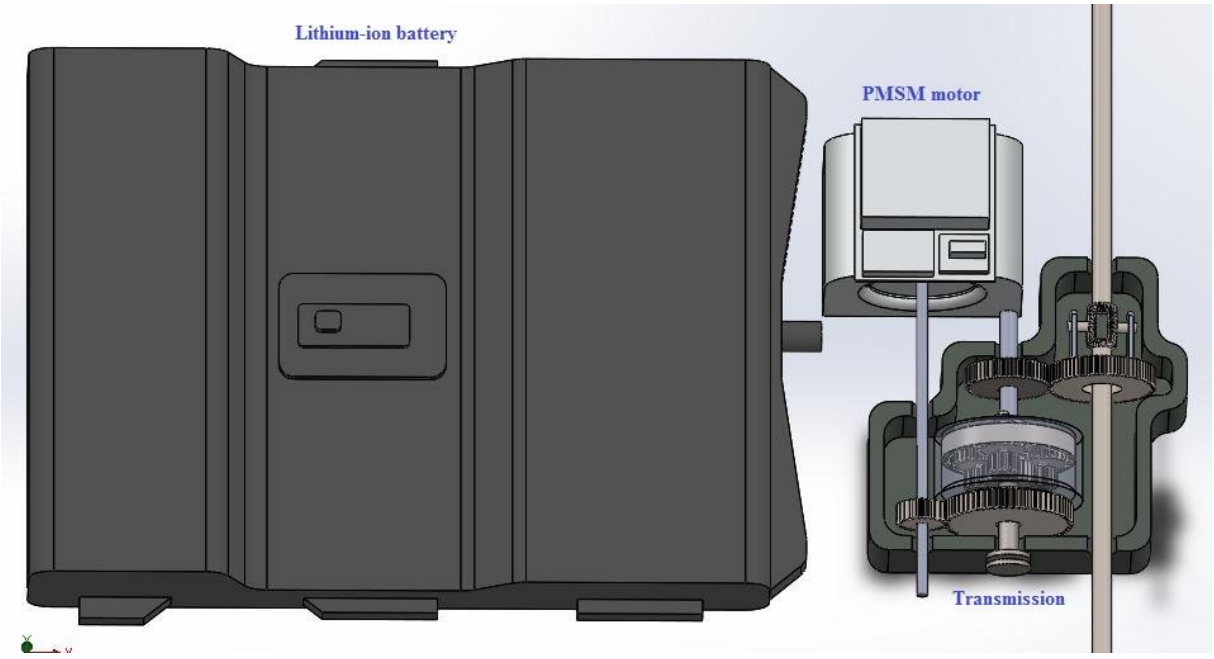

Figure III.2—1. 3D model of the powertrain in SolidWorks

However, the transmission has the largest number of components that can be divided into 2 parts; the planetary gear set and the differential set. The following table shows the design of the transmission components.

III.3 The planetary gear set modeling

The motion is transmitted from the motor to the gear M through shaft I, then it is transmitted to the gear P equipped with a cover that coincides with the gear R, so both gears have the same rotation. On the other hand, we have the sun gear S1 and S2 each attached to its own stage brake. The planetary gears P1 and P2 provide different transmission ratios according to which sun gear is fixed the movement transmitted to the carrier attached to the shaft II.

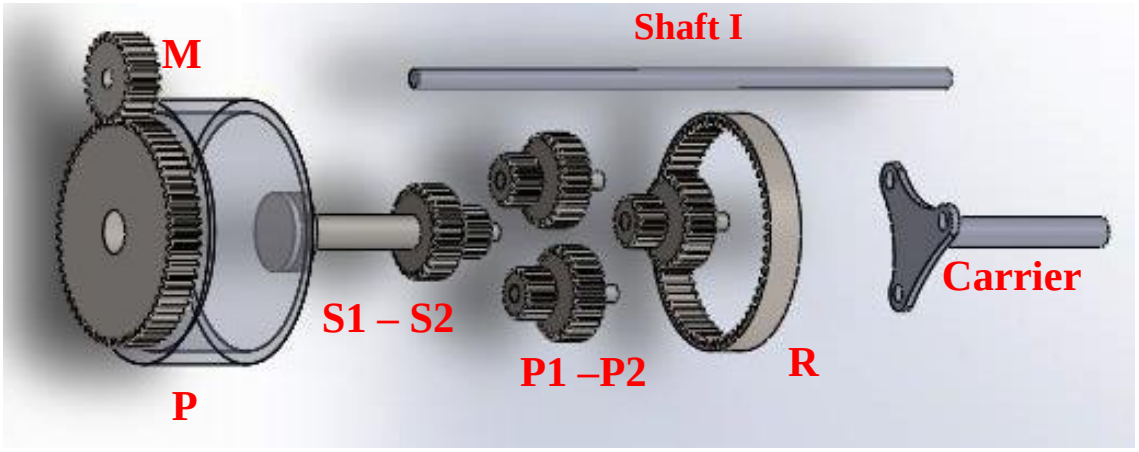

Figure III.3—1. Planetary gear set design

III.4 Differential gears

The shaft II connected to the carrier provides rotation to the gear C, which then transmits the motion to the differential gear D. this gear has two rectangular parts we refer to as connections, this allows the gear D to turn the bevel gears E and F. the final transmission is in the shaft III, it is the axle connected to the bevel pinions I and J that provide the rotation to the wheels.

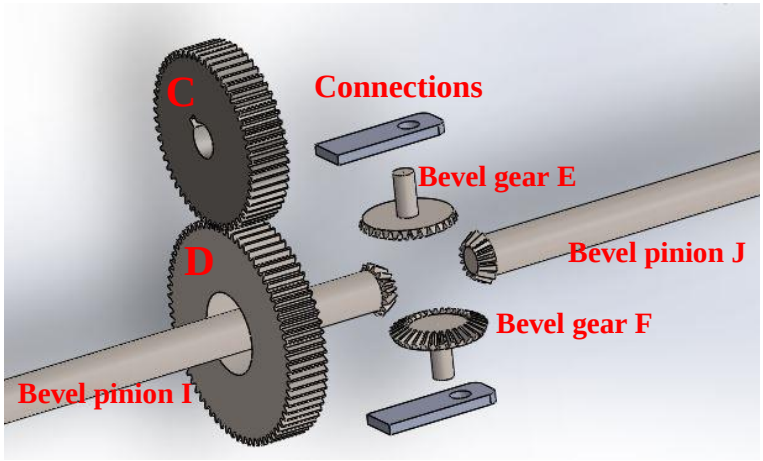

Figure III.4—1. Differential gears

III.5 Dynamic analysis parameters

A dynamic analysis of the transmission allows us to predict the stresses and deformation in its components by studying the interactions between gears and the adaptability of the shafts to support the components and transmit the required torque at a certain speed. The data that must be provided beforehand is the material properties, the fixture type, the loads acting on the part and the meshing parameters.

III.5.1 Material properties

Both the gears and the shafts in this study have the same material. The steel alloy 20CrMo5 is a tempered alloy mainly used in gears and gearboxes that require high performance. The below table (Table III.5—1) shows the mechanical properties of this steel.

Table III.5—1. 20CrMo5 Mechanical properties

20CrMo5 Mechanical properties		
Elastic modulus	$2.05 \times 10^{+11}$	N/m²
Poisson's ration	0.29	
Shear modulus	$7.99 \times 10^{+10}$	N/m²
Mass density	7858	Kg/m^3
Tensile strength	425000003.2	N/m²
Yield strength	282685049	N/m²
Thermal expansion coefficient	1.2×10^{-5}	/K
Thermal conductivity	52	W/(m.K)
Specific heat	486	J/(Kg.K)

III.5.2 Fixture and loads

To be able to perform a strength study on the designed parts, we have to input data regarding the loads applied such as forces and torques, and the fixture type of the components and the supports components, in our case bearings between the shafts and the housing. In the following study, we used the data gathered from chapter II of gear loads and the transmitted torques into the shafts.

Table III.5—2. Loads data in gears and shafts

Shaft	**Torque (N.m)**	
I	465.79	
II	336.73	
III	145.65	
Gear train	**Force 1 (N)**	**Force 2 (N)**
M – P	F (M/P) = 3531.95	F (P/M) = 10326.74
C – D	F (C/D) = 1459.04	F (D/C) = 4265.96
E - I	F (E/I) =2474.6	F(I/E) = 1239.07
Planetary set (S – P)	F (S/P) = 5163.37	F (P/S) = 5163.37
Planetary set (P – R)	F (P/R) = 10326.74	F (R/P) = 5163.37

III.5.3 Meshing parameters

Mesh control refers to specifying different element sizes at different regions in the model. A smaller element size in a region improves the accuracy of results in that region. In SolidWorks, mesh control can be specified at vertices, points, edges, faces, and components.

The mesh control parameters are:

- Element size (e) for the specified entities;
- Element growth ratio (r);

III.6 Dynamic study of gear trains in the transmission design

In this study we are concerned about the stress resulting from interactions between gears and the loads and torque effects, therefore by applying the previously mentioned data in a dynamic study we analyzed the following gear sets.

III.6.1 Gear train M – P

In the study of interactions between gear M and gear P, we assume the gears only interact between them and are treated both as solid bodies and the global contact is bonded.

Table III.6—1. Gear train M – P solid bodies

Components	Treated as	Volumetric properties
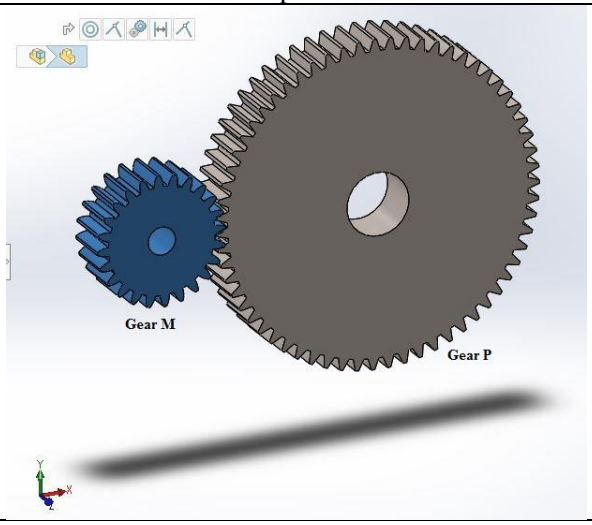	Solid body (gear M)	Mass:14.9132 kg Volume:0.0018978 m^3 Density:7858 kg/m^3 Weight:146.149 N
	Solid body (gear P)	Mass:2.09451 kg Volume:0.00026654 m^3 Density:7858 kg/m^3 Weight:20.5262 N

For study simulation in SolidWorks we used a linear dynamic analysis (nodal time history) with 15 frequencies of iteration including temperature loads as a thermal option when at zero strain, the temperature is at 298 Kelvin.

For meshing, we used a standard solid mesh with 4 Jacobean points, an element size of 11.9676 mm and 0.598382 mm for tolerance.

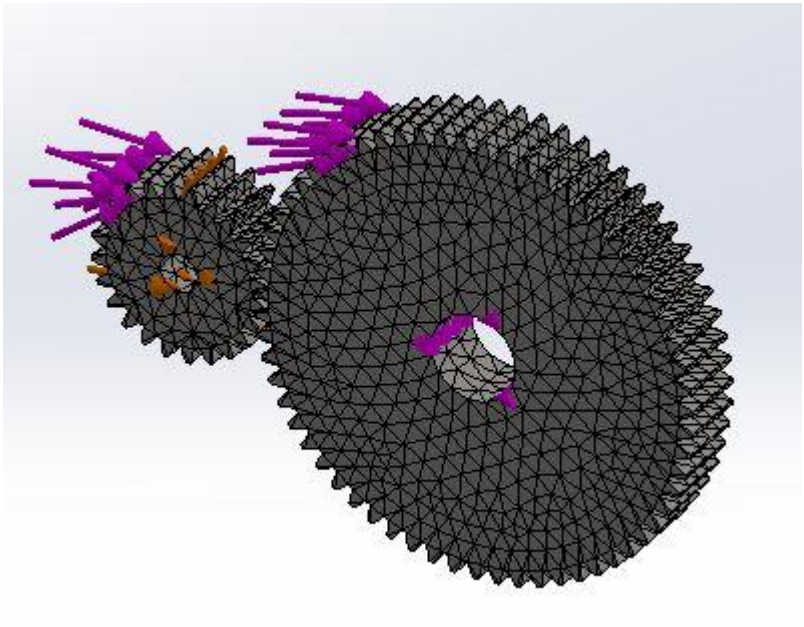

Figure III.6—1. Gear train M – P mesh type

The study will analyze the stress constraints on the gears while on load. The following table shows the applied loads.

Table III.6—2. Load application on gear train M – P

Load type	Load name	Component	Details
Normal force	Force of M on P (in purple)		Entities: 2 faces Value: 10326.7 N
	Force of P on M (in blue)		Entities: 2 faces Value: 3531.95 N
Torque	Torque on M	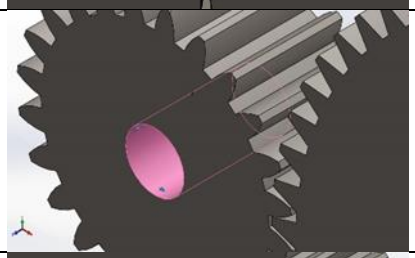	Reference: bore Value: 463.51 N.m
	Torque on P	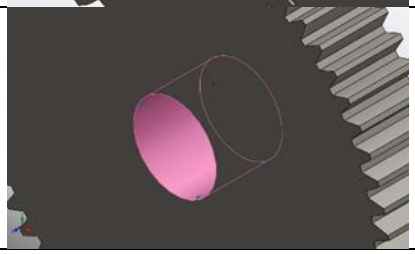	Reference: bore Value:- 336.56 N.m

The results showed the stress on the nodes applied during meshing, the Von Mises nodal stress results are plotted in the following graph.

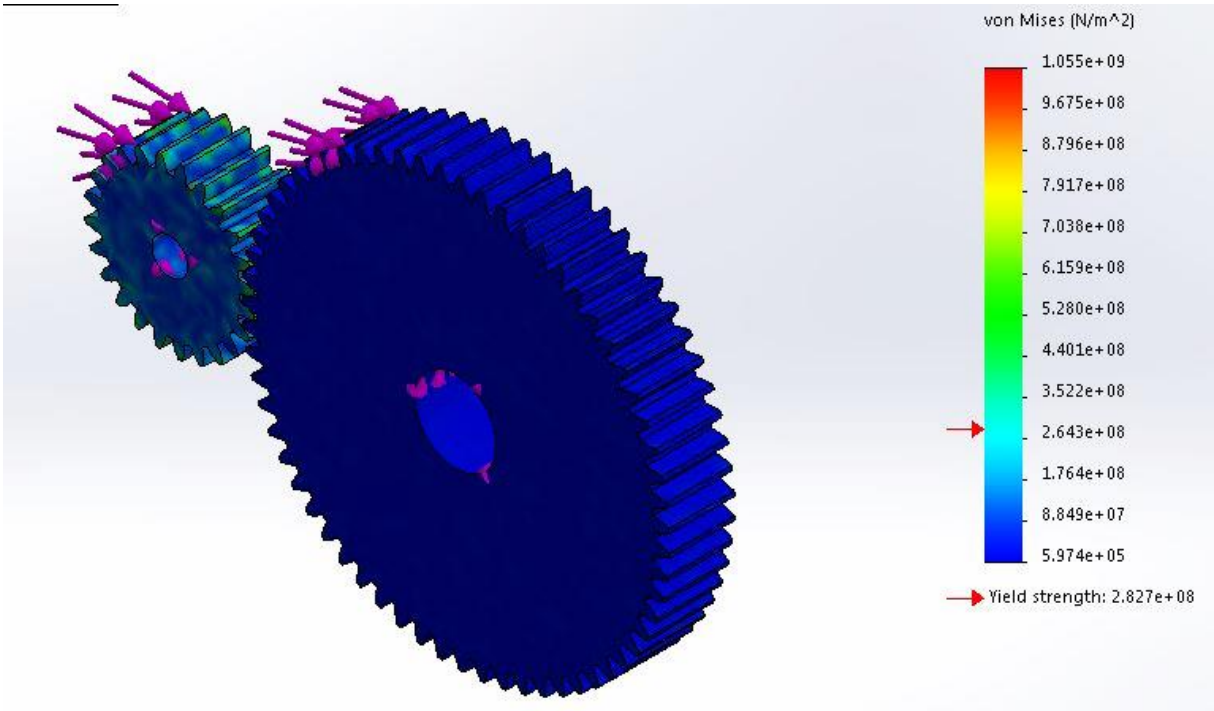

Figure III.6—2. Von Mises stress plot

By observing the dynamic analysis results, the stress values are within the permissible stress value for the gear train M – P with a mean value of $2.643 \times 10^{+8} < 2.827 \times 10^{+8}$, the stress increase in the teeth edges of gear M but still within the acceptable values. Therefore, the gear train design theoretically won't have to go through a modification.

III.6.2 Gear train C – D

In the study of interactions between gear C and gear D, we assume the gears only interact between them and are treated both as solid bodies and the global contact is bonded.

Table III.6—3. Gear train C - D solid bodies

Components	Treated as	Volumetric properties
	Solid body (gear C) In blue	Mass: 6.57161 kg Volume: 0.0008363 m^3 Density: 7858 kg/m^3 Weight: 64.4018 N

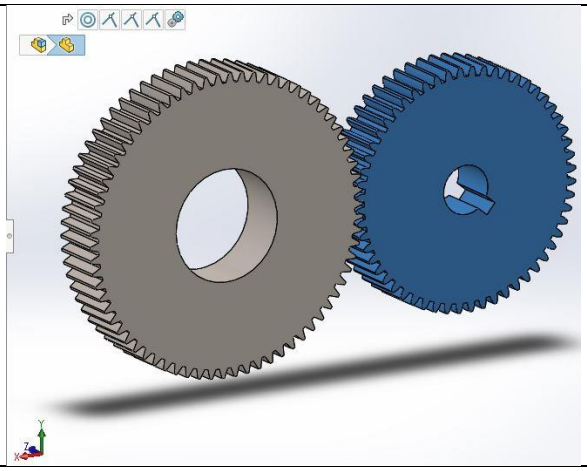	Solid body (gear D) In grey	Mass: 9.20963 kg Volume: 0.00117201 m^3 Density: 7858 kg/m^3 Weight: 90.2544 N

For study simulation in SolidWorks we used a linear dynamic analysis (nodal time history) with 15 frequencies of iteration including temperature loads as a thermal option when at zero strain, the temperature is at 298 Kelvin.

For meshing, we used a standard solid mesh with 4 Jacobean points, an element size of 11.9866 mm and with 0.599328 mm for tolerance and a maximum aspect ratio of 6.3797. However, due to the geometry of gear D, we applied a mesh control of 4.88995 mm with a ratio of 1.5 to be able to perform the analysis.

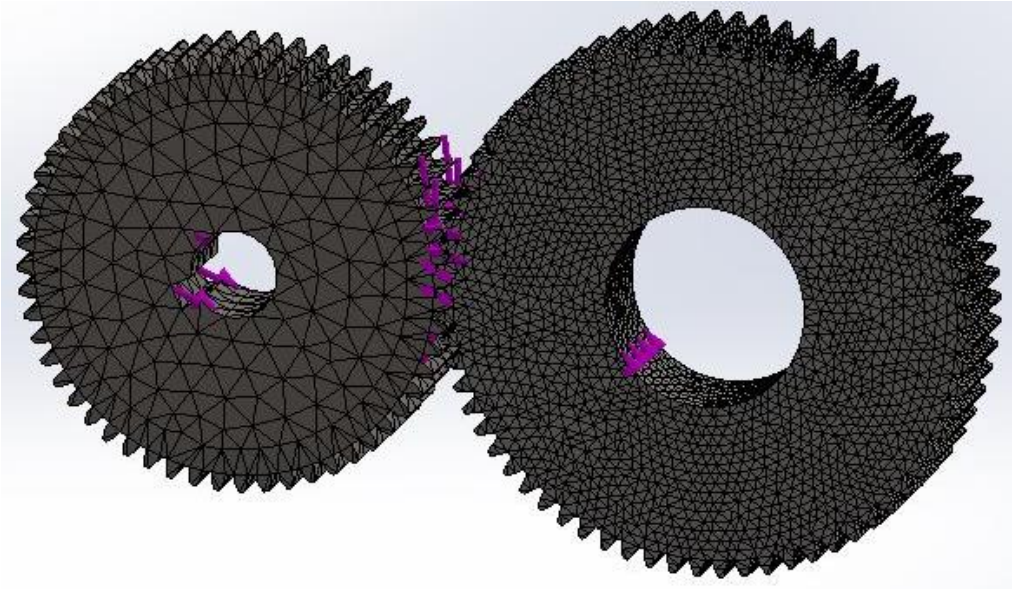

Figure III.6—3. Gear train C - D mesh type

Chapter III. 3D modelling and dynamic study of powertrain components

The study will analyze the stress constraints on the gears while on load. The following table shows the applied loads.

Table III.6—4. Load application on gear train D - C

Load type	Load name	Component	Details
Normal force	Force of C on D (on the left)		Entities: 2 faces Value: 4265.96 N
	The force of D on C (on the right)		Entities: 2 faces Value: 1459.04 N
Torque	Torque on C	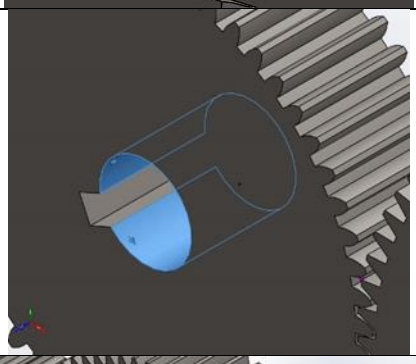	Entities: bore with a key aperture Value: 300 N.m
	Torque on D	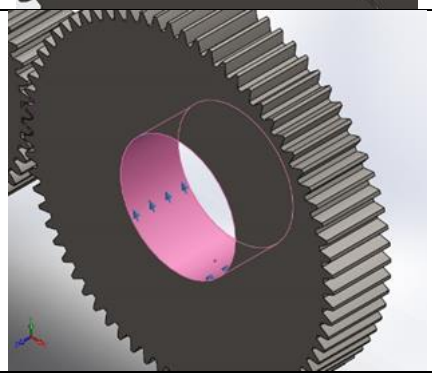	Reference: bore Value: -200 N.m

The results showed the stress on the nodes applied during meshing, the Von Mises nodal stress results are plotted in the following graph.

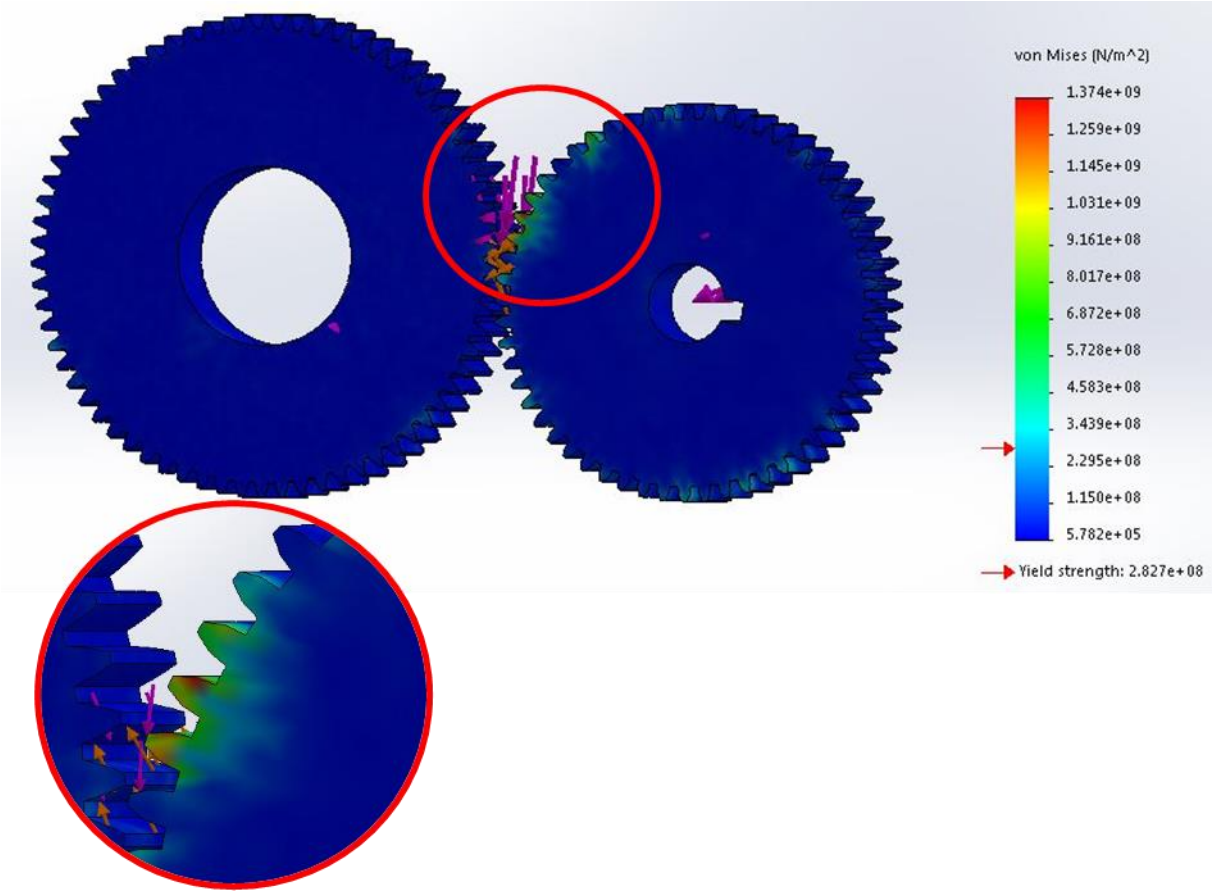

Figure III.6—4. Von Mises stress plot

By observing the dynamic analysis results, the stress values are within the permissible stress value for the gear D with a mean value of $2.295 \times 10^{+8} < 2.827 \times 10^{+8}$, the stress increase in the teeth edges of gear C on the point of contact but still within the acceptable values for medium usage. However, for extreme conditions application with increased torque, the number of teeth of gear D must increase for a better distribution of constraints along the gear increased diameter.

III.6.3 Planetary gears

In this study, we look at the interactions between the gears inside the planetary gear set. We assume the gears only interact between them, and we only consider one planet gear and all the gears are treated as solid bodies and the global contact is bonded.

Table III.6—5. The planetary gear set solid bodies

Components	Treated as	Volumetric properties
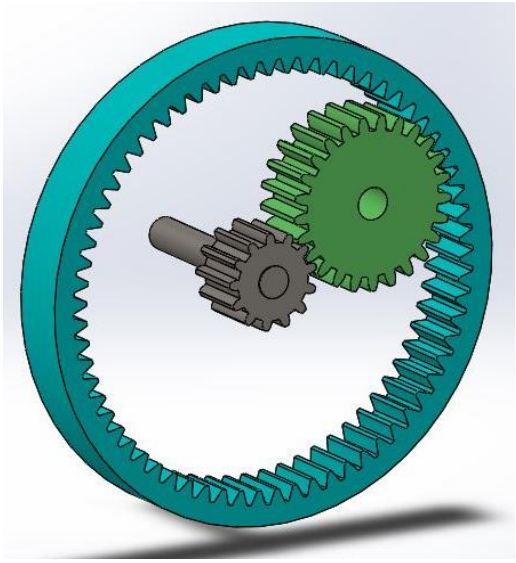	Solid body (gear P1) In blue	Mass:2.32888 kg Volume:0.00029637 m^3 Density:7858 kg/m^3 Weight:22.823 N
	Solid body (gear S1) In grey	Mass:0.928369 kg Volume:0.000118143 m^3 Density:7858 kg/m^3 Weight:9.09802 N
	Solid body (gear R) In green	Mass:4.84195 kg Volume:0.000616181 m^3 Density:7858 kg/m^3 Weight:47.4511 N

As mentioned before, for study simulation in SolidWorks we used a linear dynamic analysis (nodal time history) with 15 frequencies of iteration including temperature loads as a thermal option when at zero strain, the temperature is at 298 Kelvin.

For meshing, we used a curvature-based solid mesh with 4 Jacobean points, element size between [9.85101 – 3.28364] mm and with 0.599328 mm for tolerance and a maximum aspect ratio of 6.3797. However, due to the geometry of the sun gear S1 we applied a mesh control of 4.60977 mm with a ratio of 1.5 to be able to perform the analysis.

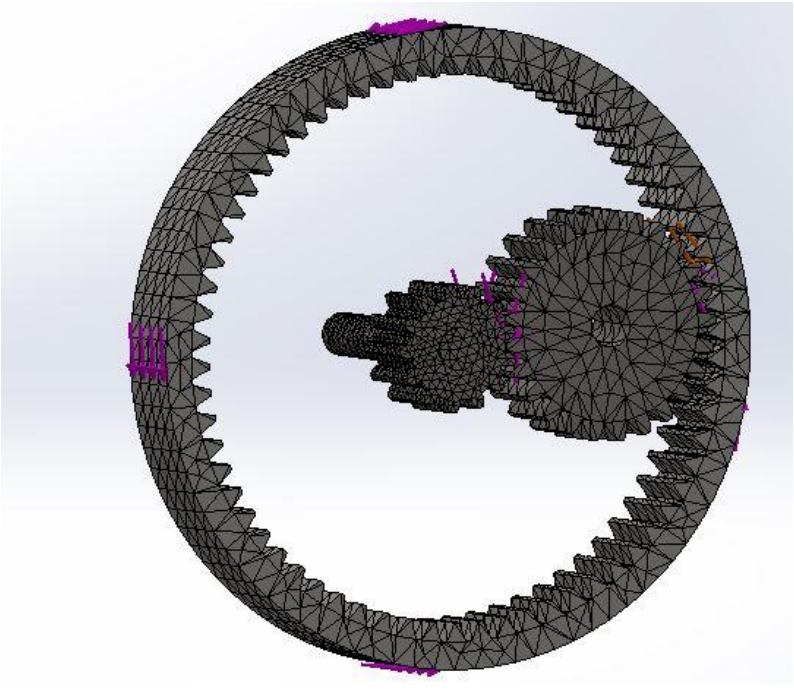

Figure III.6—5. Planetary gear set mesh type

Chapter III. 3D modelling and dynamic study of powertrain components

The study will analyze the stress constraints on the gears while on load. The following table shows the applied loads.

Table III.6—6. Load application on the planetary gear set

Load type	Load name	Component	Details
Normal force	Forces between S and P (on the left)		Entities: 1 tooth face of S and 1 tooth face of P Value: 5163.37 N
	Forces between P and R (on the right)	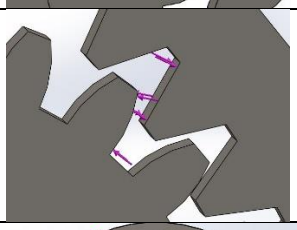	Entities: 1tooth face of P and 1 tooth face of R Value: 10326.7 N
Torque	Torque on R	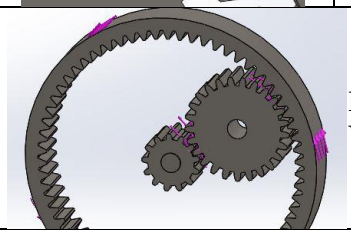	Entities: External diameter Value: 336.73 N.m

The results showed the stress on the nodes applied during meshing, the Von Mises nodal stress results are plotted in the following graph.

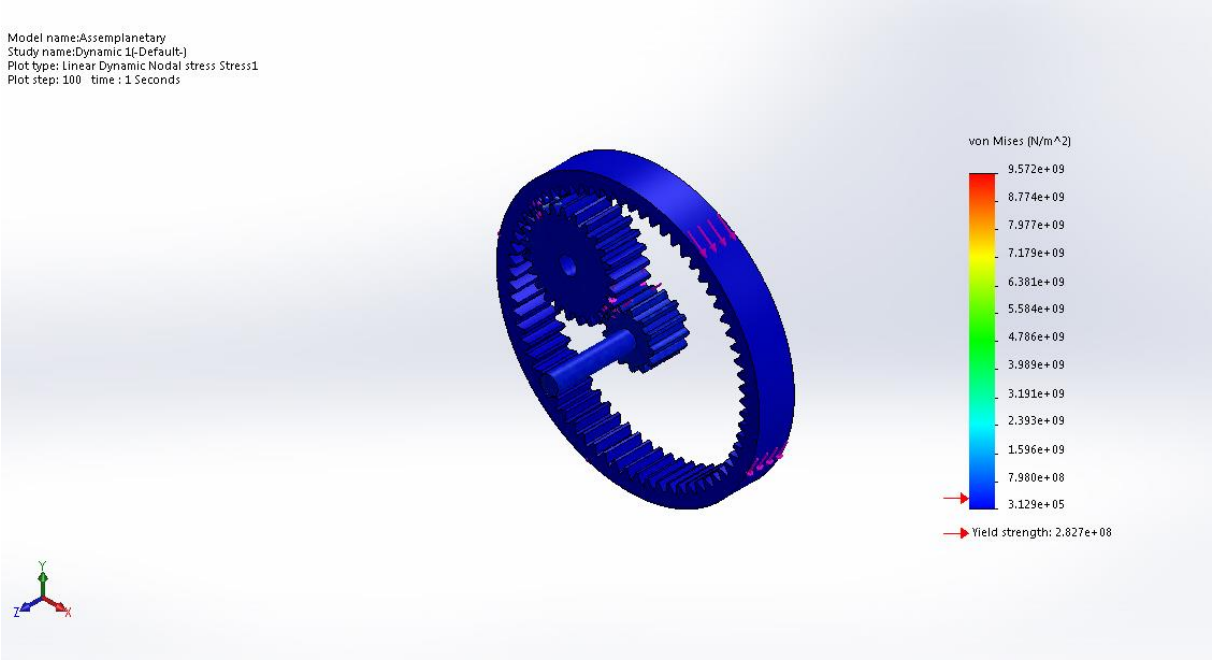

Figure III.6—6. Von Mises stress plot – planetary gear set

By observing the dynamic analysis results, the stress values are within the permissible stress value for the planetary gear set with a mean value of $3.129 \times 10^{+5} < 2.827 \times 10^{+8}$. Therefore, the design of the gear set won't have any modifications.

III.6.4 Differential bevel gears

In this study, we look at the interactions between the gears in the differential. We assume the gears only interact between them, and we only consider one gear and one pinion as the other two are similar and all the gears are treated as solid bodies and the global contact is bonded.

Table III.6—7. Differential bevel gears solid bodies

Components	Treated as	Volumetric properties
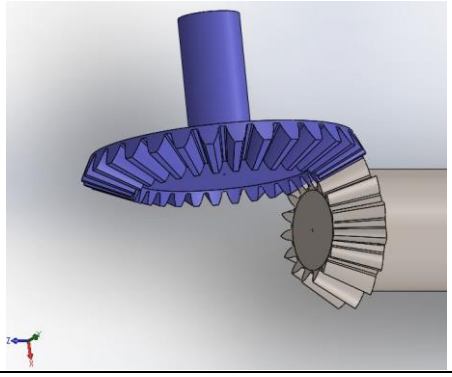	Solid body (gear E) In blue	Mass:0.519736 kg Volume:6.61411×10^{-5} m^3 Density:7858 kg/m^3 Weight:5.09342 N
	Solid body (pinion I) In grey	Mass:6.90176 kg Volume:0.00087831 m^3 Density:7858 kg/m^3 Weight:67.6373 N

As mentioned before, for study simulation in SolidWorks we used a linear dynamic analysis (nodal time history) with 15 frequencies of iteration including temperature loads as a thermal option when at zero strain, the temperature is at 298 Kelvin.

For meshing, we used a standard solid mesh with 4 Jacobean points, an element size of 11.6928 mm with 0.584639 mm for tolerance.

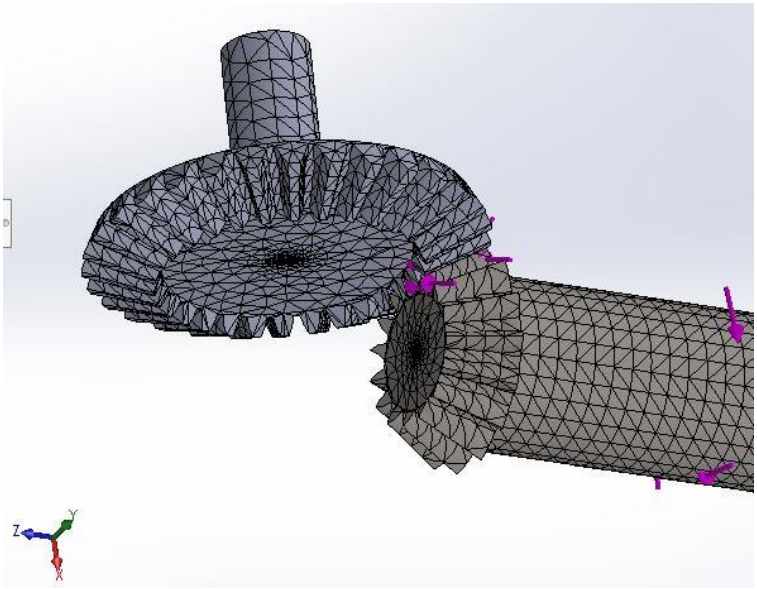

Figure III.6—7. Differential bevel gears mesh type

The study will analyze the stress constraints on the gears while on load. The following table shows the applied loads.

Table III.6—8. Load application on the differential bevel gears

Load type	Load name	Component	Details
Normal force	Force of E on I	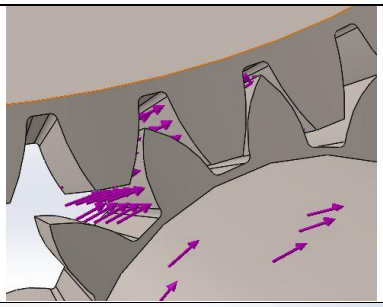	Entities: tooth face Value: 2474.7 N
	Force of I on E		Entities: tooth face Value: 1239.07 N
Torque	Torque on E	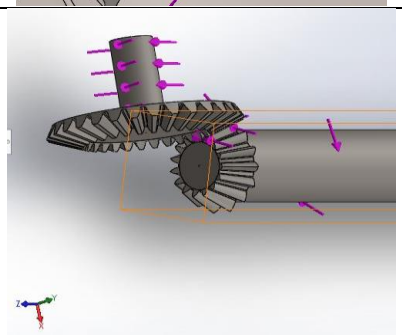	Entities: gear bore Value: 145.35 N.m
	Torque on I		Entities: pinion bore Value: -145.36 N.m

The results showed the stress on the nodes applied during meshing, the Von Mises nodal stress results are plotted in the following graph.

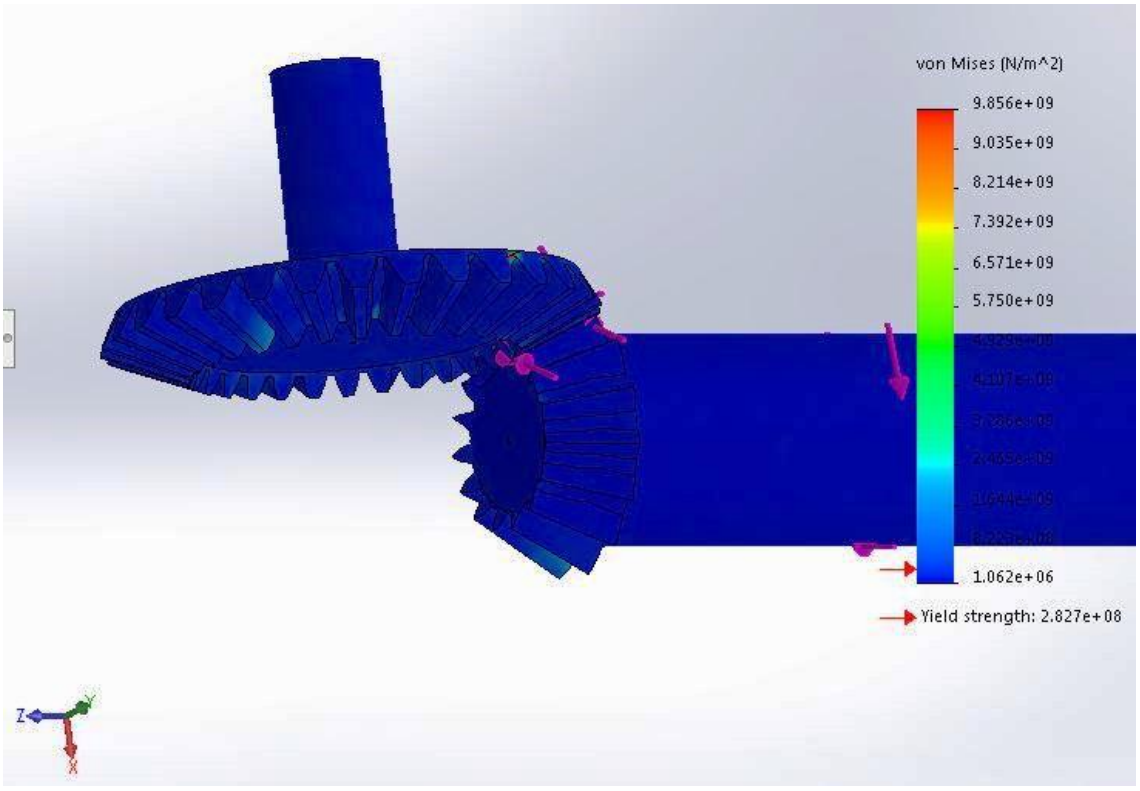

Figure III.6—8. Von Mises stress plot – Differential bevel gears

By observing the dynamic analysis results, the stress values are within the permissible stress value for the planetary gear set with a mean value of $1.062 \times 10^{+6} < 2.827 \times 10^{+8}$. Therefore, the design of the gear set won't have any modifications.

III.7 Dynamic study of shafts in the transmission design

In the dynamic study of the shafts, we include the housing and we set a connection between it and the shaft as a bearing connection, also the gears will be simulated as remote masses acting on the shafts as loads.

III.7.1 Shaft I

In this study, we analyze the strength of the shafts and look at the stress concentration areas when the shaft is on load and supported by bearings.

Table III.7—1. Shaft I solid bodies and connections

Components	Treated as	Volumetric properties
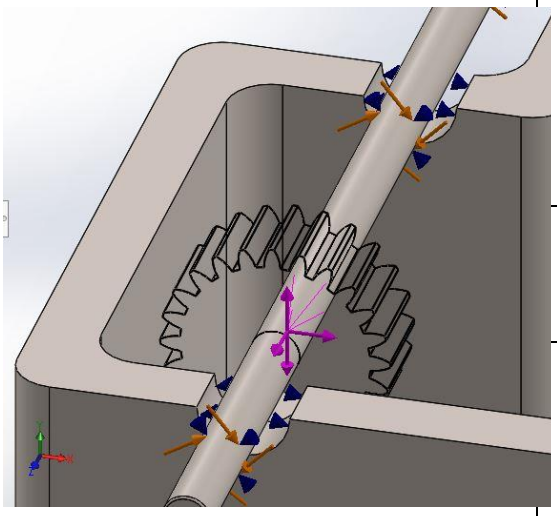	Solid-body (shaft I)	Mass:2.04869 kg Volume:0.0002661 m^3 Density:7700 kg/m^3 Weight:20.0772 N
	Solid-body (housing)	Mass:117.031 kg Volume:0.0151988 m^3 Density:7700 kg/m^3 Weight:1146.9 N
	Bearing connector	Number of connectors: 2 Entities: shaft cylindrical face and housing cylindrical aperture

Same as in gears, for study simulation in SolidWorks we used a linear dynamic analysis (nodal time history) with 15 frequencies of iteration including temperature loads as a thermal option when at zero strain, the temperature is at 298 Kelvin.

For meshing, we used a standard solid mesh with 4 Jacobean points, an element size of 24.9178 mm with 1.24589 mm for tolerance.

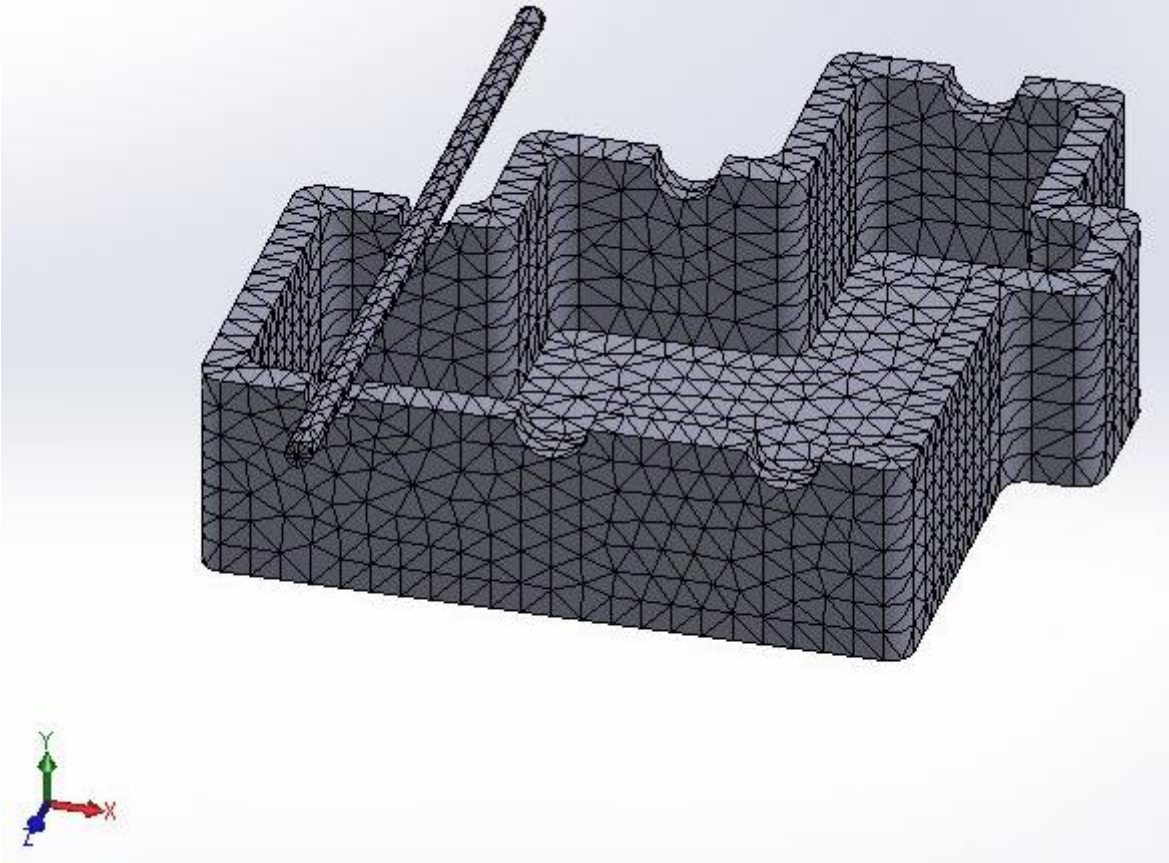

Figure III.7—1. Shaft I mesh type

The study will analyze the stress constraints on the gears while on load. The following table shows the applied loads.

Table III.7—2 Load application on shaft I

Load type	Load name	Component	Details
Normal force	Remote mass (gear)	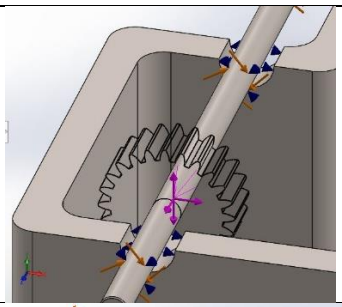	Remote Mass: 2.0524 kg Coordinate System: Global Cartesian coordinates Force Values: 0, -3531.95, 0 N
Torque	Torque on the shaft I	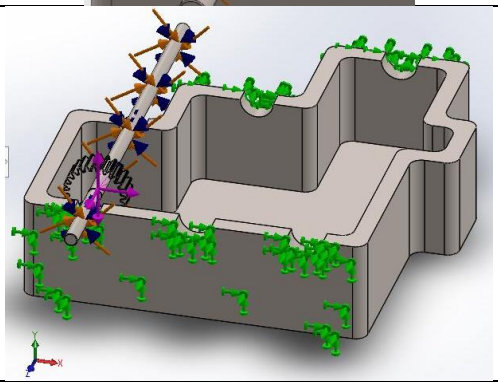	Entities: 1 cylindrical face Value: - 465.79 N.m
Fixed geometry	Housing fixture		Entities : 3 housing faces Reaction force: 4.71962 N

The results showed the stress on the nodes applied during meshing, the Von Mises nodal stress results are plotted in the following graph.

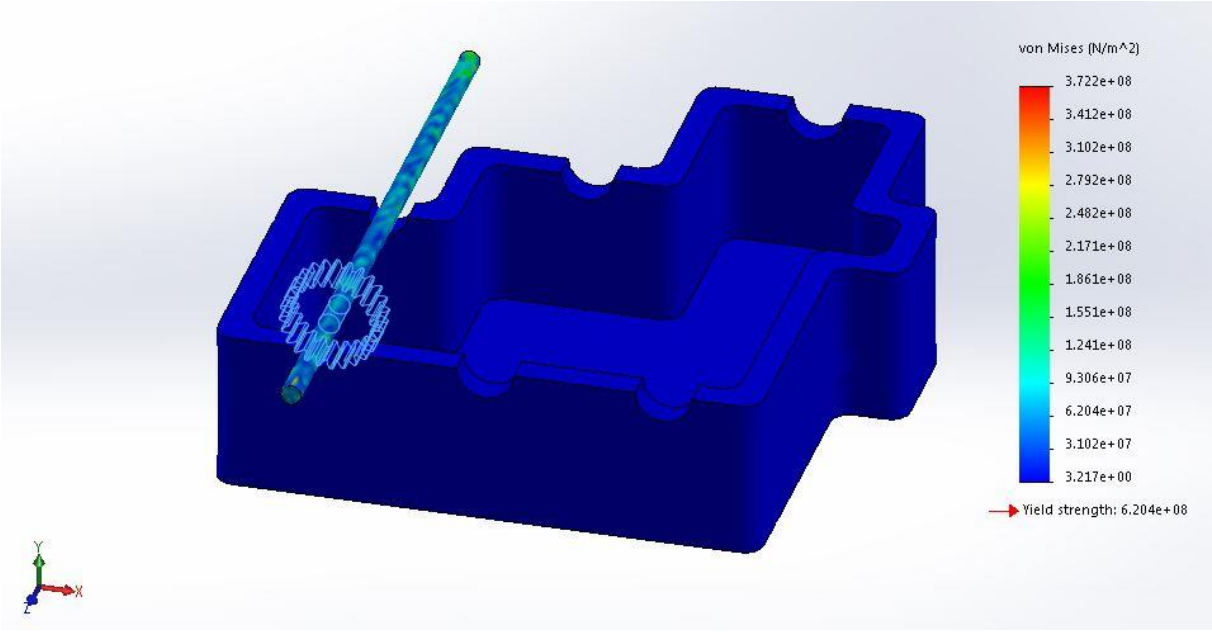

Figure III.7—2. Von Mises stress plot – Shaft I

By observing the dynamic analysis results, the stress values are within the permissible stress value for shaft I with a maximum value of $3.722 \times 10^{+8} < 6.204 \times 10^{+8}$. Therefore, the design of shaft I won't have any modifications.

III.7.2 Shaft II

In this study, we analyze the strength of the shafts and look at the stress concentration areas when the shaft is on load and supported by bearings.

Table III.7—3. Shaft II solid bodies and connections

Components	Treated as	Volumetric properties
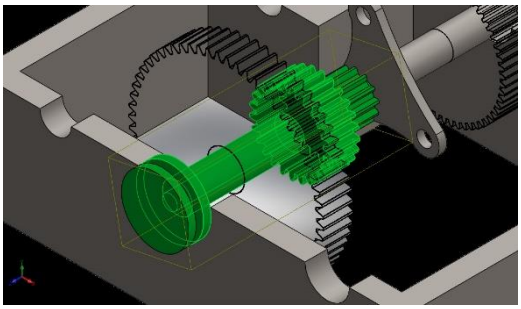	Solid-body (planetary sun gears)	Mass:3.91499 kg Volume:0.00049822 m^3 Density:7858 kg/m3 Weight:38.3669 N
	Solid body (carrier)	Mass:2.6839 kg Volume:0.00034155 m^3 Density:7858.01 kg/m^3 Weight:26.3023 N
	Solid-body (housing)	Mass:86.0628 kg Volume:0.0109523 m^3 Density:7858 kg/m^3 Weight:843.415 N

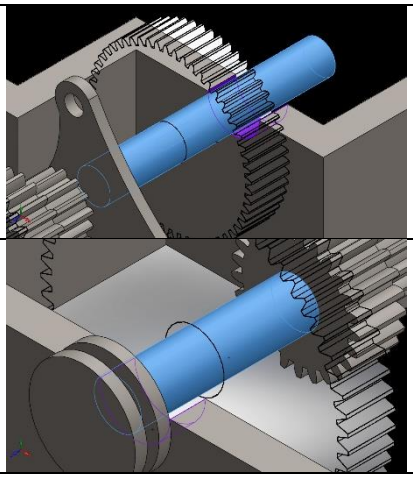	Bearing connector	Number of connectors: 2 Entities: shaft cylindrical face and housing cylindrical aperture

Same as in gears, for study simulation in SolidWorks we used a linear dynamic analysis (nodal time history) with 15 frequencies of iteration including temperature loads as a thermal option when at zero strain, the temperature is at 298 Kelvin.

For meshing, we used a standard solid mesh with 4 integration points, an element size of 22.6228 mm with 1.13114 mm for tolerance and a maximum aspect ratio of 11.993. However, to be able to run the simulation, we opted for a mesh control on the shaft side containing the sun gears with a size of 9.73639 mm and a ratio of 1.5.

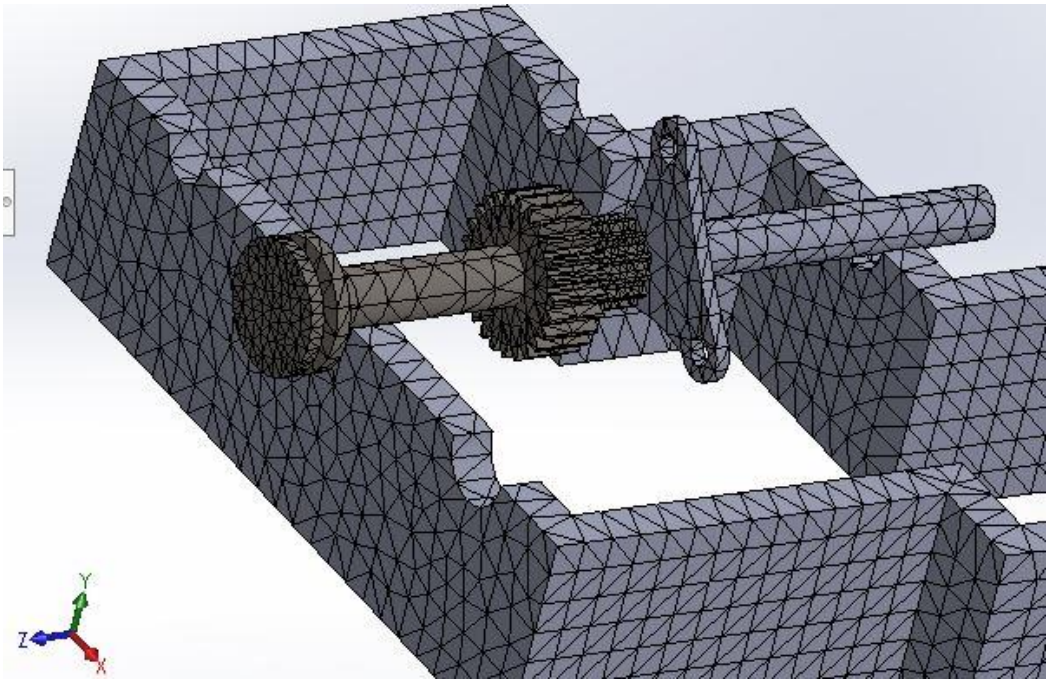

Figure III.7—3. Shaft II mesh type

Chapter III. 3D modelling and dynamic study of powertrain components

The study will analyze the stress constraints on the gears while on load. The following table shows the applied loads.

Table III.7—4. Load application on shaft II

Load type	Load name	Component	Details
Normal force	Remote mass (gear C)	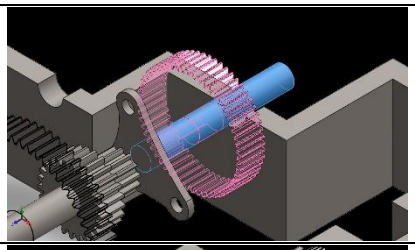	Remote Mass: 6.57161 kg Coordinate System: Global Cartesian coordinates Force Values: 0, 1459.04, 0 N
	Remote mass (gear P)	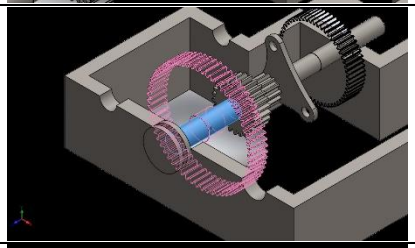	Remote Mass: 14.9132 kg Coordinate System: Global Cartesian coordinates Force Values: 0, 10326.7, 0 N
Torque	Torque on shaft II	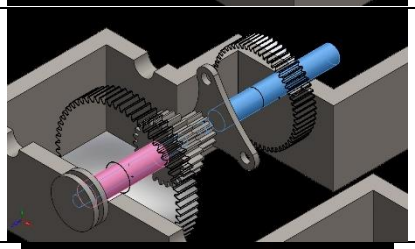	Entities: 2 cylindrical face Value: - 336.73 N.m
Fixed geometry	Housing fixture	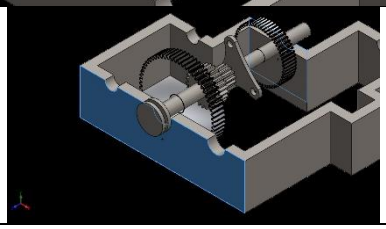	Entities: 2 housing faces Reaction force : 0.0125 N

The results showed the stress on the nodes applied during meshing, the Von Mises nodal stress results are plotted in the following graph.

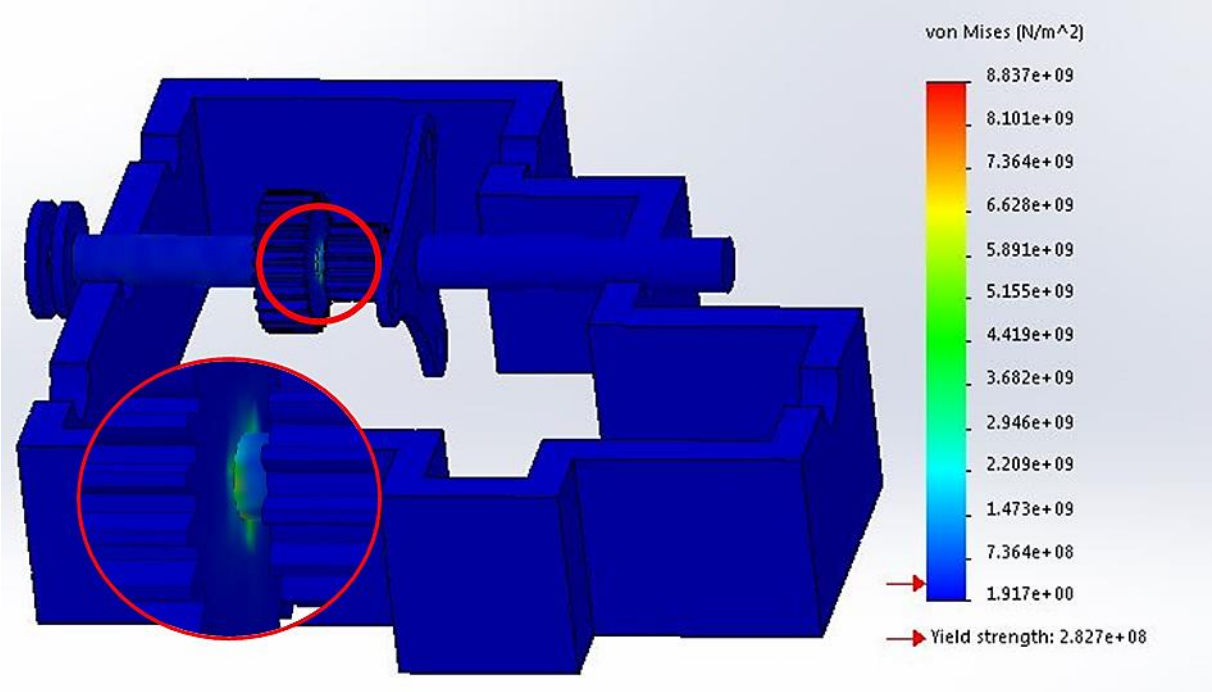

Figure III.7—4. Von Mises stress plot – Shaft II

By observing the dynamic analysis results, the stress values are within the permissible stress value for shaft II pictured as a blue area. However, there is a concentration of stresses on the shaft section located between the sun gear which must be modified by adding a filet.

III.7.3 Shaft III

In this study, we analyze the strength of the shafts and look at the stress concentration areas when the shaft is on load and supported by bearings.

Table III.7—5. Shaft III solid bodies and connections

Components	Treated as	Volumetric properties
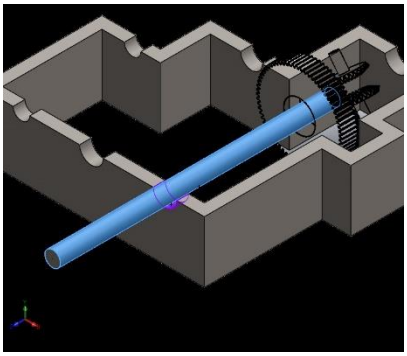	Solid-body (shaft)	Mass:6.90176 kg Volume:0.00087831 m^3 Density:7858 kg/m^3 Weight:67.6373 N
	Solid-body (housing)	Mass:86.0628 kg Volume:0.0109523 m^3 Density:7858 kg/m^3 Weight:843.415 N
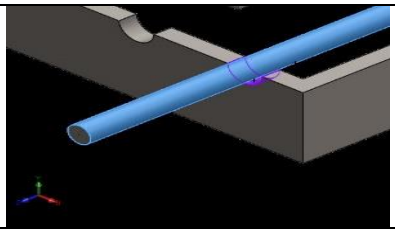	Bearing connector	Number of connectors: 1 Entities: shaft cylindrical face and housing cylindrical aperture

Same as in gears, for study simulation in SolidWorks we used a linear dynamic analysis (nodal time history) with 15 frequencies of iteration including temperature loads as a thermal option when at zero strain, the temperature is at 298 Kelvin.

For meshing, we used a standard solid mesh with 4 Jacobean points, an element size of 28.4867 mm with 1.13947 mm for tolerance.

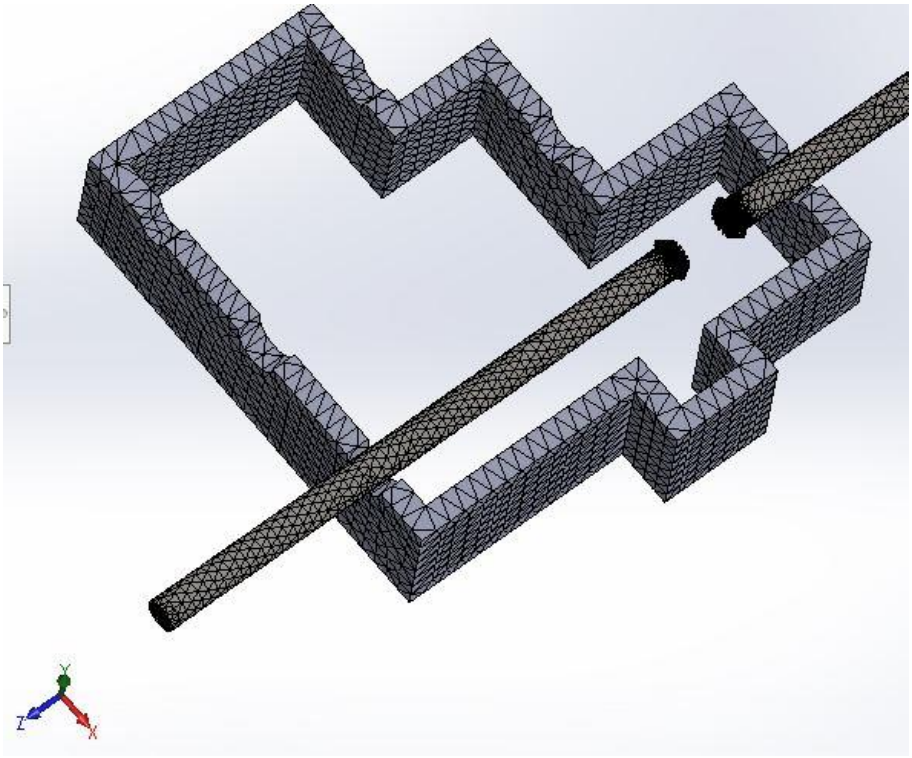

Figure III.7—5. Shaft III mesh type

Chapter III. 3D modelling and dynamic study of powertrain components

The study will analyze the stress constraints on the gears while on load. The following table shows the applied loads.

Table III.7—6. Load application on shaft III

Load type	Load name	Component	Details
Normal force	Remote mass (gear D)	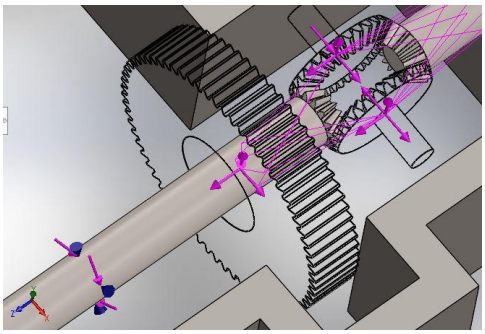	Remote Mass: 9.20963 kg Coordinate System: Global Cartesian coordinates Force Values: 0, 4265.96, 0 N
	Remote mass (bevel gears E and F)		Remote Mass: 2.519736 kg x 2 Coordinate System: Global Cartesian coordinates Force Values: 0, ± 1239.07, 0 N
Torque	Torque on shaft III	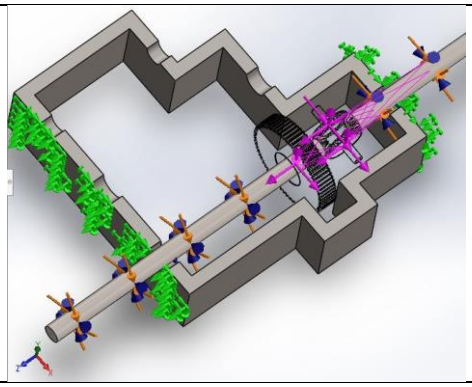	Entities: 2 cylindrical face Value: -145.65 N.m
Fixed geometry	Housing fixture		Entities: 2 housing faces Reaction force : 0.133523 N

The results showed the stress on the nodes applied during meshing, the Von Mises nodal stress results are plotted in the following graph.

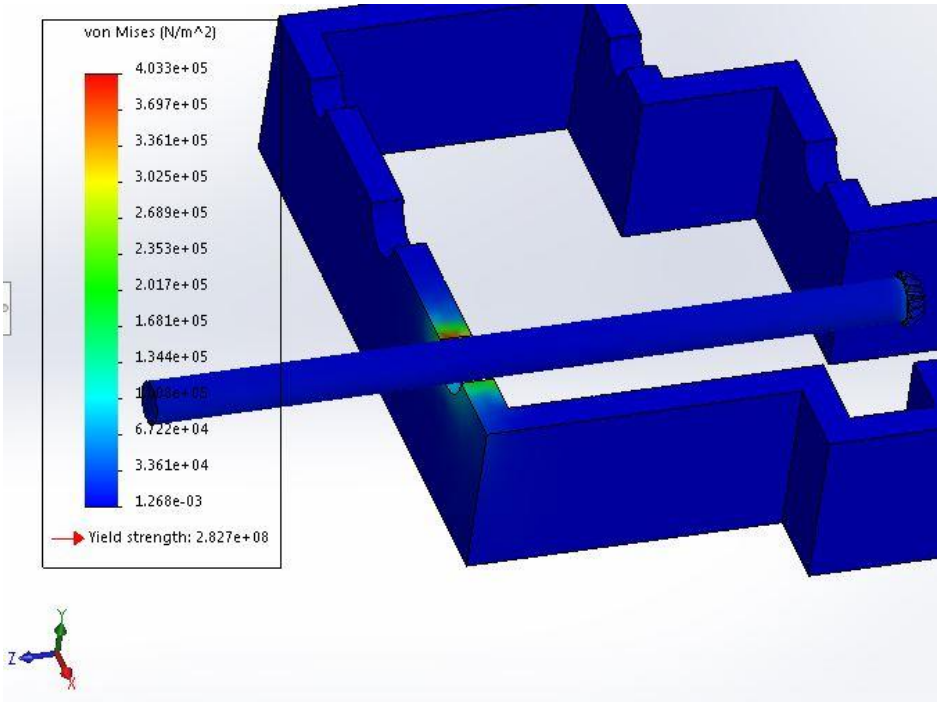

Figure III.7—6. Von Mises stress plot – Shaft III

By observing the dynamic analysis results, the stress values are within the permissible stress value for shaft III pictured as a blue area. However, there is a concentration of stresses on the housing in the location of the bearing, since the shaft is long, more area is needed for support.

III.8 Design modifications

The shaft II section between the sun gear shows a rough edge, the modification in design consist of adding a fillet of 1 mm as shown below.

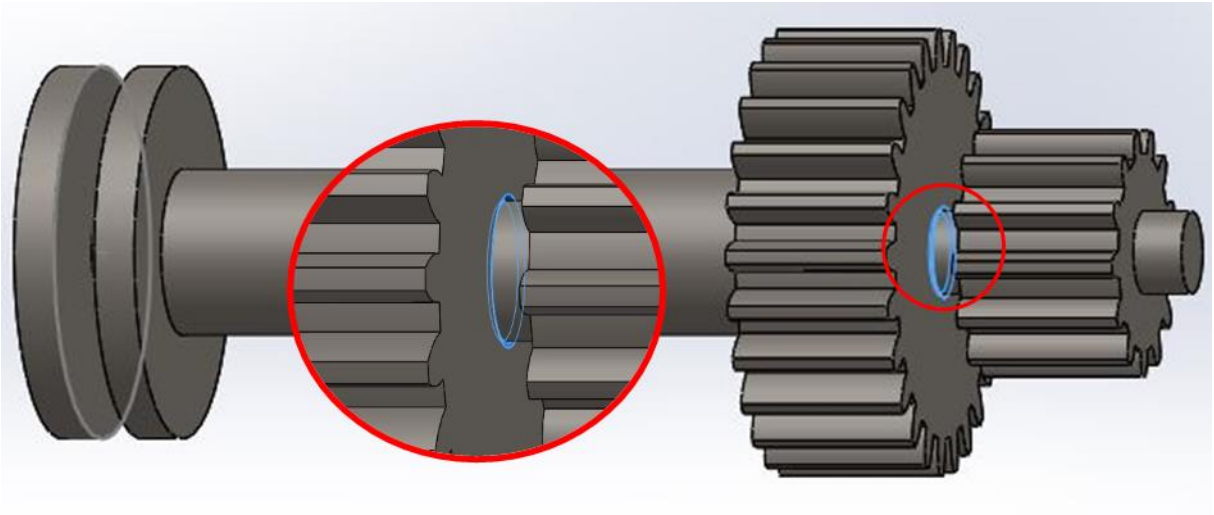

Figure III.8—1. Shaft II modification

For shaft III, the section holding the bearings needed a diameter adjustment to fit the shaft III, so the diameter was decreased to 15 mm.

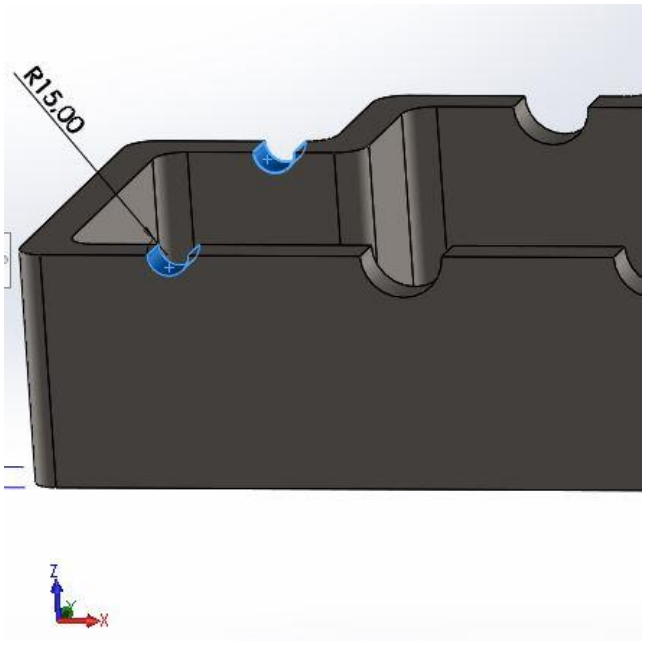

Figure III.8—2. Housing modification

III.9 Conclusion

Through the result analysis of the gears and shaft, we assume that the design will function in the established conditions. However, some modifications are needed in the housing section holding shaft III and the shaft section between the sun gears in shaft II. All designed components including the modified are attached in (Appendix A4).

Conclusions

In this thesis, the design and the study of a powertrain for an electric vehicle providing a two-speed transmission were performed. The two-transmission offers two-speed ranges suited for rural and urban drive cycles for flexible adaptability on the road. It is powered by a PMSM motor with an integrated inverter and a mechanical standard differential is also provided.

in chapter one, a background research study was an important step to understand the geometry and the kinematics in the current EV models, also an insight on the industry provided us with necessary data to work on certain areas such as the driving range and the multiple speed options.

Then in the second chapter, we focused on the transmission components design such as gears, shafts and bearing selection through calculation and MitCalc software calculation analysis of the shafts strength. Before that, we performed a battery and a motor selection on the commercial models existing in the market then we checked the adaptability of the motor to the required vehicle performances.

In the third chapter, we designed the powertrain components according to the previous calculations and selection catalogs for the motor and battery. Then we performed a dynamic linear analysis on each gear train and the shafts through SolidWorks simulation. The results showed theoretically the components are apt to work on the chosen condition. However, some changes in the design of shaft II and the housing were required. All the components drawings are presented in the appendices.

The electric vehicle transmission design, despite the alleged simplicity compared to internal combustion engine vehicle transmissions, still integrates a vast number of variables that form a network and influence each other. This makes the design an intricate project, constantly changing. Given that there are still several topics that could be considered, some future work is a compact transmission with two motors, integration of an electric vehicle and a multi-speed transmission.

References

1. *Standard gears*, C. Morse, Editor.
2. 2020, *Electric Vehicle Charging Station Market to Reach USD 264.80 Billion by 2026*, NASDAQ OMX's News Release Distribution Channel: New York.
3. 2021, NASDAQ OMX's News Release Distribution Channel; New York.
4. 2021-2022, C. Motion, Editor: 7929 SW Burns Way, Suite F,Wilsonville, OR 97070-7678 USA.
5. Algérie, T.d.e.*Oussama Touaba – ce chercheur qui a fabriqué une voiture électrique 100% algérienne*. [cited 2021; Available from: https://topdestinationsalgerie.com/oussama-touaba-ce-chercheur-qui-a-fabrique-une-voiture-electrique-100-algerienne/.
6. Amor, O. and N. Parera, 2018, *Electric and Hybrid Vehicles Crash Test Protocol Improvements*,in., Springer International Publishing: Cham. p. 351-362.
7. Arora, S., W. Shen, and A. Kapoor, 2016, *Review of mechanical design and strategic placement technique of a robust battery pack for electric vehicles.* Renewable & sustainable energy reviews. **60**(Journal Article): p. 1319-1331.
8. Bandi, M., et al., 2020, *Design and Modeling of Fuel Cell Hybrid Electric Vehicle for Urban Transportation*,in., Springer Singapore: Singapore. p. 1-31.
9. Bengang Gong, R.L., Xiaoqi Zhang, 2020, *Market acceptability assessment of electric vehicles based on an improved stochastic multicriteria acceptability analysis-evidential reasoning approach.* Cleaner Production: p. 12.
10. Bhandari, V.B., *Objective type questions for Design of machine elements*. 3rd edition ed. New Delhi: Hill publishing company limited.
11. Carfolio. *2020, Wuling Hong Guang MINI EV CN*. [cited 2021; Available from: https://www.carfolio.com/wuling-hong-guang-mini-ev-728145#a_chassis.
12. Chevalier, A., 2004, *Guide du dessinateur industriel*. ed.: Hachette technique.
13. CleanTechnica. *World Plugin Vehicle Sales (January - December 2020).* [cited 2021; Available from: https://cleantechnica.com/2021/02/04/global-electric-vehicle-top-20-ev-sales-report/.
14. Dhinakaran, V., et al., 2020, *Study on Electric Vehicle (EV) and Its Developments Based on Batteries, Drive System and Charging Methodologies in Modern World*,in., Springer Singapore: Singapore. p. 103-118.

15. EVcompare. *Hyundai Kona Electric 39 kWh*. [cited 2021; Available from: https://www.evcompare.io/cars/hyundai/hyundai_kona_electric_standard-range_2018

16. Fabricio A. Machado, P.J.K., Daniel G. Barroso, and Ali Emadi, *Multi-speed Gearboxes for Battery Electric Vehicles: Current Status and Future Trends*. IEEE Open Journal of Vehicular Technology.

17. Faraz, A., et al., 2020, *Battery Electric Vehicles (BEVs)*,in., Springer Singapore: Singapore. p. 137-160.

18. G.J. Os´orio, M.L., M.Gough, M.Javadi, H. Espassandim, M.Shafie-khah, J. Catalao, 2021, *Modeling an electric vehicle parking lot with solar rooftop participating in the reserve market and in ancillary services provision.* Cleaner Production: p. 15.

19. Gillespie, T.D., 1992, *Fundamentals Of Vehicle Dynamics*. 1st edition ed.: Society of Automotive Engineers, Inc.

20. Group, O. *Types of Electric Cars and Working Principles*. [cited 2021; Available from: https://www.omazaki.co.id/en/types-of-electric-cars-and-working-principles/.

21. Group, S. 2021, *The Surprisingly Interesting History of Electric Cars*.

22. Group,V. *Chosing the right bearing*. [cited 2022; Available from: http://www.cbkbearings.com/index.php?sec=56&subsec=107&itm=139&subitm=30.

23. Grunditz, E.A., 2016, *Design and Assessment of Battery Electric Vehicle Powertrain, with Respect to Performance, Energy Consumption and Electric Motor Thermal Capability*, in *Department of Energy and Environment*, Chalmers University of technology: Göteborg, Sweden. p. 229.

24. Hasan, S., 2021, *Assessment of electric vehicle repurchase intention: A survey-based study on the Norwegian EV market.* Transportation Research Interdisciplinary Perspectives p. 13.

25. Jae-Oh Han, J.-W.S., Jae-Chang Kim and Se-Hoon Oh, 2019, *Design 2-Speed Transmission for Compact Electric Vehicle Using Dual Brake System.* MDPI applied sciences.

26. Matulka, R. 2014, *The History of the Electric Car*.

27. Mauro Erriquez, T.M., Pierre-Yves Moulière, and Philip and Schäfer.2017, *Trends in electric-vehicle design*. 2017 12/102021]; Available from: https://www.mckinsey.com/industries/automotive-and-assembly/our-insights/trends-in-electric-vehicle-design

28. NN, A., *Nissan Leaf Battery Pack*.

29. R.Bernal, D.O., M.Negrete-Pincetic, Á.Lorca, 2020, *Management of EV charging stations under advance reservations schemes in electricity markets.* Sustainable Energy, Grids and Networks: p. 11.

30. Renault. *Renault Zoe E-Tech Electric*. [cited 2021; Available from: https://www.renault.co.uk/electric-vehicles/zoe/battery.html.

31. Rodrigues, C.D.P., 2018, *Design of a high-speed transmission for an electric vehicle*, in *Department of Mechanical Engineering*, University of Porto: Porto, Portugal. p. 335.

32. Sanguesa, J.A., et al., 2021, *A Review on Electric Vehicles: Technologies and Challenges.* Smart Cities. **4**(1): p. 372.

33. Singh, H., et al., 2020, *Plug-In Hybrid Electric Vehicles (PHEVs),*in., Springer Singapore: Singapore. p. 53-72.

34. Sungsoon Jang, J.Y.C., 2021, *Which consumer attributes will act crucial roles for the fast market adoption of electric vehicles? Estimation on the asymmetrical & heterogeneous consumer preferences on the EVs.* Energy Policy: p. 11.

35. Tesla.*Tesla Model 3*. [cited 2021; Available from: https://www.tesla.com/model3.

36. Tesla.*Tesla model Y*. [cited 2021; Available from: https://www.tesla.com/en_eu/modely.

37. U.S. Department of Energy, E.E.a.R.E.*Alternative Fuels Data Center*. [cited 2021; Available from: https://afdc.energy.gov/vehicles/.

38. Wilson, K.A. 2018, *Worth the Watt: A Brief History of the Electric Car, 1830 to Present*. **2021**.

List of figures

List of tables

Appendices

Appendix A1. Lithium-ion battery dimensions

Appendix A2. CM200 inverter and HVH250 motor (Cascadia Motion Catalog)

Appendix A3 – 1. Cylindrical roller bearing without outer ring (CBK BEARINGS)

Appendix A3 – 2. Taper roller bearings metric size (CBK BEARINGS)

Appendix A4 – 1. Planetary gear set drawing

Appendix A4 – 2. Planet – sun gear assembly drawing

Appendix A4 – 3. Stage brakes drawing

Appendix A4 – 4. Spur gear P drawing

Appendix A4 – 5 . Cover drawing

Appendix A4 – 6. Internal spur gear drawing

Appendix A4 – 7 . Carrier drawing

Appendix A4 – 8 . Differential drawing

Appendix A4 – 9. Spur gear D drawing

Appendix A4 – 10 . Straight bevel gear drawing

Appendix A4 – 11. Straight bevel pinion drawing

Appendix A4 – 12. Connection drawing

Appendix A4 – 13. Transmission drawing

Appendix A4 – 14 . Housing drawing

Appendix A4 – 15. Gear C drawing

Appendix A4 – 16. Gear M drawing

Appendix A4 – 17. Key C drawing

Appendix A4 – 18. Key M drawing

Appendix A4 – 19. Shaft I drawing

Appendix A1

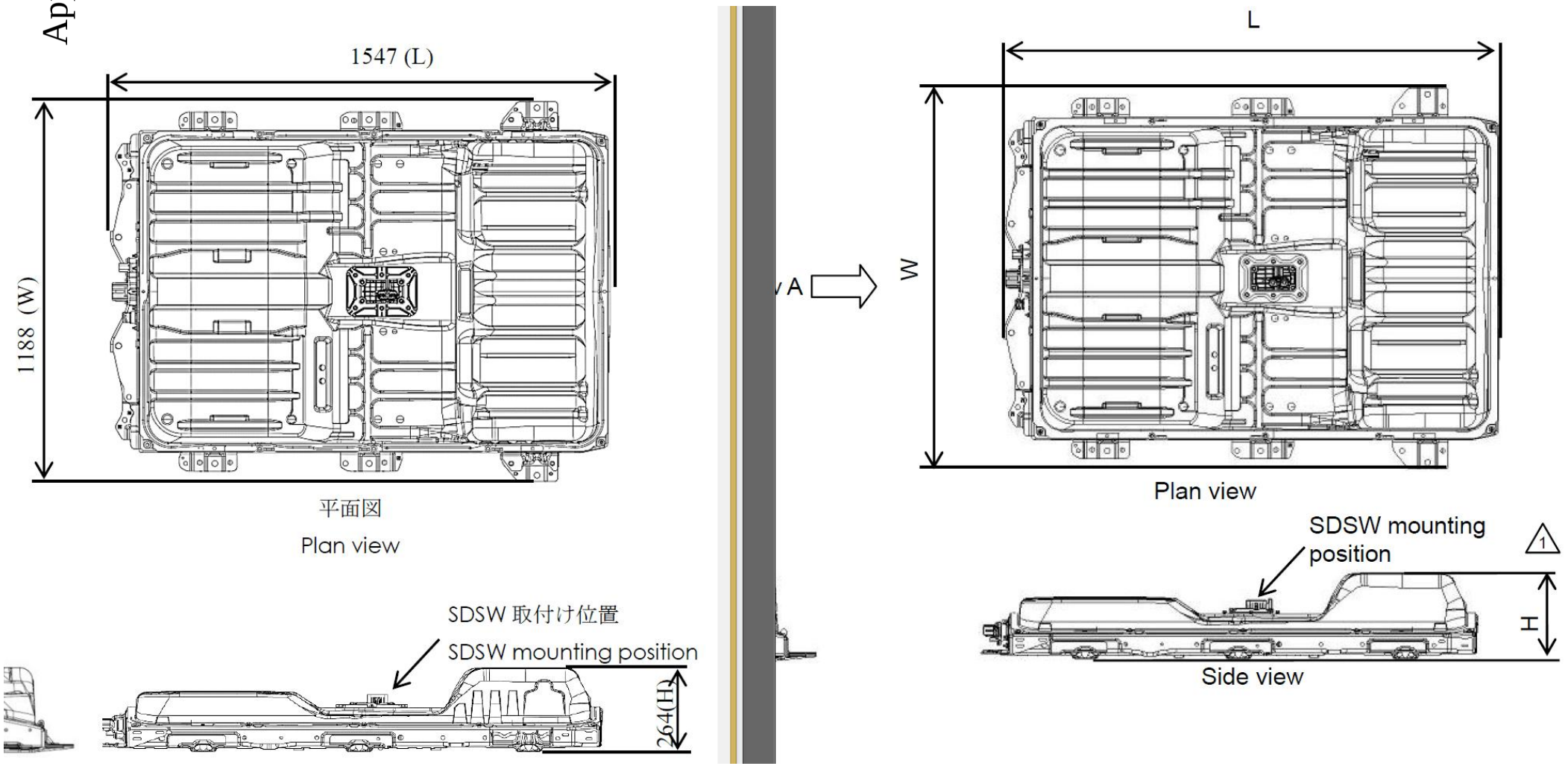
1547 (L)
1188 (W)
平面図
Plan view
SDSW 取付け位置
SDSW mounting position
264(H)
v A
L
W
Plan view
SDSW mounting position
1
H
Side view

iM-225-DX-D (INTEGRATED MODULE)

Made with BorgWarner HVH250-115D motor core

Built using the CM200 inverter and HVH250 motor core, this integrated module packs a 500Nm punch within a compact package. It's loaded with integrated features like an oil pump, oil cooler, oil sump and water pump.

Peak Torque	500Nm
Peak Power	225kW
Continuous Torque	230Nm
Continuous Power	110-135 kW
Maximum Speed	12000rpm
Weight	64 kg
Motor Cooling Medium	Dexron VI
Inverter Cooling Medium	50% E.G. / 50% Water
Maximum Water Temperature	80°C (Peak performance below 60°C, Mild Derate 60-80°C, No Torque at 100°C)
Combined Efficiency	95% peak (@200Nm, 5500rpm)

FEATURES

- 480Vdc maximum voltage (with CM200DX inverter)
- Integrated oil pump
- Integrated water pump
- Integrated oil cooler
- Shallow sump depth, 170mm from shaft centerline to bottom
- Only 300mm in axial length and 405mm in total height
- Auxiliary ports provided for optional external oil connections
- Provided transmission connection bolt patterns:
  - 6-bolt 'Cascadia pattern'
  - 16-bolt 'Remy pattern' (e.g. 31-03 connection)
  - 4-bolt Porsche G50 pattern

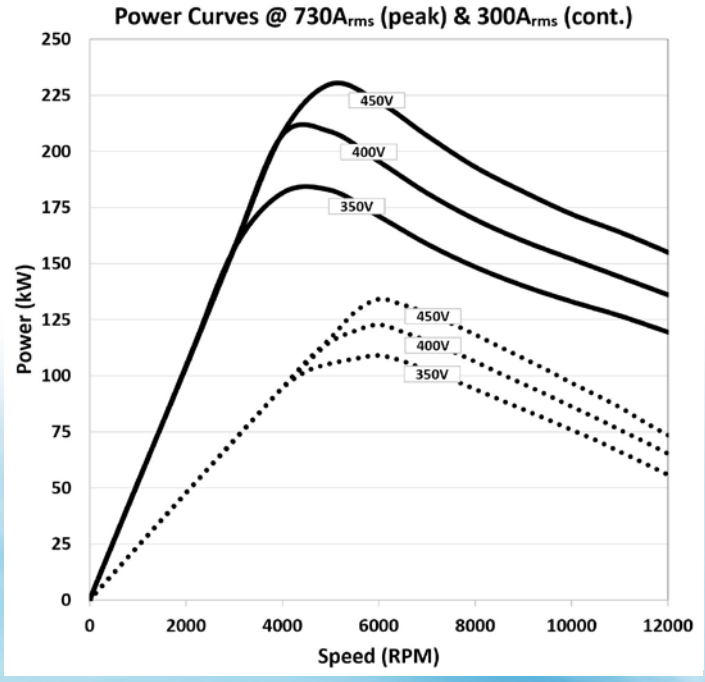

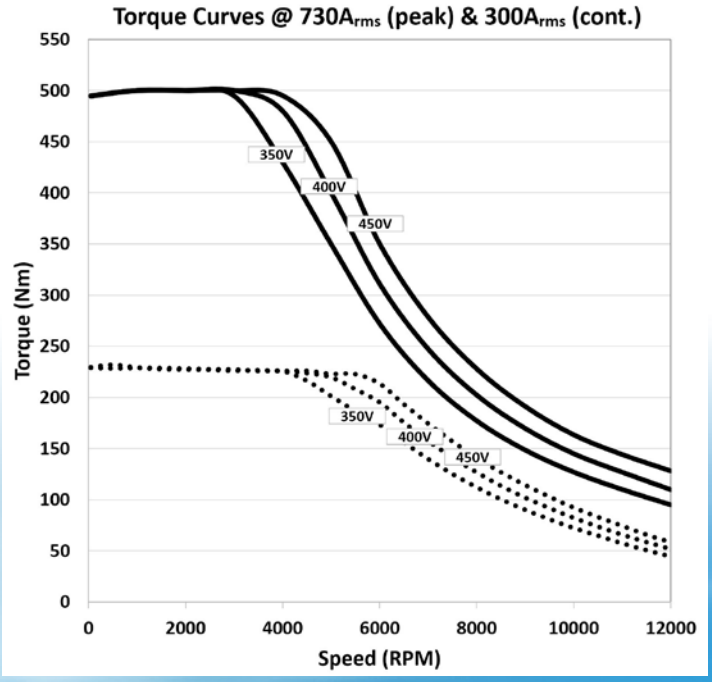

Point Camera Here

To View Manuals

CASCADIA MOTION

cascadiamotion.com +1-503-344-5085

iM-225-DZ-S Also Available

Appendix A2 - 1

Search

>

Site Map

- Home
- Business
- Products
  - Rolling Bearings Program
    - Deep groove ball bearings
    - Special ball bearings
    - Self-aligning ball bearings
    - Cylindrical roller bearings
      - Cylindrical roller bearing without inner ring
      - Cylindrical roller bearing without outer ring
    - Special cylindrical roller bearings
    - Taper roller bearings metric size
    - Taper roller bearings inch size and special
    - Spherical roller bearings
    - Thrust ball bearings
    - Ball bearings Units
    - Ball bearing inserts
    - Farm implement ball bearing inserts
    - Drawn cup needle roller bearings
    - Drawn cup roller clutches
    - Cylindrical roller clutch and ball bearing assemblies
    - Needle roller and cage assemblies for connecting rod bearing arrangement
    - Needle roller bearing full complement
    - Needle roller bearing double row
    - Needle roller bearings without inner ring
    - Thrust needle roller and cage assemblies
    - Thrust washers
    - Yoke type track roller bearings
    - Inner rings
    - Spherical plains bearings
    - Angular contact spherical plain bearings
    - Rod ends - Metric sizes
    - Injection rod ends
    - Rod ends Sizes - Inch sizes
  - Linear Motion Program
- Catalogues
- Contact

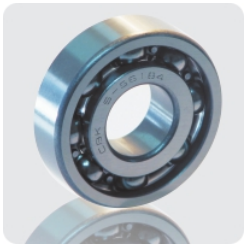

Cylindrical roller bearing without outer ring

CBK Keeps Moving

Cylindrical roller bearings:

Without inner ring - RNU
Without outer ring - RN

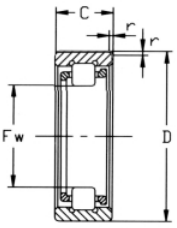

RNU

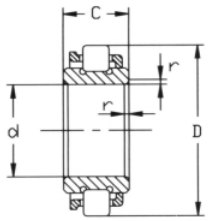

RN

Shaft Diameter (mm)	Bearing Designation		Boundary Dimensions (mm)				Basic Load Rating (N)		Limiting Speed (rpm)		Weight (kg)
	Current Designation	Original Designation	Fw / d	D/Ew	C	rs min	Cr Dynamic	Cor Static	Grease	Oil	
20	RN204	502204	20	40	14	1	15800	13100	13800	16400	0.055
	RN304	502304	20	44	15	1.1	21800	17700	11400	13800	0.079
22	SZ-204		22	32	9	0.3	7800	8100	16000	19000	0.024
22.1	RNU203ETN1		22.1	40	12	0.6	16900	13800	16000	19000	0.052
22.9	RNU203	292203	22.9	40	12	0.6	11400	9100	16000	19000	0.065
25	LRN205/YA	922205	25	52	15	0.6	38400	34700	11400	13800	0.151
	RN205	502205	25	45	15	1	17000	14900	11400	13800	0.071
27	RNU204		27	47	14	1.0	14400	13100	13800	16400	0.080
27.5	RNU6/27.5	292604E	27.5	52	21	1.1	42000	38700	9200	11400	0.168
28	RNU304	292304	28	52	15	1.1	21800	17700	11400	13800	0.119
30	RN206	502206	30	53.5	16	1	23900	22200	9400	11300	0.112
	RN306	502306	30	62	19	1.1	35900	31900	7800	9200	0.197
	SZ-201		30	62	27	1.1	74500	77400	7000	8500	0.316
32	RNU205	292205	32	52	15	1	17000	14900	11400	13800	0.096
35	RN207	502207	35	61.8	17	1.1	31400	28900	8300	9900	0.156
	RN307	502307	35	68.2	21	1.5	46400	43000	7800	9200	0.245
	RNU305	292305	35	62	17	1.1	29100	25200	9200	11400	0.179
38.5	RNU206	292206	38.5	62	16	1	23900	22200	8900	10500	0.154
40	RN308	502308	40	77.5	23	1.5	58600	56900	6600	7900	0.360
42	RNU306	292306	42	72	19	1.1	35900	31900	7800	9200	0.250
43.8	RNU207	292207	43.8	72	17	1.1	31400	28900	8300	9900	0.222
45	RN309	502309	45	86.5	25	1.5	72900	69900	5900	7000	0.458
46.2	RNU307		46.2	80	21	1.5	46400	43000	7700	9200	0.357
50	RN210		50	80.4	20	1.1	48100	50900	5900	7000	0.287
	RN310	502310	50	95	27	2	88900	88800	5400	6500	0.622
	RNU208	292208	50	80	18	1.1	43700	42900	7300	8700	0.278
	RNU208/P6		50	80	18	1.1	43700	42900	7300	8700	0.278
53.5	RNU308		53.5	90	23	1.5	58600	56900	6600	7900	0.497
55	RN211		55	88.5	21	1.5	57900	62200	6000	7100	0.356
60	RN212	502212	60	97.5	22	1.5	71800	79800	5400	6500	0.490
60.4	RNU210	292210	60.4	90	20	1.1	48100	50900	6600	7900	0.339
65	RNU310	292310	65	110	27	2	88900	88800	5400	6300	0.853
66.5	RNU211		66.5	100	21	1.5	57900	62200	6000	7100	0.458
70	RN214		70	110.5	24	1.5	82100	93500	4800	5700	0.645
73.5	RNU212	292212	73.5	110	22	1.5	71800	79800	5400	6500	0.588
84.5	RNU214		84.5	125	24	1.5	82100	93500	4800	5700	0.845
90	RN90X115X23		90	115	23	1	64100	111200	------	-------	0.485
96.5	RNU1017	292117	96.5	130	22	1.1	68900	86800	4500	5400	0.718

Clearence - C2 - C3 - C4 - According DIN 620 - Are available under request.

CBK Keeps Moving

Taper roller bearings metric size

PREFIX	
A	Modified internal design-increased capacity
P6	Accurracy to ISO tolerance class 6
X	Boundary dimensions altered to conform to ISO standards
FD	Solid collapsible steel cage

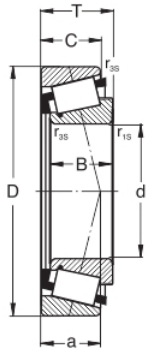

Shaft Diameter (mm)	Current Designation	Boundary Dimensions (mm)									Basic Load Rating (N)		Limiting Speed (rpm)		Weight (kg)
		d	D	B	C	T	r1s min	r2s min	r3s min	a ~	Cr Dynamic	Cor Static	Grease	Oil	
15	30202A	15	35	11	10	11.75	0.6	0.6	0.3	10	15	14.3	12000	16000	0.057
17	30203A	17	40	12	11	13.25	1	1	0.3	10	19.3	18.8	9000	13000	0.07
	30303A	17	47	14	12	15.25	1	1	0.3	10	26	25.7	8500	12000	0.13
	32303A	17	47	19	16	20.25	1	1	0.3	12	35.3	36.3	8000	11000	0.17
20	30204A	20	47	14	12	15.25	1	1	0.3	11	27.5	28	8000	11000	0.12
	30304A	20	52	15	13	16.25	1.5	1.5	0.6	11	31.6	32	8000	11000	0.17
	32304A	20	52	21	18	22.25	1.5	1.5	0.6	11	44	45.5	7500	11000	0.23
25	30205A	25	52	15	13	16.25	1	1	0.3	12	32.6	35.5	7500	10000	0.16
	31305A	25	62	17	13	28.25	1.5	1.5	0.6	20	38	40	5600	7500	0.22
	32305A	25	62	24	20	25.25	1.5	1.5	0.6	15	65	69.3	6000	8000	0.36
	30305A	25	62	17	15	18.25	1.5	1.5	0.6	13	44.6	43	6700	9000	0.26
	31305A	25	62	17	13	18.25	1.5	1.5	0.6	20	40.5	43.5	5600	7500	0.26
	32205A	25	52	18	15	19.25	1	1	0.3	18	41.3	49.2	7000	9500	0.19
	33205A	25	52	22	18	22	1	1	0.3	14	47.1	55.8	6700	9000	0.23
30	30206A	30	62	16	14	17.25	1	1	0.3	14	40.2	44	6300	8500	0.23
	32206A	30	62	20	17	21.25	1	1	0.3	15	50.1	57	6300	8500	0.29
	33206A	30	62	25	19.5	25	1	1	0.3	16	63.8	75.4	5600	7500	0.37
	30306A	30	72	19	16	20.75	1.5	1.5	0.6	15	56.1	56	5600	7500	0.39
	32306A	30	72	27	23	28.75	1.5	1.5	0.6	18	76.5	85	5300	7000	0.54
	31306A	30	72	19	14	20.75	1.5	1.5	0.6	22	47.3	50	5000	6700	0.37
35	32007X	35	62	18	14	18	1	1	0.3	15	36.4	47.1	6000	8000	0.22
	30207A	35	72	17	15	18.25	1.5	1.5	0.6	15	51.2	56	5300	7000	0.33
	32207A	35	72	23	19	24.25	1.5	1.5	0.6	17	66	78	5300	7000	0.49
	30307A	35	80	21	18	22.75	2	1.5	0.6	16	72.1	73.5	5000	6700	0.52
	32307A	35	80	31	25	32.75	2	1.5	0.6	20	95.2	106	4800	6300	0.72
	31307A	35	80	21	15	22.75	2	1.5	0.6	25	59.7	63.9	4500	6000	0.50
40	32008X	40	68	19	14.5	19	1	1	0.3	15	54	71	5300	7000	0.27
	30208A	40	80	18	16	19.75	1.5	1.5	0.6	16	63.4	70.2	4800	6300	0.42
	32208A	40	80	23	19	24.75	1.5	1.5	0.6	19	74.8	86.5	4800	6300	0.53
	30308A	40	90	23	20	25.25	2	1.5	0.6	19	85.8	95	4500	6000	0.74
	32308A	40	90	33	27	35.25	2	1.5	0.6	23	117.9	142.7	4000	5300	0.99
	31308A	40	90	23	17	25.25	2	1.5	0.6	28	73.7	81.5	4000	5300	0.68
45	32009A	45	75	20	15.5	20	1	1	0.3	52	61	86.5	4800	6300	0.34
	30209A	45	85	19	16	20.75	1.5	1.5	0.6	18	66	76.5	4500	6000	0.47
	32209A	45	85	23	19	24.75	1.5	1.5	0.6	20	80.9	98	4500	6000	0.59
	33209X	45	85	32	25	32	1.5	2	0.5	22	99.5	124	4000	5300	0.82
	30309A	45	100	25	22	27.25	2	1.5	0.6	21	108	120	4000	5300	0.99
	32309A	45	100	36	30	38.25	2	1.5	0.6	25	140	170	3600	4800	1.33
	31309A	45	100	25	18	27.25	2	1.5	0.6	31	87.6	101.1	3400	4500	0.91

Taper roller bearings metric size

Shaft Diameter (mm)	Current Designation	Boundary Dimensions (mm)									Basic Load Rating (N)		Limiting Speed (rpm)		Weight (kg)
		d	D	B	C	T	r1s min	r2s min	r3s min	a ~	Cr Dynamic	Cor Static	Grease	Oil	
50	32010X	50	80	20	15.5	20	1	1	0.3	18	61.1	89	4500	6000	0.37
	33110A	50	85	26	20	26	1.5	1.5	0.6	20	89.3	124.1	4300	5600	0.59
	30210A	50	90	20	17	21.75	1.5	1.5	0.6	19	76.5	91.5	4300	5600	0.54
	32210A	50	90	23	19	24.75	1.5	1.5	0.6	21	82.5	100	4300	5600	0.63
	30310A	50	110	27	23	29.25	2.5	2	0.6	23	131.4	150	3600	4800	1.20
	32310AX1	50	110	40	33	42.25	2.5	2	0.6	27	174	244	3200	4300	1.74
	31310A	50	110	27	19	29.25	2.5	2	0.6	34	105	138	3200	4300	1.16
55	32011A	55	90	23	17.5	23	1.5	1.5	0.6	20	80.2	117.2	4000	5300	0.56
	30211A	55	100	21	18	22.75	2	1.5	0.6	20	90.3	106.3	3800	5000	0.72
	32211A	55	100	25	21	26.75	2	1.5	0.6	22	106	129	3800	5000	0.84
	33211A	55	100	35	27	35	2	1.5	0.6	25	138	190	3400	4500	1.20
	30311A	55	120	29	25	31.5	2.5	2	0.6	24	135	179	3200	4300	1.53
	32311A	55	120	43	35	45.5	2.5	2	0.6	29	200	275	3000	4000	2.20
	31311A	55	120	29	21	31.5	2.5	2	0.6	37	118.3	131.8	2800	3800	1.50
60	32012X	60	95	23	17.5	23	1.5	1.5	0.6	21	81.7	122.2	3800	5000	0.59
	30212A	60	110	22	19	23.75	2	1.5	0.6	22	98	125	3400	4500	0.86
	32212A	60	110	28	24	29.75	2	1.5	0.6	24	126	174	3400	4500	1.10
	30312A	60	130	31	26	33.5	3	2.5	1	26	167	210	3000	4000	1.90
	32312A	60	130	46	37	48.5	3	2.5	1	31	229	323	2600	3600	2.80
	31312A	60	130	31	22	33.5	3	2.5	1	39	134	172	2600	3600	1.83
65	32013X	65	100	23	17.5	23	1.5	1.5	0.6	22	84.2	127	3400	4500	0.63
	30213A	65	120	23	20	24.75	2	1.5	0.6	23	115	150	3000	4000	1.10
	32213A	65	120	31	27	32.75	2	1.5	0.6	27	160.9	221.7	3000	4000	1.50
	33213A	65	120	41	32	41	2	1.5	0.6	29	202.2	281.6	2800	3800	2.05
	30313A	65	140	33	28	36	3	2.5	1	28	194	249	2600	3600	2.30
	32313A	65	140	48	39	51	3	2.5	1	33	260	360	2400	3400	3.40
	31313A	65	140	33	23	36	3	2.5	1	42	156	197	2200	3200	2.25
70	32014X	70	110	25	19	25	1.5	1.5	0.6	23	101	153	3200	4300	0.84
	30214A	70	125	24	21	26.25	2	1.5	0.6	25	125	166	3000	4000	1.22
	32214A	70	125	31	27	33.25	2	1.5	0.6	28	155	228	2800	3800	1.56
	30314A	70	150	35	30	38	3	2.5	1	29	220	282	2400	3400	2.90
	32314A	70	150	51	42	54	3	2.5	1	36	296	429	2200	3400	4.10
	31314A	70	150	35	25	38	3	2.5	1	45	176	224	2000	3000	2.85
75	32015X	75	115	25	19	25	1.5	1.5	0.6	25	103.1	160.2	3000	4000	0.90
	30215A	75	130	25	22	27.25	2	1.5	0.6	27	135	182	2800	3800	1.33
	32215A	75	130	31	27	33.25	2	1.5	0.6	29	160	234	2600	3600	1.62
	30315A	75	160	37	31	40	3	2.5	1	31	242	318	2200	3200	3.40
	32315A	75	160	55	45	58	3	2.5	1	38	344	494	2000	3000	5.00
	31315A	75	160	37	26	40	3	2.5	1	50	194	250	1800	2600	3.50
	33215A	75	130	41	31	41	2	1.5	0.6	32	192	302	2400	3400	2.25
80	32016X	80	125	29	22	29	1.5	1.5	0.6	27	138	216	2600	3600	1.30
	33116A	80	130	37	29	37	2	2	0.6	30	181	317	2600	3600	1.60
	30216A	80	140	26	22	28.25	2.5	2	0.6	28	147	203	2400	3400	1.59
	32216A	80	140	33	29	35.25	2.5	2	0.6	30	184	263	2400	3400	2.00
	30316A	80	170	39	33	42.5	3	2.5	1	33	271	377	2000	3000	4.00
	32316A	80	170	58	48	61.5	3	2.5	1	41	378	545	1900	2800	5.90
85	33117A	85	140	41	32	41	2.5	2	0.6	32	215.7	354.2	2400	3400	2.45
	30217A	85	150	28	24	30.5	2.5	2	0.6	30	171	239	2200	3200	2.00
	32217A	85	150	36	30	38.5	2.5	2	0.6	33	212	309	2200	3200	2.50
	30317A	85	180	41	34	44.5	4	3	1	35	305	399	1900	2800	4.70
	32317A	85	180	60	49	63.5	4	3	1	42	406	597	1800	2600	6.95

Appendix A4 - 1

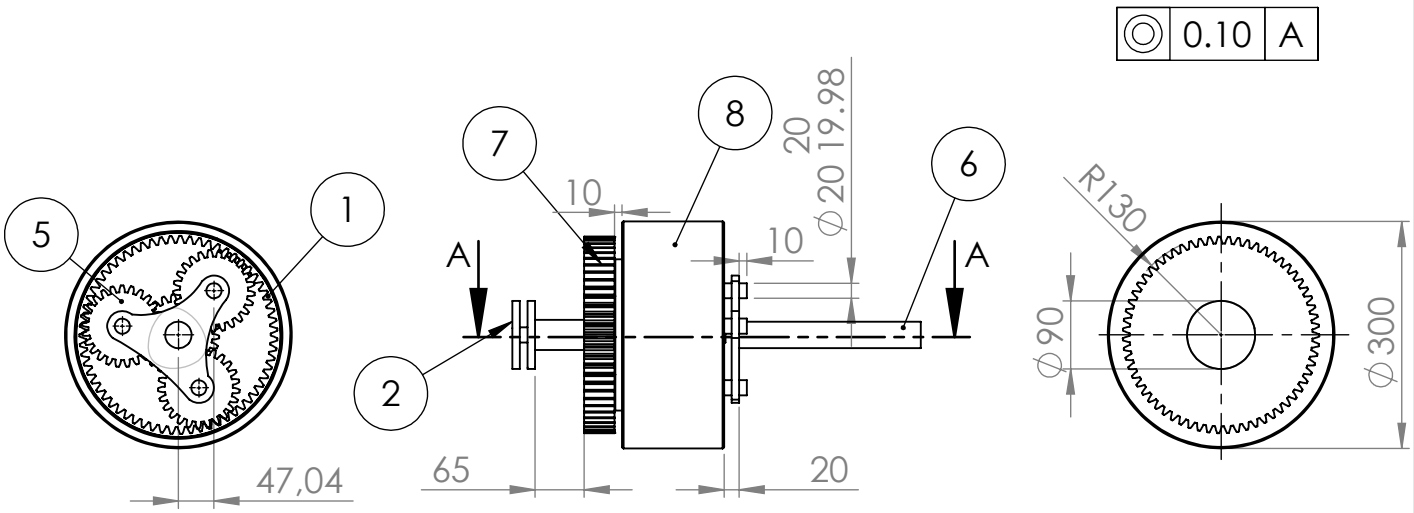

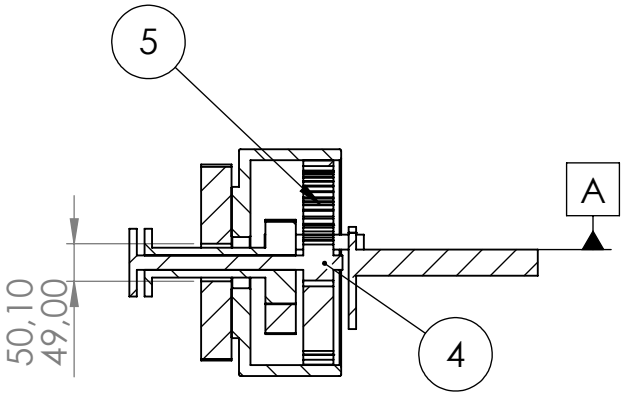

SECTION A-A

Tolerancing

00 = ± 0.3
R 00 = ± 0.01
00.00 = ± 0.005
angular = ± 0°'30

Component N°	Component name	Details	Quantity
1	Internal spur gear	ISO - 4M63T20PA40FW	1
2	Stage brakes	-	2
4	Sun gear	4M15T	4
5	Planet gear	4M30T	4
6	Carrier	-	1
7	Spur gear	4M63T20PA40FW	1
8	Cover	-	1

Scale:1/2	Planetary gear set	AMINI Dahbia Date: 14/01/2022
A4	Thesis drawing Master's in mechanical design	University Mouloud Mammeri of Tizi Ozou Faculty of construction engineering Department of mechanical engineering

Appendix A4 - 2

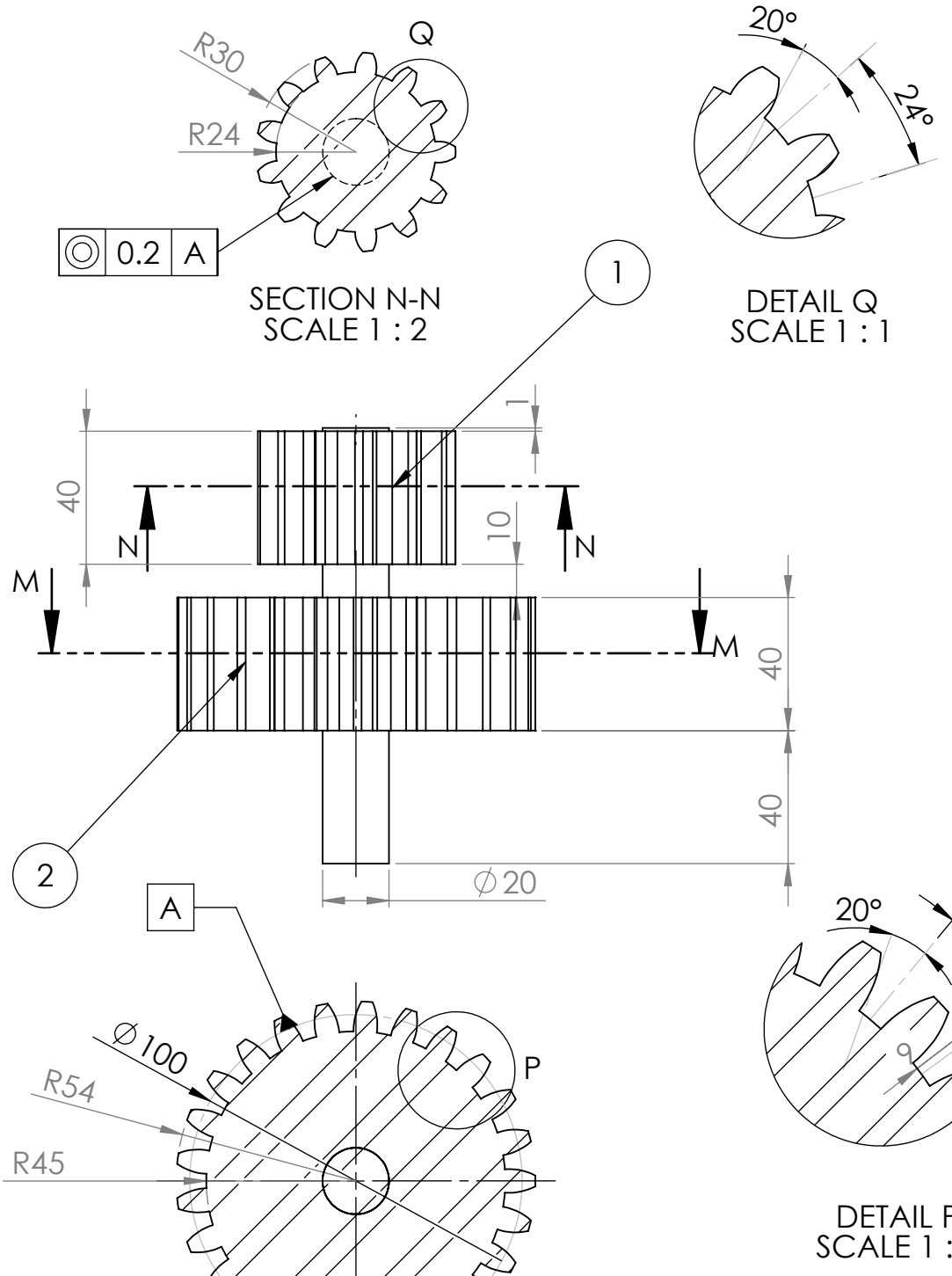

Tolerancing

00 = ± 0.2
R 00.0 = ± 0.1
angular = ± 0°'30

General roughness Ra = 0.36 um
Teeth roughness Ra<0.25um

Component N°	Component name
1	Sun gear
2	Planet gear

Scale:1/2

Planet - sun gears assembly

AMINI Dahbia

Date: 14/01/2022

A4

Thesis drawing
Master's in mechanical design

University Mouloud Mammeri of Tizi Ozou
Faculty of construction engineering
Department of mechanical engineering

Appendix A4 - 3

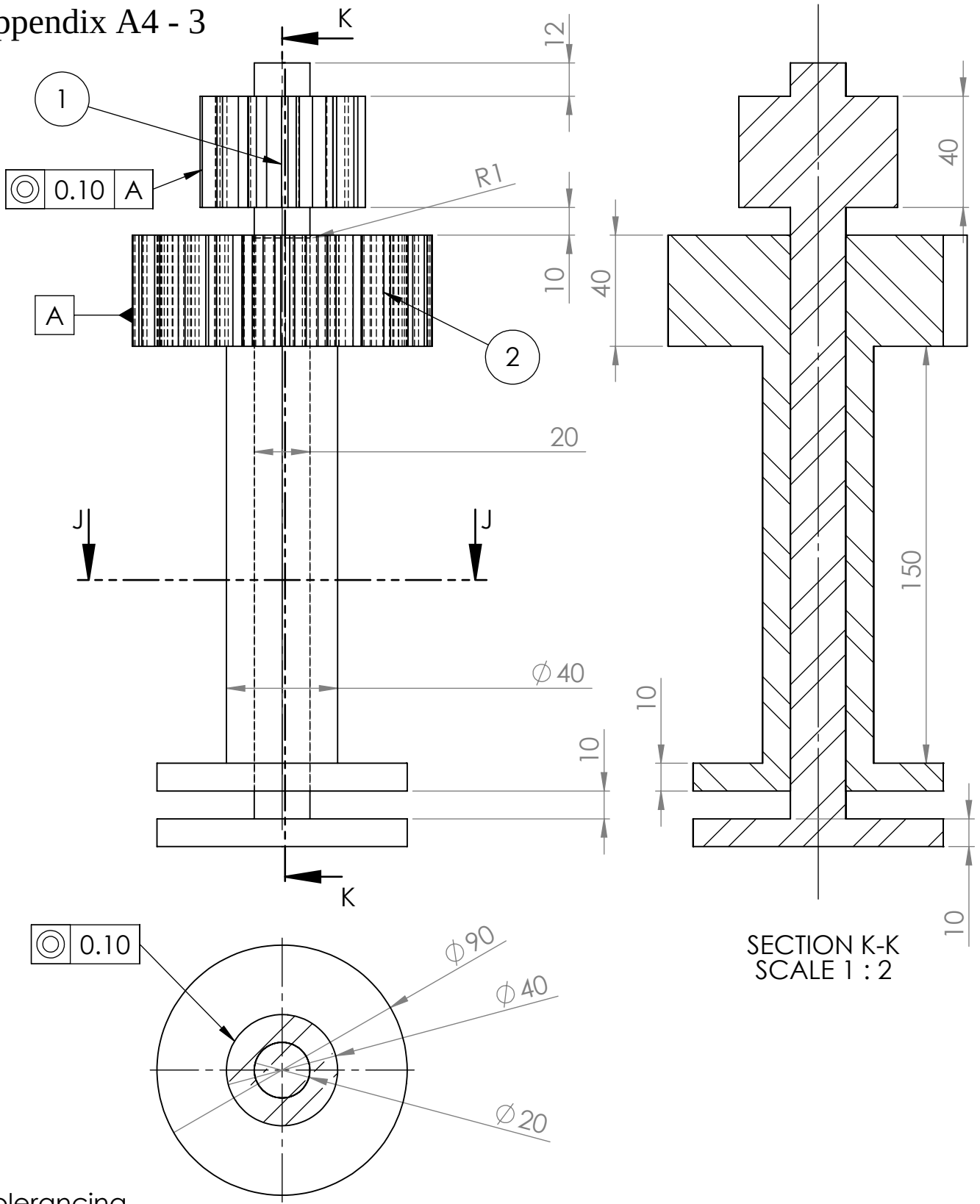

SECTION K-K
SCALE 1 : 2

SECTION J-J
SCALE 1 : 2

Tolerancing

00 = ± 0.3
∅ 00.0 = ± 0.1

Component N°	Component name
1	Sun gear
2	Planet gear

Scale:1/2

Stage brakes

AMINI Dahbia

Date: 14/01/2022

A4

Thesis drawing
Master's in mechanical design

University Mouloud Mammeri of Tizi Ozou
Faculty of construction engineering
Department of mechanical engineering

General roughness Ra = 0.36 um
Teeth roughness Ra<0.25um

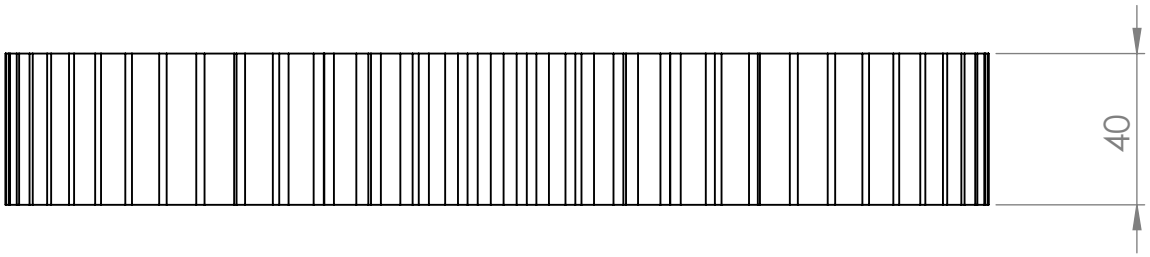

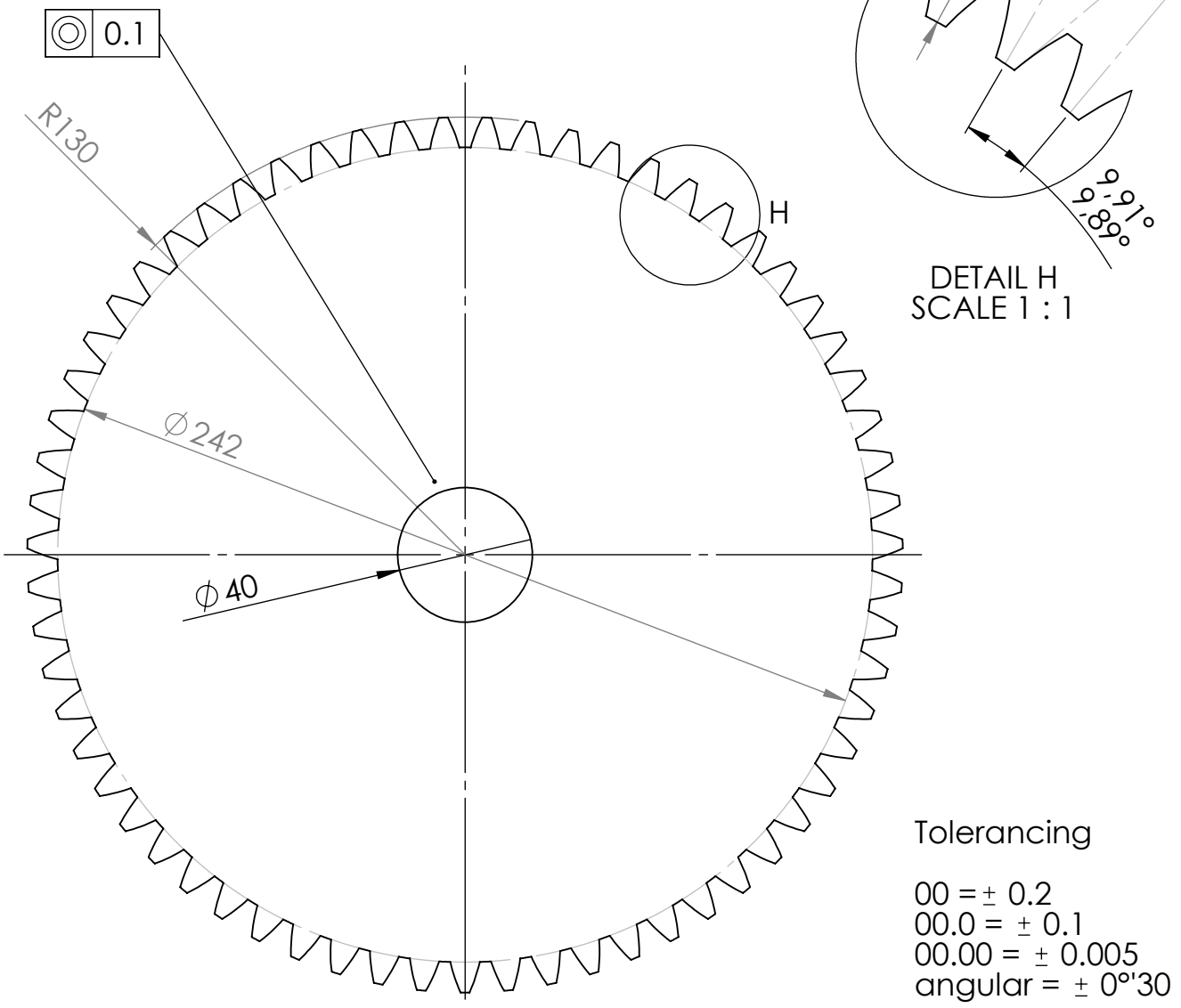

DETAIL H
SCALE 1 : 1

Tolerancing

00 = ± 0.2
00.0 = ± 0.1
00.00 = ± 0.005
angular = ± 0°'30

Scale:1/2	Spur gear P	AMINI Dahbia
		Date: 14/01/2022
A4	Thesis drawing Master's in mechanical design	University Mouloud Mammeri of Tizi Ozou Faculty of construction engineering Department of mechanical engineering

Appendix A4 - 5

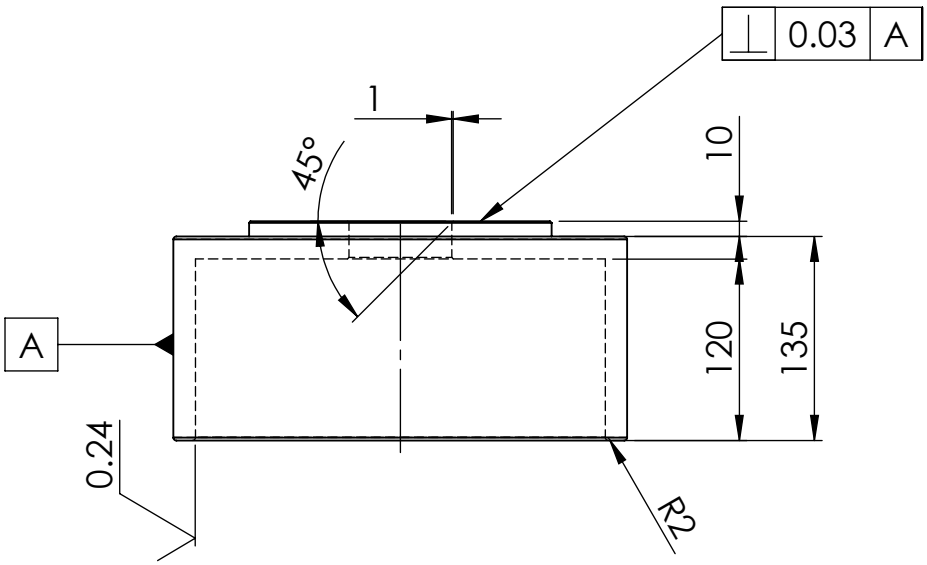

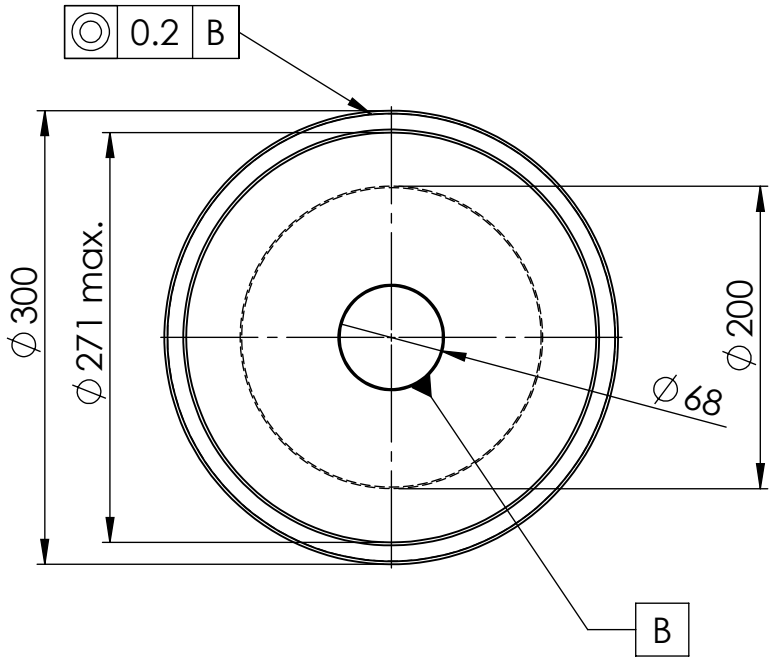

Tolerancing

00 = ± 0.15
R 00.0 = ± 0.1
angular = ± 0°'30

General roughness Ra = 0.36 um

Scale:1/5	Cover	AMINI Dahbia
		Date: 14/01/2022
A4	Thesis drawing Master's in mechanical design	University Mouloud Mammeri of Tizi Ozou Faculty of construction engineering Department of mechanical engineering

Appendix A4 - 6

General roughness Ra = 0.36 um
Teeth roughness Ra<0.25um

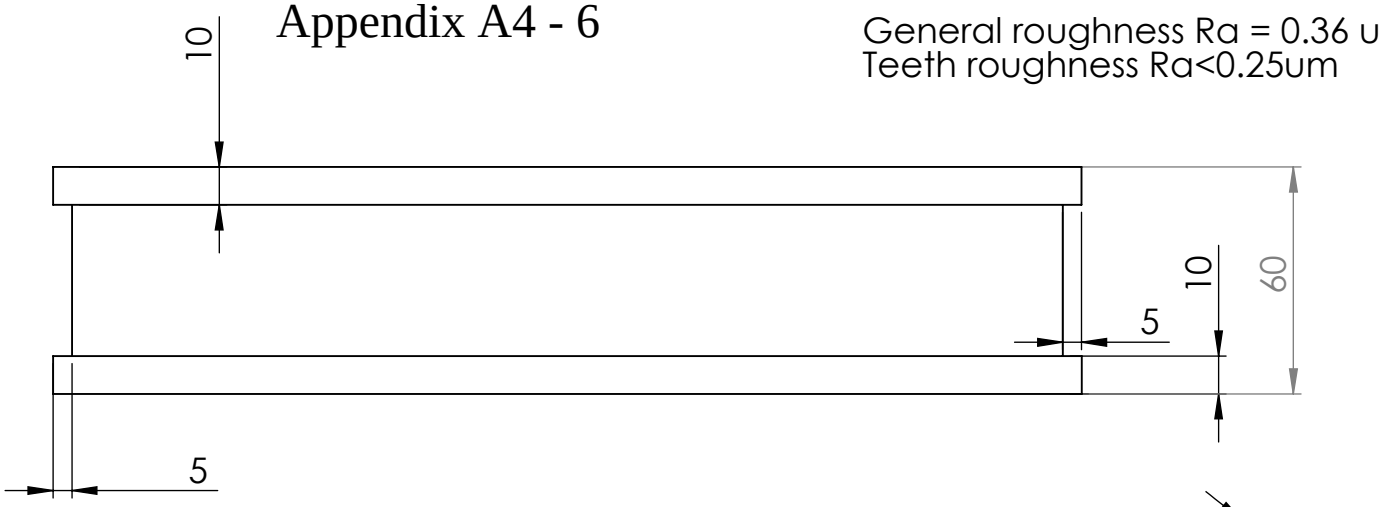

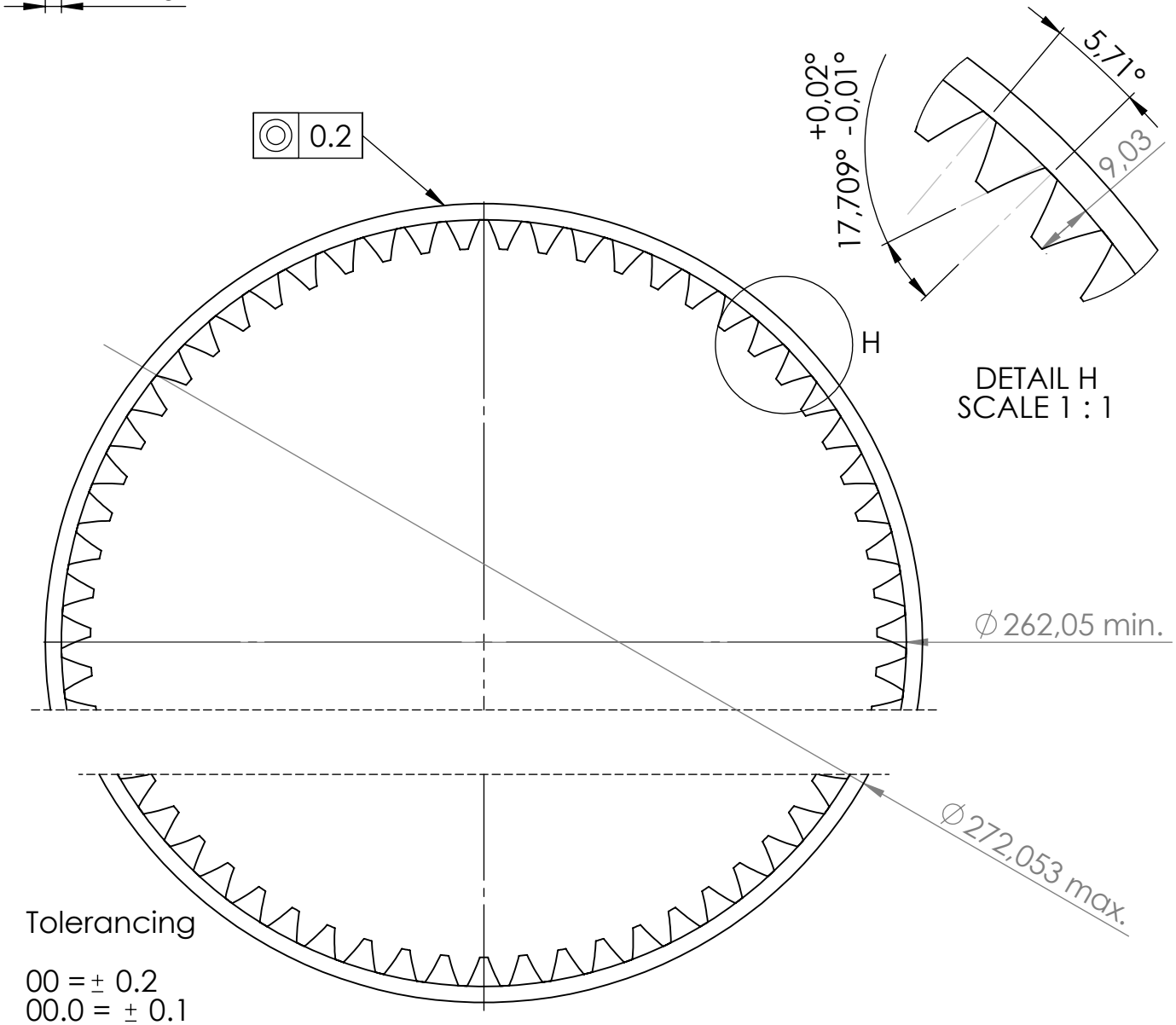

Tolerancing

00 = ± 0.2
00.0 = ± 0.1
00.00 = ± 0.005
angular = ± 0°'30

Scale:1/2	Internal spur gear	AMINI Dahbia
		Date: 14/01/2022
A4	Thesis drawing Master's in mechanical design	University Mouloud Mammeri of Tizi Ozou Faculty of construction engineering Department of mechanical engineering

Tolerancing

00 = ± 0.2
00.00 = ± 0.05

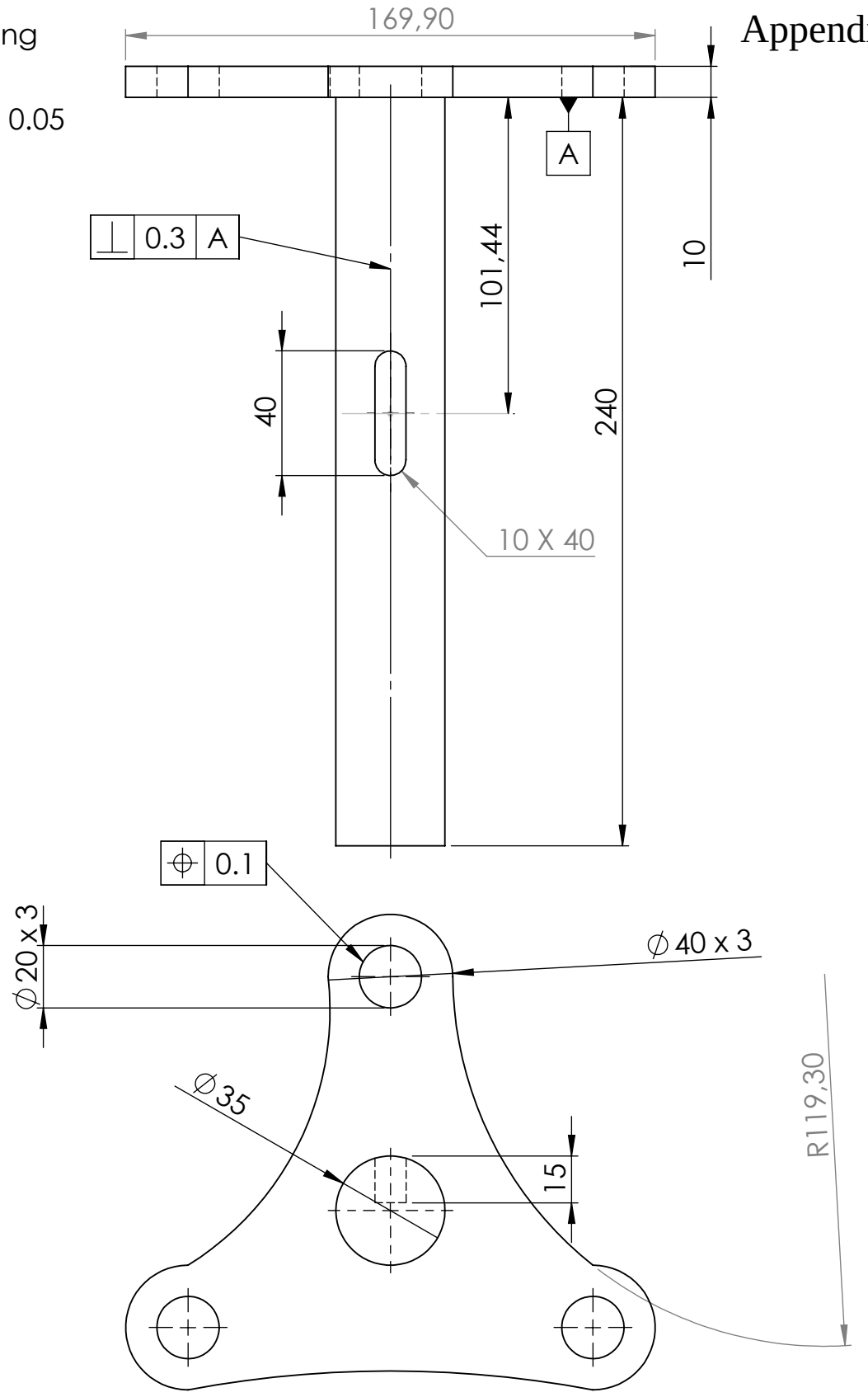

General roughness Ra = 0.36 um
Holes roughness Ra<0.25um

Scale:1/2	Carrier	AMINI Dahbia
		Date: 14/01/2022
A4	Thesis drawing Master's in mechanical design	University Mouloud Mammeri of Tizi Ozou Faculty of construction engineering Department of mechanical engineering

Appendix A4 - 8

General roughness Ra = 0.36 um
Teeth roughness Ra<0.25um

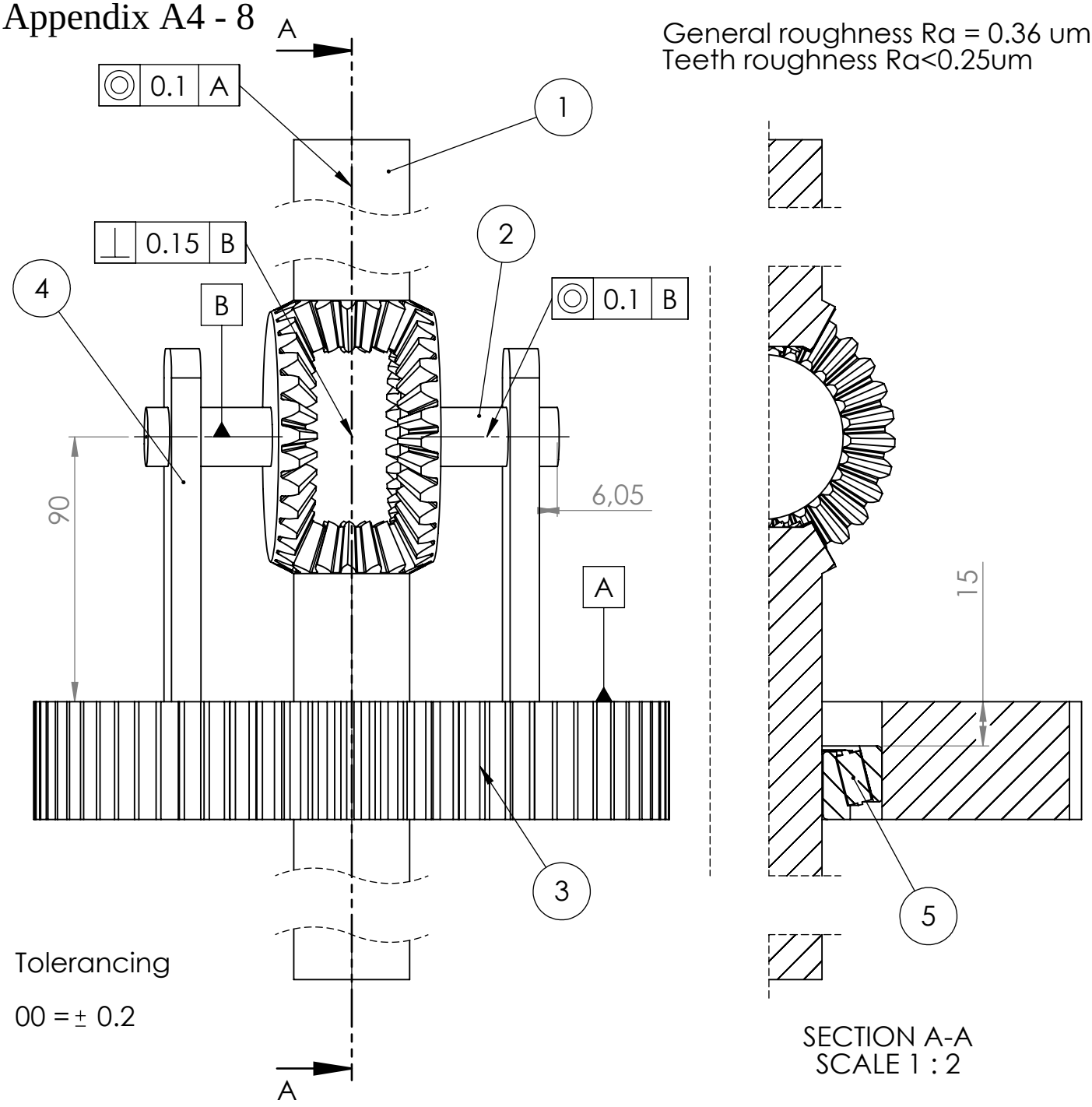

Tolerancing

00 = ± 0.2

SECTION A-A
SCALE 1 : 2

Component N°	Component name	Details	Quantity
1	Straight bevel pinion	3M15PT30GT20PA 17FW	2
2	Straight bevel gear	3M30GT15PT20PA FW17	2
3	Spur gear	3M70t20PA40FW	1
4	Connection	-	2
5	Tapered roller bearing	ISO 355 - 3 - 3DC40 -16,DE, PC 16	1

Scale:1/2

Differential

AMINI Dahbia

Date: 14/01/2022

A4

Thesis drawing
Master's in mechanical design

University Mouloud Mammeri of Tizi Ozou
Faculty of construction engineering
Department of mechanical engineering

Appendix A4 - 9

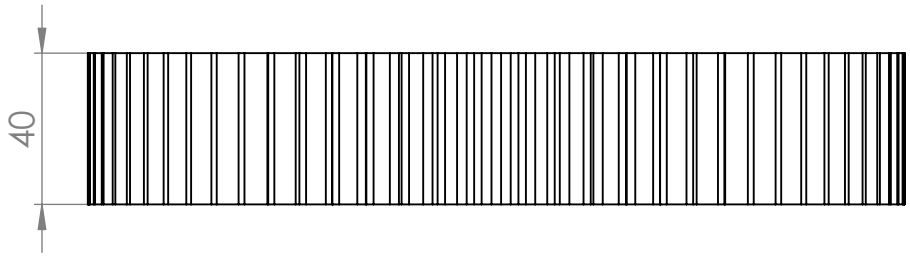

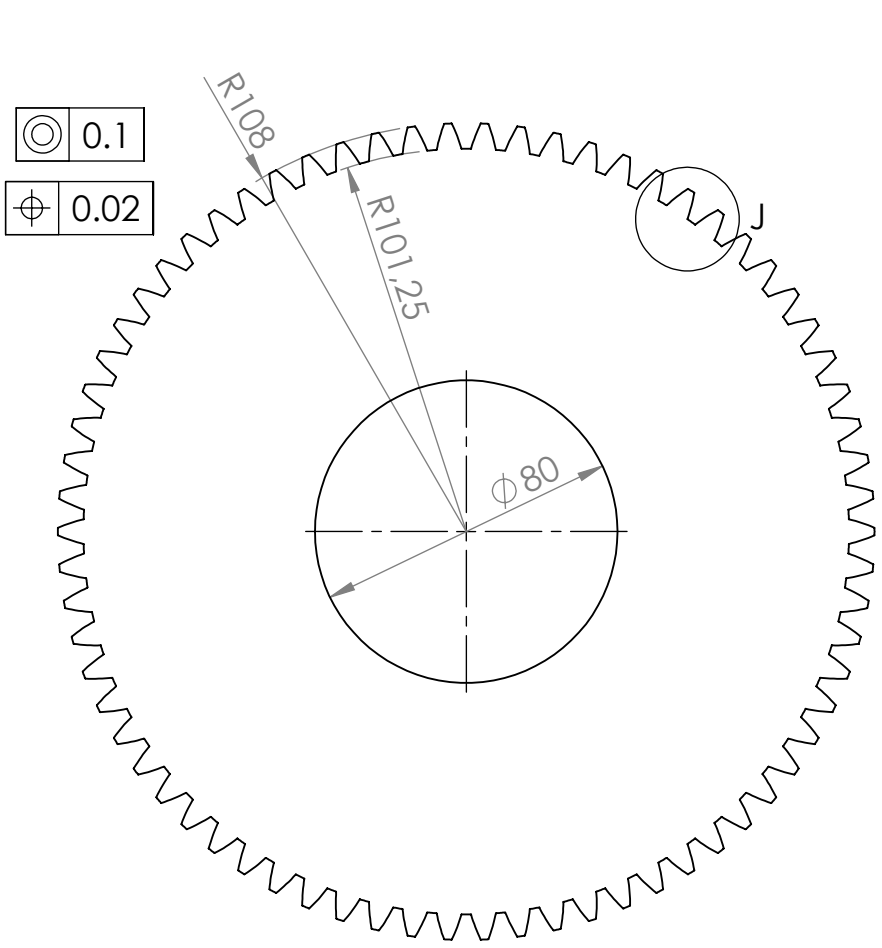

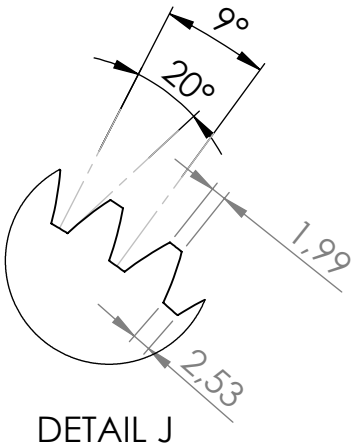

DETAIL J
SCALE 1 : 1

Tolerancing

00 = ± 0.2
00.0 = ± 0.1
00.00 = ± 0.005
angular = ± 0°'30

General roughness Ra = 0.36 um
Teeth roughness Ra<0.25um

Scale:1/2	Spur gear D	AMINI Dahbia
		Date: 14/01/2022
A4	Thesis drawing Master's in mechanical design	University Mouloud Mammeri of Tizi Ozou Faculty of construction engineering Department of mechanical engineering

Appendix A4 - 10

Tolerancing

00 = ± 0.2
00.0 = ± 0.1
00.00 = ± 0.005
angular = ± 0°'30

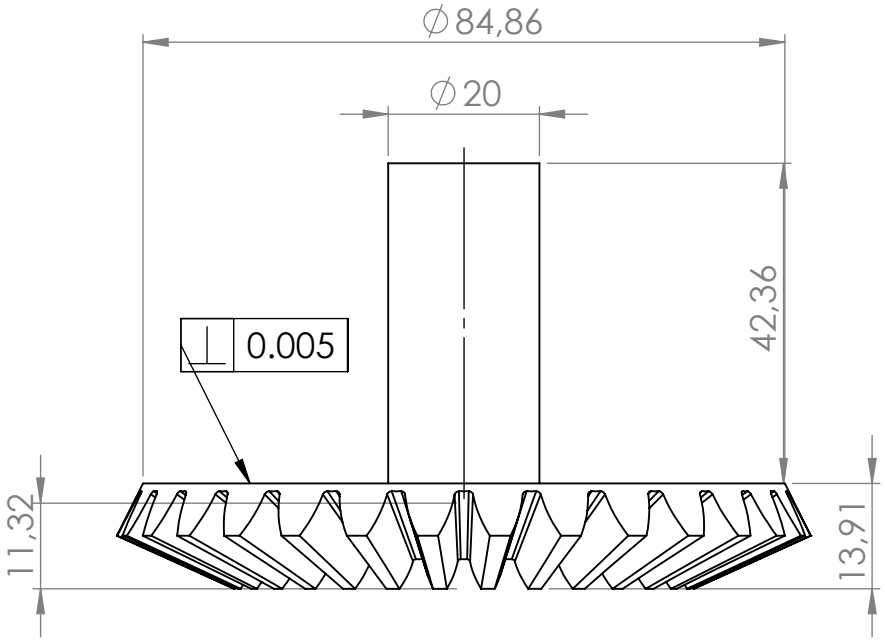

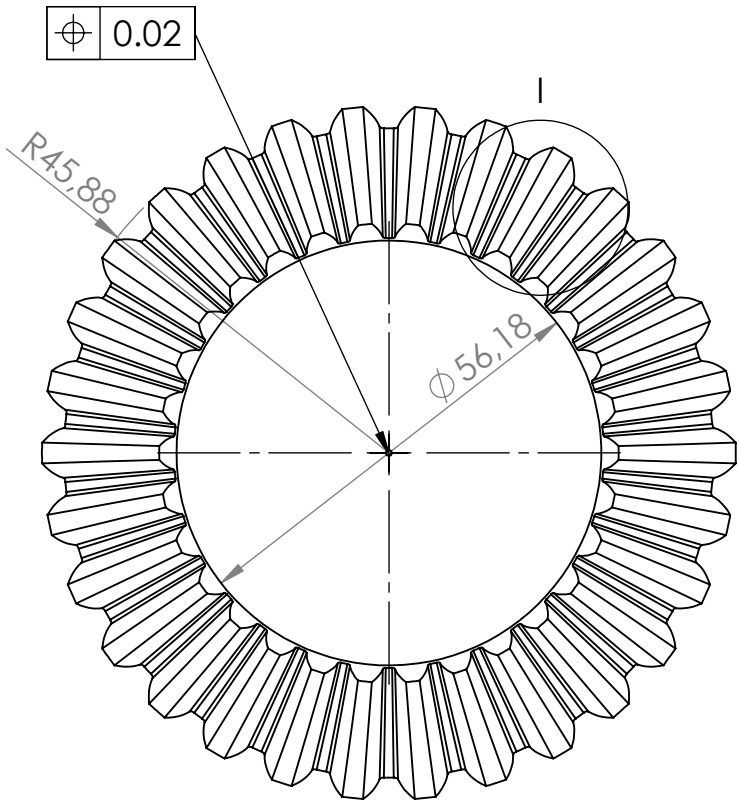

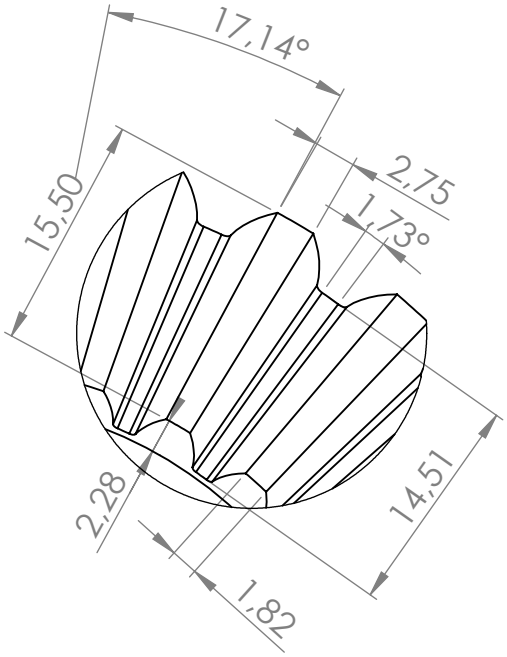

DETAIL I
SCALE 2 : 1

General roughness Ra = 0.36 um
Teeth roughness Ra<0.25um

Scale:1/1	Straight bevel Gear	AMINI Dahbia
		Date: 14/01/2022
A4	Thesis drawing Master's in mechanical design	University Mouloud Mammeri of Tizi Ozou Faculty of construction engineering Department of mechanical engineering

Appendix A4 - 11

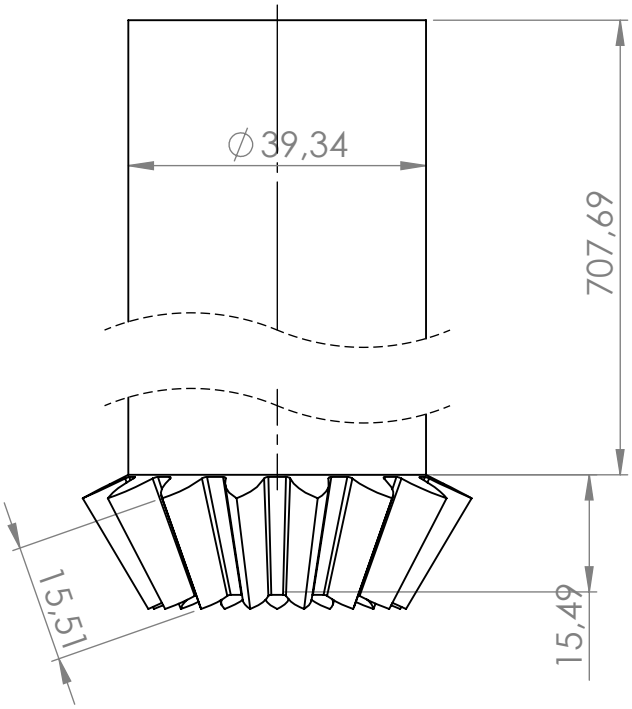

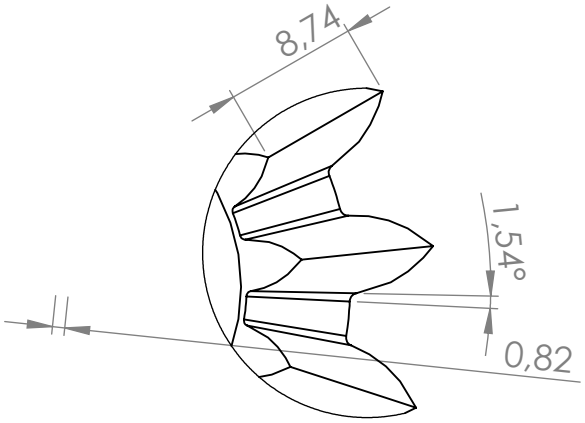

DETAIL H
SCALE 2 : 1

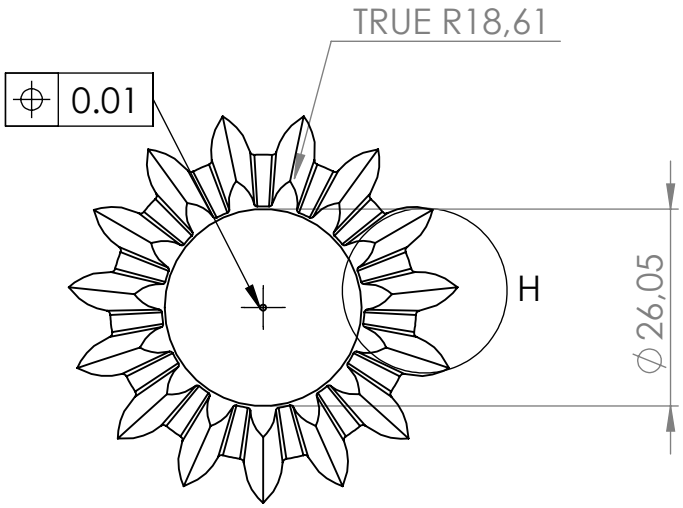

Tolerancing

00 = ± 0.5
00.0 = ± 0.1
00.00 = ± 0.005
angular = ± 0°'30

General roughness Ra = 0.36 um
Teeth roughness Ra<0.25um

Scale:1/1	Straight bevel pinion	AMINI Dahbia
		Date: 14/01/2022
A4	Thesis drawing Master's in mechanical design	University Mouloud Mammeri of Tizi Ozou Faculty of construction engineering Department of mechanical engineering

Appendix A4 - 12

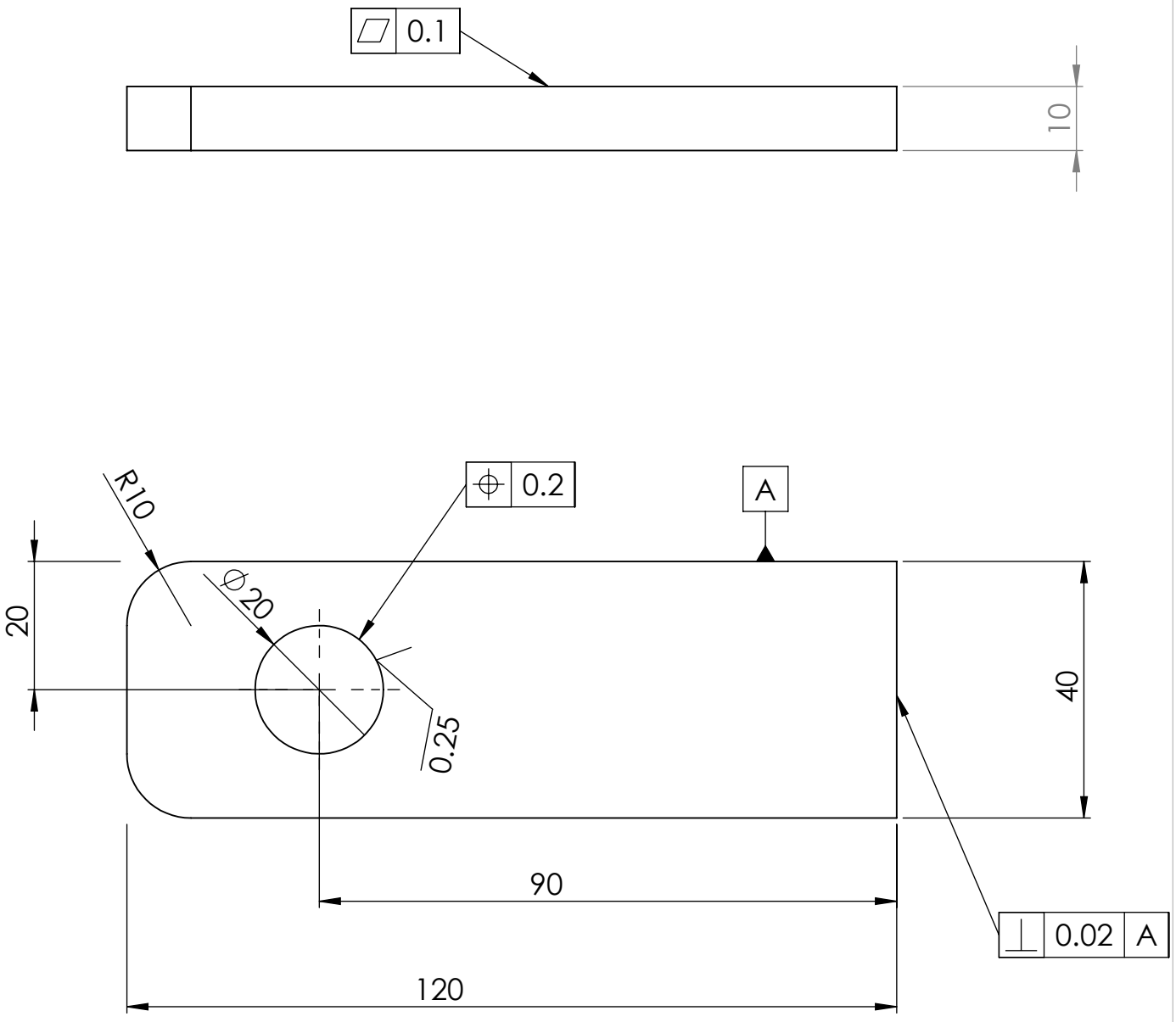

Tolerancing

00 = ± 0.2
∅00 = ± 0.1

General roughness Ra = 0.36 um

Scale:1/1	Connection	AMINI Dahbia
		Date: 14/01/2022
A4	Thesis drawing Master's in mechanical design	University Mouloud Mammeri of Tizi Ozou Faculty of construction engineering Department of mechanical engineering

Appendix A4 - 13

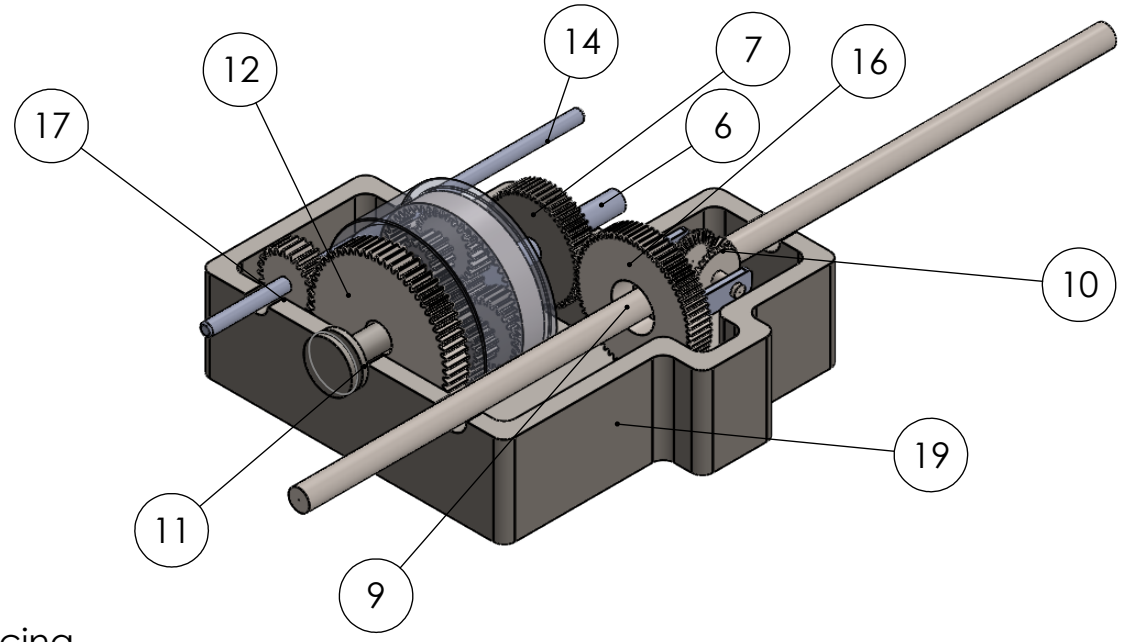

Tolerancing

00 = ± 0.2
00.0 = ± 0.1
00.00 = ± 0.005
angular = ± 0°'30

General roughness Ra = 0.36 um
Teeth roughness Ra<0.25um

Component N°	Component Name	Details	Material
6	Sahft II	35D 550L	20CrMo5
7	Gear C	3M56T	
9	Shaft III	60D 1600L	
10	Differential	-	
11	Gear P	4M63T	
12	Planetary gear set	-	
14	Shaft I	22D180L	
16	Gear D	3M70T	
17	Gear M	4M24T	
19	Housing	-	-

Scale:1/10

Transmission

AMINI Dahbia

Date: 14/01/2022

A4

Thesis drawing
Master's in mechanical design

University Mouloud Mammeri of Tizi Ozou
Faculty of construction engineering
Department of mechanical engineering

Appendix A4 - 14

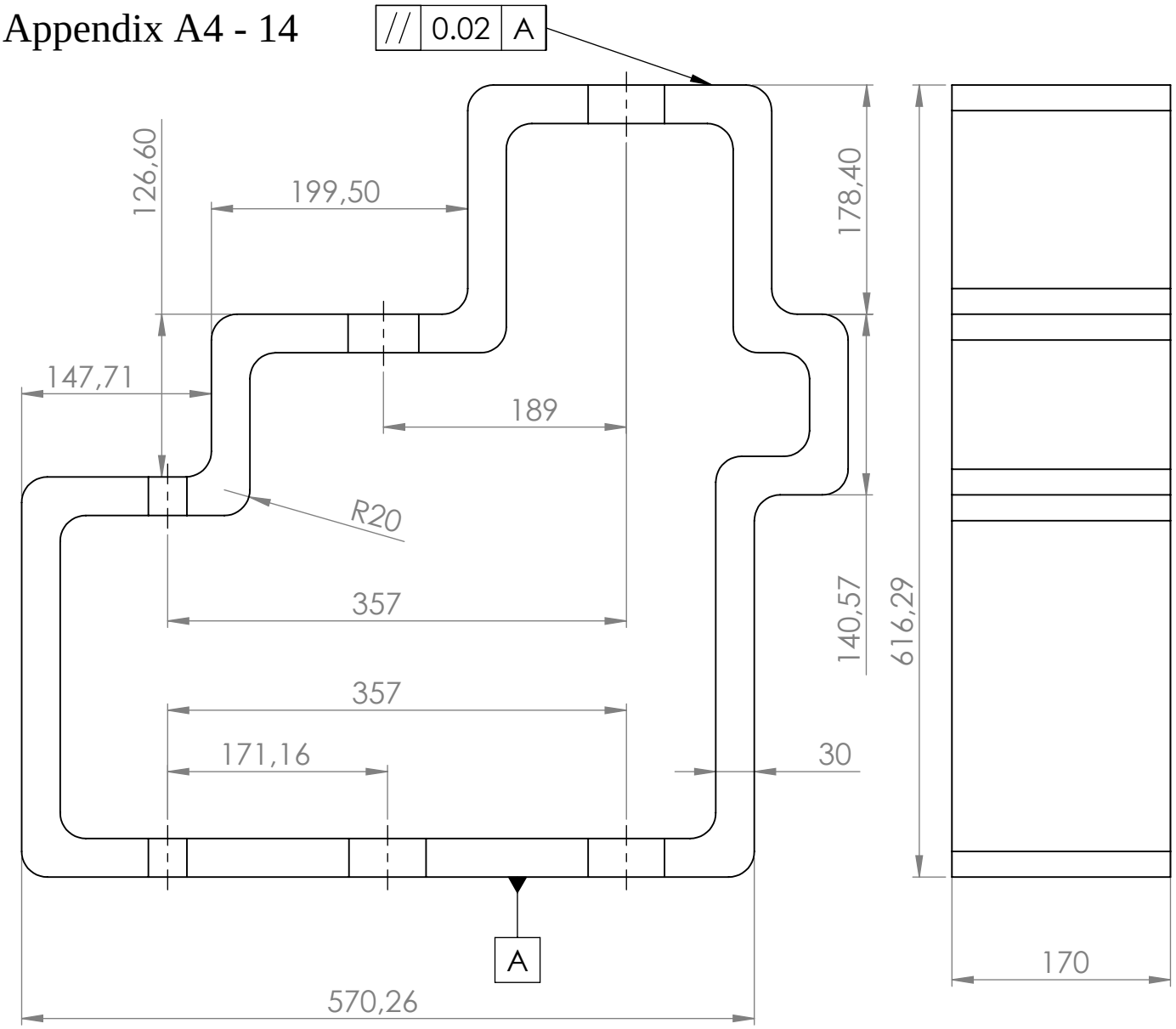

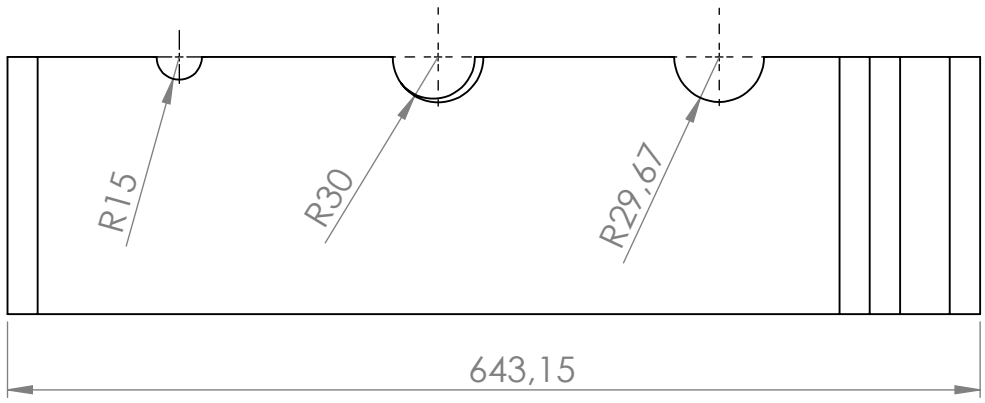

Tolerancing

00 = ± 0.2
R 00.0 = ± 0.1
00.00 = ± 0.005

General roughness Ra = 0.35 um
Roughness on edges Ra = 0.25um

Scale:1/10	Housing	AMINI Dahbia
		Date: 14/01/2022
A4	Thesis drawing Master's in mechanical design	University Mouloud Mammeri of Tizi Ozou Faculty of construction engineering Department of mechanical engineering

Appendix A4 - 15

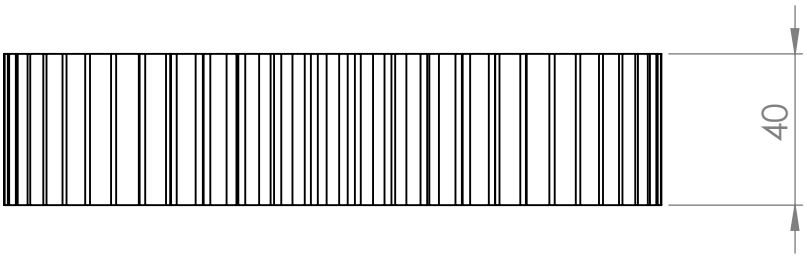

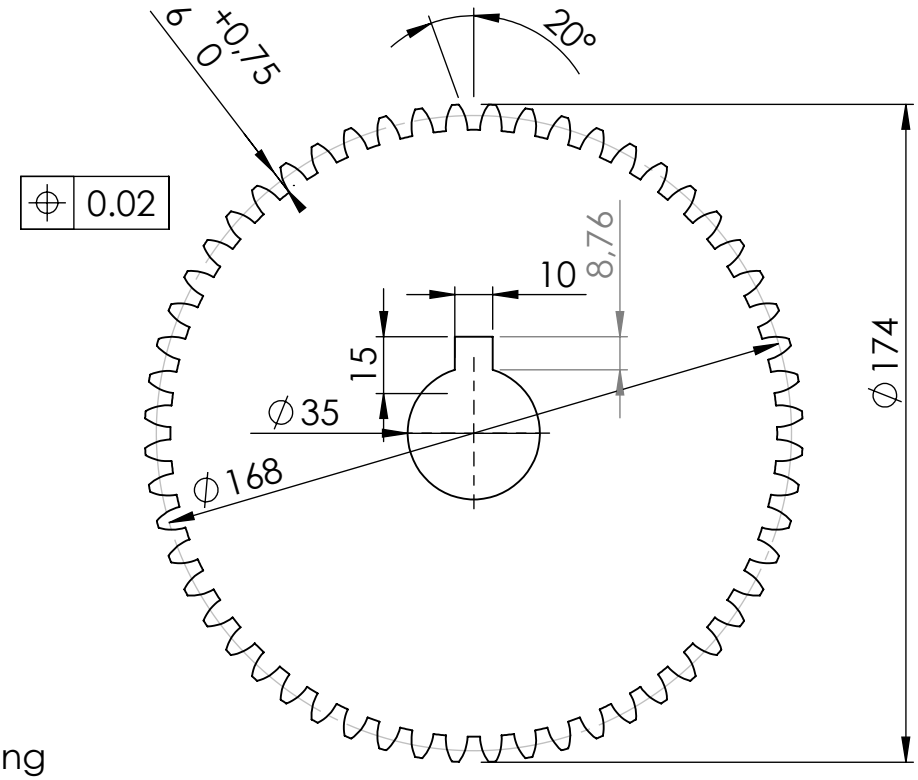

Tolerancing

00 = ± 0.5
00.0 = ± 0.2
00.00 = ± 0.005
angular = ± 0°'30

General roughness Ra = 0.36 um
Teeth roughness Ra<0.25um

Scale:1/2	Gear C	AMINI Dahbia
		Date: 14/01/2022
A4	Thesis drawing Master's in mechanical design	University Mouloud Mammeri of Tizi Ozou Faculty of construction engineering Department of mechanical engineering

General roughness Ra = 0.36 um
Teeth roughness Ra<0.25um

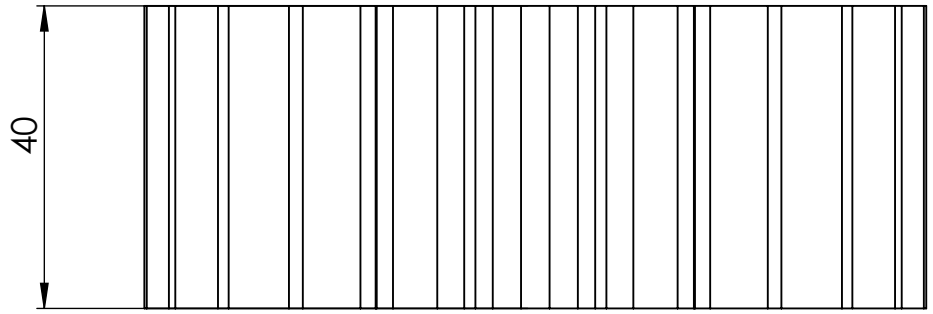

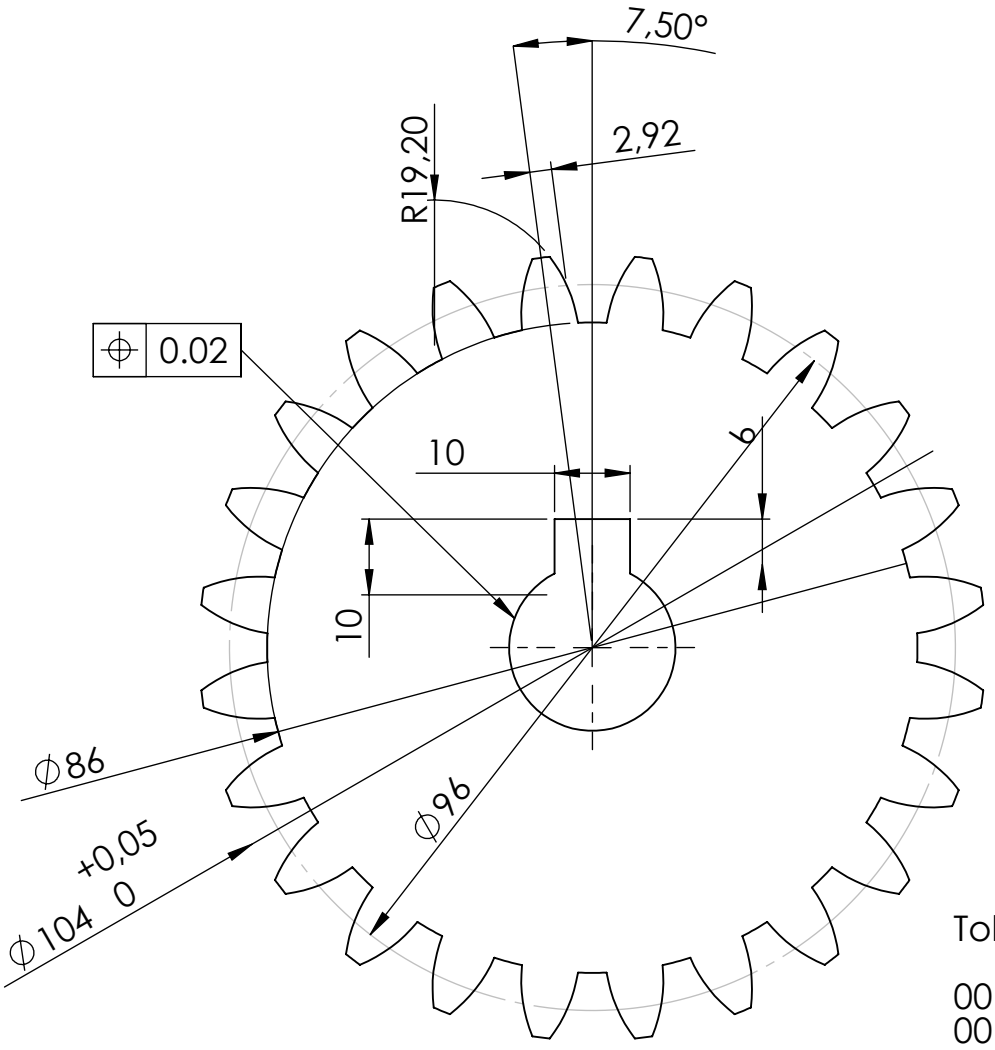

Tolerancing

00 = ± 0.2
00.0 = ± 0.1
00.00 = ± 0.005
angular = ± 0°'30

Scale:1/1	Gear M	AMINI Dahbia
		Date: 14/01/2022
A4	Thesis drawing Master's in mechanical design	University Mouloud Mammeri of Tizi Ozou Faculty of construction engineering Department of mechanical engineering

Appendix A4 - 17

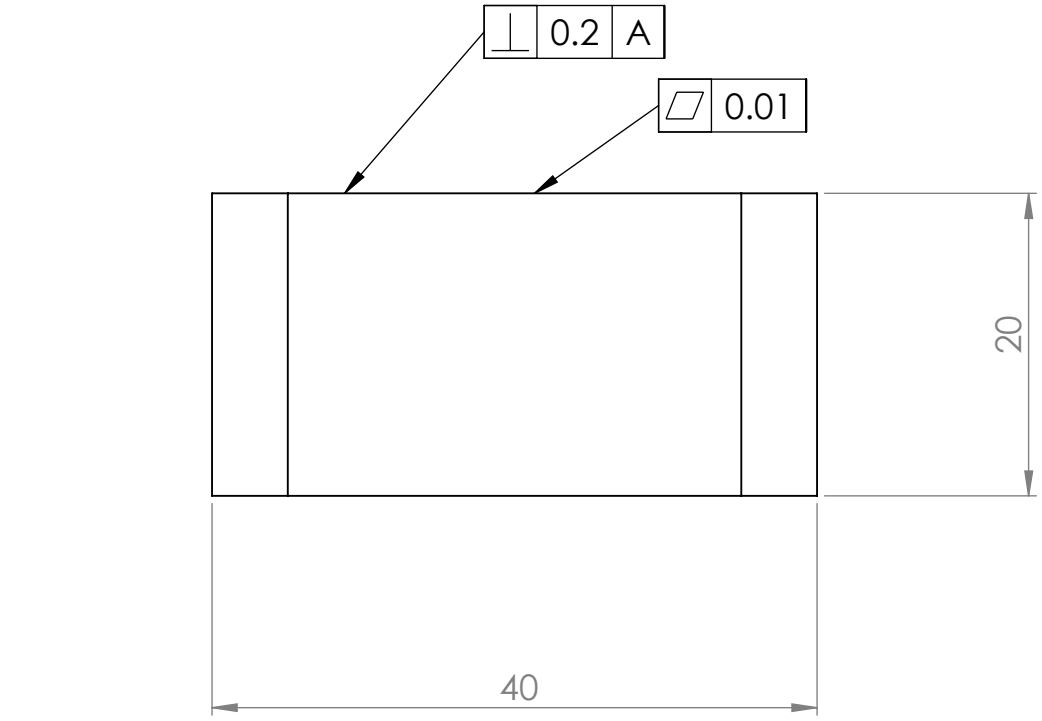

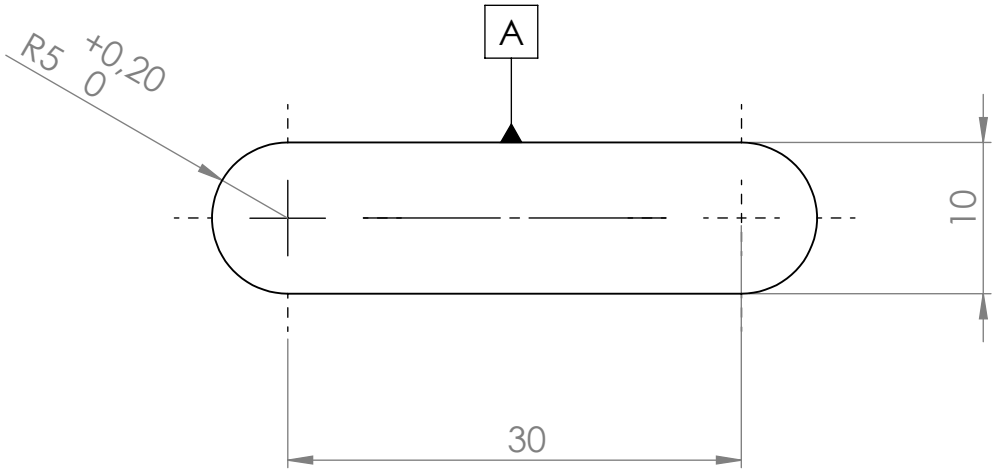

General roughness Ra = 0.24 um
General tolerance 00 = ±0.02

Scale:2/1	Key C	AMINI Dahbia
		Date: 14/01/2022
A4	Thesis drawing Master's in mechanical design	University Mouloud Mammeri of Tizi Ozou Faculty of construction engineering Department of mechanical engineering

Appendix A4 - 18

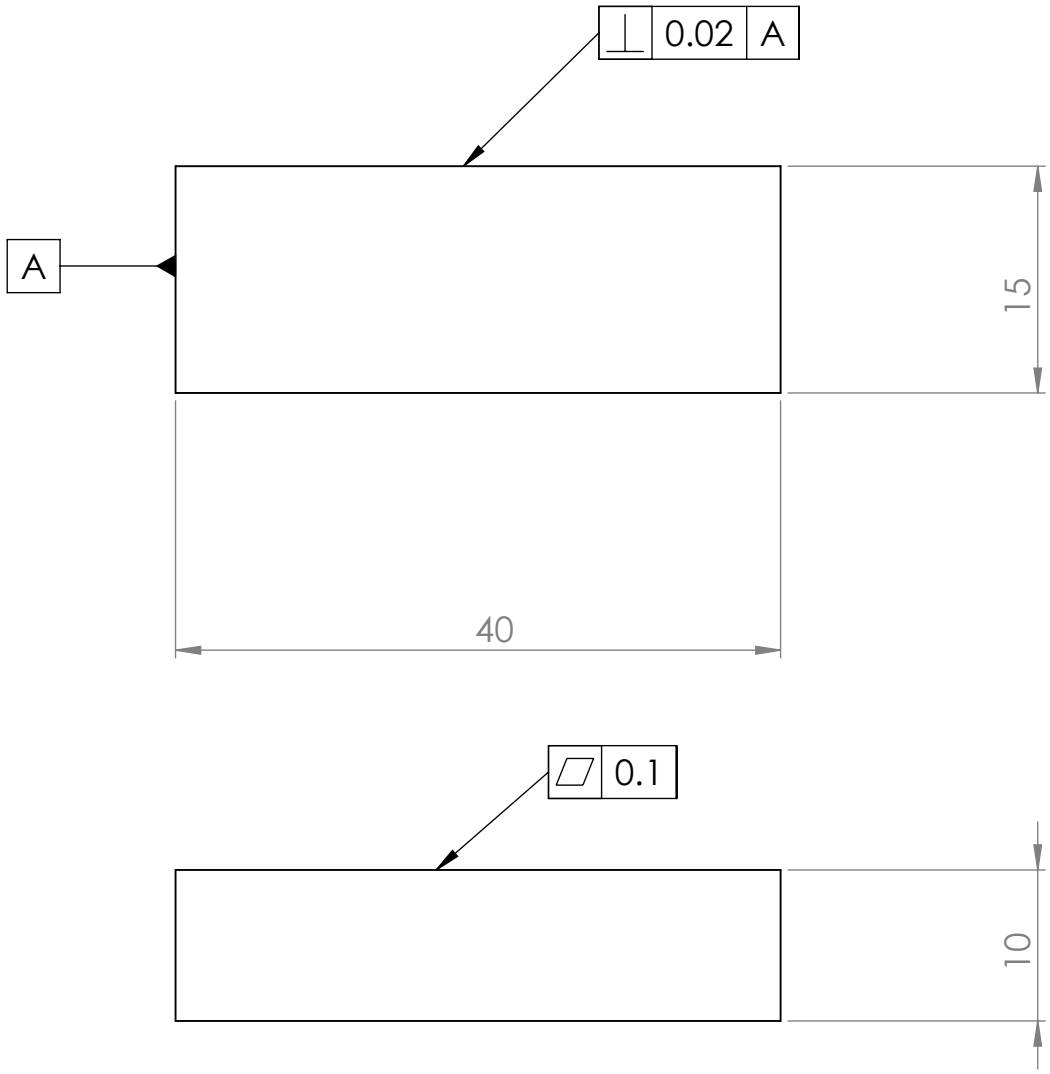

Tolerancing

00 = ± 0.2

General roughness Ra = 0.24 um

Scale:2/1	Key M	AMINI Dahbia
		Date: 14/01/2022
A4	Thesis drawing Master's in mechanical design	University Mouloud Mammeri of Tizi Ozou Faculty of construction engineering Department of mechanical engineering

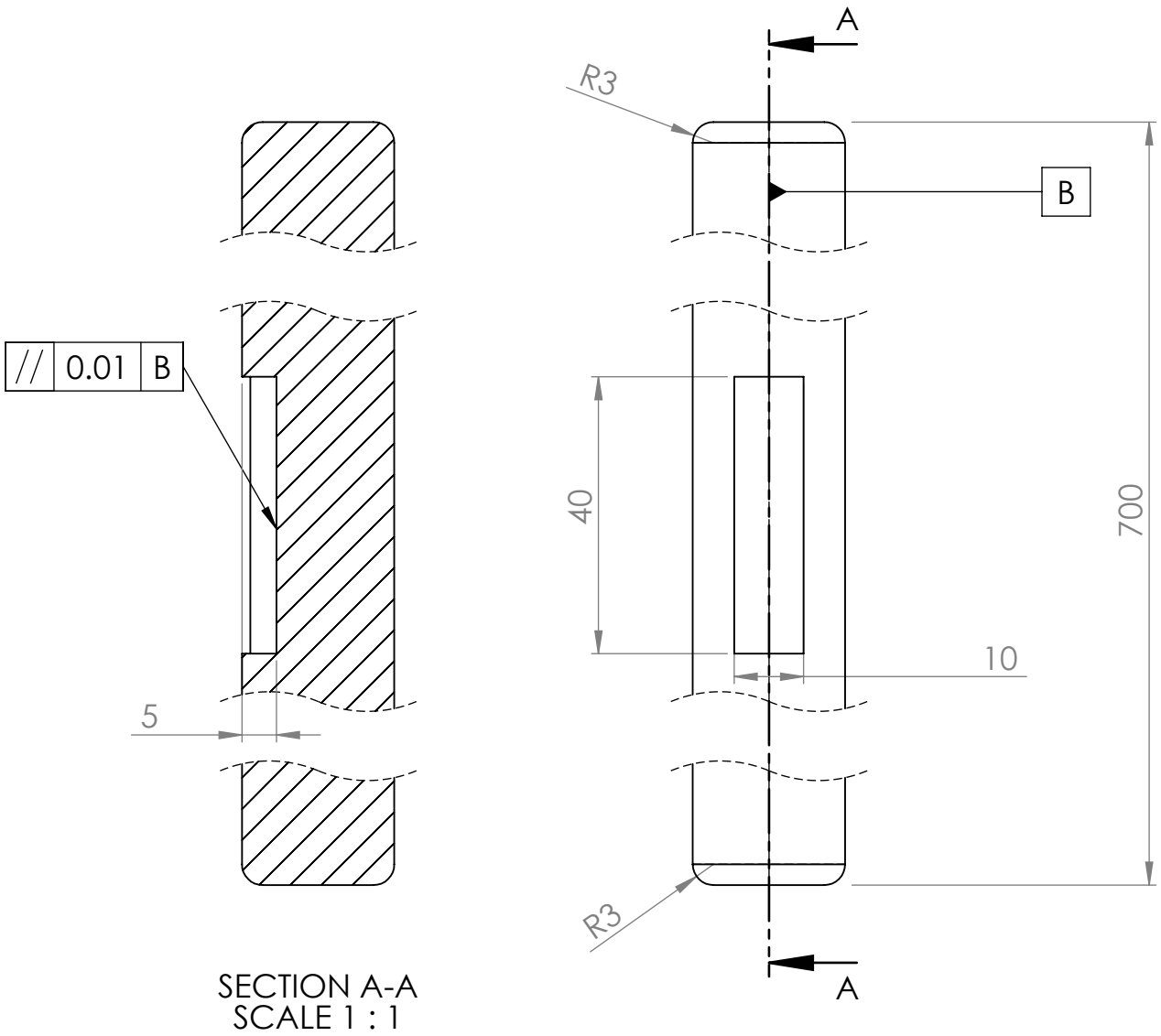

SECTION A-A
SCALE 1 : 1

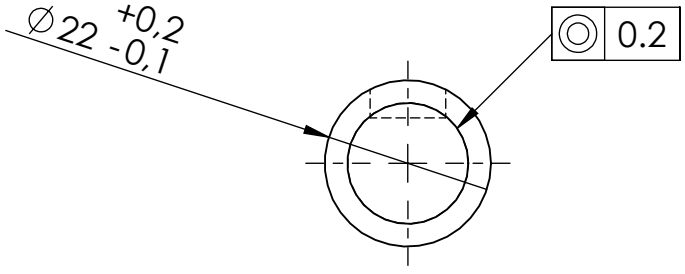

Tolerancing

00 = ± 0.1
R 00 = ± 0.01

General roughness Ra = 0.36 um

Scale:1/1	Shaft I	AMINI Dahbia
		Date: 14/01/2022
A4	Thesis drawing Master's in mechanical design	University Mouloud Mammeri of Tizi Ozou Faculty of construction engineering Department of mechanical engineering